UNIVERSITY OF THE
FREE STATE
UNIVERSITEIT VAN DIE
VRYSTAAT
YUNIVESITHI YA
FREISTATA

UFS
UV

PREPARATION AND IMMUNOGENICITY OF A CANDIDATE REPLICON BASED YELLOW FEVER VACCINE

Natalie Viljoen

December 2014

FAKULTEIT GESONDHEIDSWETENSKAPPE
FACULTY OF HEALTH SCIENCES

PREPARATION AND IMMUNOGENICITY OF A CANDIDATE REPLICON BASED YELLOW FEVER VACCINE

Natalie Viljoen

M.Med.Sc. Virology

Submitted in fulfilment of the requirements in respect of the M.Med.Sc. Virology degree completed in the Department of Medical Microbiology and Virology in the Faculty of Health Sciences at the University of the Free State

Promoter: Professor Felicity Jane Burt
Department of Medical Microbiology and Virology
Faculty of Health Sciences
University of the Free State

The financial assistance of the National Research Foundation and the Poliomyelitis Research Foundation is hereby acknowledged. Opinions expressed and conclusions arrived at are those of the author and are not necessarily attributed to these institutions.

University of the Free State, Bloemfontein, South Africa
December 2014

Table of content

Declaration

I, Natalie Viljoen, certify that the dissertation hereby submitted for the M.Med.Sc Virology qualification at the University of the Free State is my independent effort and has not previously been submitted for a qualification at another university/faculty. I furthermore waive copyright of the dissertation in favour of the University of the Free State.

X 

Natalie Viljoen

Acknowledgements

I hereby acknowledge and extend my wholehearted appreciation to the following:

- First and foremost, I would like to thank my heavenly Father.

"For I can do everything through Christ, who gives me strength"
Philippians 4:13 (New Living Translation)

- My esteemed supervisor, Prof. Felicity Jane Burt, for guidance, support and her willingness to assist. Your enthusiasm is contagious and this is reflected within the research group.

- Prof. Mark Heise from the Department of Microbiology and Immunology at the University of North Carolina in the United States of America (USA) for providing the DNA-launched replicon construct and granting permission for use in this study.

- The University of the Free State, Faculty of Health Sciences, Department of Medical Microbiology and Virology and National Health Laboratory Services for providing the facilities required for completion of the research project.

- The National Health Laboratory Service Research Trust for funding of the research project.

- The National Research Foundation, the Poliomyelitis Research Foundation and the University of the Free State School of Medicine for providing financial assistance.

- My family, friends and colleagues for moral support and encouragement.

- The University of the Free State's Animal Unit, Dr Stephen Robinson, Prof. Felicity Jane Burt, Riaan van Zyl, Seb Lamprecht and Lehlohonolo Mathengtheng for assistance with animal housing, inoculation, handling, monitoring and exsanguination.

List of figures

Chapter 1:

Chapter 2:

Chapter 3:

List of tables

Chapter 2:

Chapter 3:

List of abbreviations

2X TY	2X tryptone yeast
2X TY/kan	2X TY containing kanamycin to a final concentration of 50µg/ml
ABTS	2,2'-azino-bis(3-ethylbenzothiazoline-6-sulphonic acid)
ACIP	Advisory Committee on Immunisation Practices
AIDS	acquired immunodeficiency syndrome
APS	ammonium persulphate
ATCC	American Type Culture Collection
BBS	borate-buffered saline
BGH	bovine growth hormone
BHK	baby hamster kidney
bp	base pairs
C	capsid
CAI	Codon Adaptation Index
CDC	Centres for Disease Control and Prevention
cfu	colony forming units
con A	concanavalin A
COS	CV-1 in Origin, carrying SV40
CPE	cytopathic effect
CTL	cytotoxic T-lymphocyte
DC	dendritic cells
DEN	dengue virus
DMEM	Dulbecco's Modified Eagle Medium
DNA	deoxyribonucleic acid
E	envelope
ED-lll	envelope domain lll
EDTA	ethylenediaminetetraacetic acid
ELISA	enzyme-linked immunosorbent assay
EMEM	Eagle's Minimal Essential Medium
ER	endoplasmic reticulum
F	phenylalanine
FBS	foetal bovine serum
FDA	Food and Drug Administration
FITC	fluorescein isothiocyanate
FNV	French neurotropic virus
FVV	French viscerotropic virus
GAVI	Global Alliance for Vaccines and Immunisation

GFP	green fluorescent protein
GRO	growth-related oncogenes
H	haemagglutinin
HCl	hydrochloric acid
hCMV	human cytomegalovirus
HEK	human embryonic kidney
HIV	human immunodeficiency virus
HRPO	horseradish peroxidase
I	isoleucine
IFA	immunofluorescence assay
IFN	interferon
Ig	immunoglobulin
IL	interleukin
IL-1RA	interleukin-1 receptor antagonist
IM	intramuscular
IMAC	immobilised metal ion affinity chromatography
IP	inducible protein
IPTG	isopropyl β-D-1-thiogalactopyranoside
IV	intravenous
JCat	JAVA Codon Adaptation Tool
JEV	Japanese encephalitis virus
kb	kilobases
L	leucine
LB	Luria-Bertani
LB/amp	Luria-Bertani containing ampicillin to a final concentration of 100µg/ml
LD	lethal dose
LEW	lysis-equilibrium-wash
L-glu	L-glutamine
M	membrane (protein)
MCP-1	monocyte chemo-attractant protein 1
MCS	multiple cloning site
MEM	minimum essential media
MHC	major histocompatibility complex
MOI	multiplicity of infection
m-RNA	messenger ribonucleic acid
NCR	non-coding region
NEAA	non-essential amino acid

NS	non-structural
Oas	2’-5’ oligoadenylate synthetase
OD	optical density
ORF	open reading frame
o/n	overnight
PBS	phosphate buffered saline
PCR	polymerase chain reaction
pen/strep	penicillin and streptomycin
poly A	polyadenylation A
prM	pre-membrane
PRNT	plague reduction neutralisation test
PVDF	polyvinylidene fluoride
RANTES	regulated upon activation normal T-cell expressed and secreted
rpm	rotations per minute
RNA	ribonucleic acid
RSA	Republic of South Africa
RT-PCR	reverse-transcriptase polymerase chain reaction
RYF	yellow fever virus-specific repeat sequence
SDS	sodium dodecyl sulphate
SDS-PAGE	sodium dodecyl sulphate polyacrylamide gel electrophoresis
SFV	Semliki Forest virus
SINV	Sindbis virus
SOC	Super Optimal broth with Catabolite repression
STAT	signal transducers and activators of transcription
TAE	trisaminomethane-acetate-ethylenediaminetetraacetic acid
TAP	transporter associated protein
TBS	trisaminomethane-buffered saline
TEMED	tetramethylethylenediamine
TGF-β	transforming growth factor β
Th	T-helper
TMB	3,3’,5,5’-tetramethylbenzidine
TNF	tumour necrosis factor
Tris	trisaminomethane
t-RNA	transfer ribonucleic acid
UK	United Kingdom
U/ml	units per millilitre
USA	United States of America

UTR	untranslated region
VEE	Venezuelan equine encephalitis virus
WHO	World Health Organisation
WNV	West Nile virus
x *g*	gravitational force
X-gal	5-bromo-4-chloro-3-indolyl-β-D-galactopyranoside
Y	tyrosine
YFV	yellow fever virus

Presentations and publications

Oral presentations:

- Preparation of a DNA-launched replicon encoding the ED-lll protein of yellow fever virus. 18th Biennial Conference of the South African Society for Microbiology, Bela-Bela, South Africa from 24-27 November 2013.

- Immune response elicited by a candidate DNA-based vaccine against yellow fever virus. 47th University of the Free State Faculty of Health Sciences Research Forum, Bloemfontein, South Africa from 28-29 August 2014.

- Immune response elicited by a candidate DNA-based vaccine against yellow fever virus. 3rd Annual Free State Provincial Health Research Day, Bloemfontein, South Africa from 30-31 October 2014.

Poster presentations:

- DNA-launched Sindbis virus based replicon encoding the yellow fever virus ED-lll protein. 16th International Congress on Infectious Diseases, Cape Town, South Africa from 2-5 April 2014.

Publications:

- Viljoen N, Heise M, Burt FJ. DNA-launched Sindbis virus based replicon encoding the yellow fever virus ED-lll protein. Int J Infect Dis 2014; 21(Suppl 1):431.

- Viljoen N, Heise M, Burt FJ. Immunogenicity of a DNA-launched replicon encoding the yellow fever virus envelope domain lll protein. (Manuscript in preparation)

Ethics approval

Ethics approval for conducting this study was obtained from the Ethics Committee of the Faculty of Health Sciences, University of the Free State as an extension study (ECUFS NR 34/2013B) of the project *Development and evaluation of novel vaccines for medically significant arboviral diseases* (ECUFS NR 34/2013A) (refer to appendix G for letter of approval).

Ethics approval for conducting a mouse immunisation study was obtained from the Animal Ethics Committee, University of the Free State (ECUFS NR 24/2011) (refer to appendix G for letter of approval).

Note

All figures and tables herein have been self-constructed.

CHAPTER 1: Literature review, problem identification, aim and objectives

1.1 Literature review

1.1.1 Introduction and brief history of yellow fever virus

Yellow fever virus (YFV), a re-emerging virus that belongs to the family *Flaviviridae* and genus *Flavivirus*, originated in Africa and was imported into the Americas and Europe due to intercontinental slave trade (Chang *et al.*, 1995; Wang *et al.*, 1996). Massive outbreaks were recorded in the 18th and 19th centuries in the port cities on the eastern seaboard of North America, in Europe and in the tropical regions of South and Central America. In 1648, the first reliable description of a yellow fever outbreak was reported in Yucatan. Whereas the first well documented yellow fever outbreak in Africa only occurred in 1778, which originated in the Cape Verde Islands and subsequently spread to Gambia, the Gold Coast, Senegal and Sierra Leone. However, retrospective analysis revealed that YFV may have been the causative agent of an outbreak reported by Finlay dating back to 1494 in the Canary Islands, on the shipping route between Europe and Western Africa, at which time the disease was called contagion (Augustin, 1909). Initially, *Bacillus icteroides* was suggested to be the causative agent of yellow fever by Giuseppe Sanarelli (Sanarelli, 1897), whose hypothesis was later proven to be erroneous by Walter Reed and colleagues (Reed *et al.*, 1900). The cause of yellow fever and malaria was also incorrectly attributed to environmental mists and there were many contradictory theories regarding the transmission of yellow fever. At the time, yellow fever was thought to be transmitted by fomites rather than mosquitoes (Gorgas, 1902).

In 1848, after ingenious reasoning, Josiah Nott revealed that yellow fever and malaria may possibly be transmitted by an insect or animalcule, which is a microscopic animal or protozoa bred on the ground, and named the mosquito as a possible vector (Augustin, 1909). In 1881, Carlos Finlay suggested that yellow fever may be transmitted by *Culex fasciatus* mosquitoes, today known as *Aedes aegypti* mosquitoes (Finlay, 1903). The *A. aegypti* mosquito was suggested to be a possible vector due to the correlation observed between the resurgence of yellow fever cases and the abundance of these mosquitoes. Subsequently Finlay initiated experiments to confirm his theory (Augustin, 1909). However, Finlay's theory was only later confirmed by Walter Reed and colleagues, who demonstrated the primary mode of transmission of yellow fever occurs by the bite of an infected female *A. aegypti* mosquito. Walter Reed and colleagues contradicted the transmission of yellow fever by fomites (Reed *et al.*, 1901) and suggested that yellow fever is caused by a filterable agent (Reed & Carroll, 1902) shown to be present in the blood of yellow fever patients during the

early stages of disease (Reed *et al.*, 1901). In 1901, stringent anti-mosquito measures were implemented in Havana, which led to a substantial reduction in the prevalence of yellow fever (Gorgas, 1902).

In 1927, YFV was first isolated from Asibi, a Ghanaian patient, who exhibited mild symptoms of yellow fever. In 1928, an animal model was established by intraperitoneal inoculation of *Macacus rhesus* monkeys with the prototypic strain of YFV, which was designated the Asibi strain. YFV was shown to be transmissible from monkey to monkey not only by inoculation with infected blood, but also by the bite of an infected *A. aegypti* mosquito. Furthermore, YFV was determined to be filterable and mosquitoes that had been infected with YFV remained infective for the duration of their lives, which in some cases exceeded three months (Stokes *et al.*, 1997). In 1930, a mouse model was developed by Max Theiler, which subsequently led to the development of a neutralising antibody assay using mice infected with YFV. The presence of anti-YFV neutralising antibody in the serum of a patient injected into mice would neutralise YFV and permit survival against a lethal YFV challenge (Theiler, 1930; Sawyer & Lloyd, 1931). This assay facilitated the delineation of yellow fever endemic geographical regions by detection of neutralising antibodies against YFV in various populations, which subsequently led to an increased understanding of the epidemiology of YFV (Sawyer & Lloyd, 1931). The application of animal models greatly assisted the identification of mosquito species with the ability to transmit YFV between human and non-human primates. In 1928, Bauer proved that YFV can be transmitted by the bite of mosquitoes other than *A. aegypti* in Africa (Bauer, 1928) and later Davis and Shannon demonstrated transmission by mosquitoes other than *A. aegypti* in South America (Davis & Shannon, 1929). In 1930, three additional species of *Aedes* mosquitoes with the ability to transmit YFV were identified in West Africa (Philip, 1930).

In 1930, Theiler reported that serial passage of YFV in mice led to the attenuation of the virus in monkeys and rendered the monkeys immune to virulent strains of YFV (Theiler, 1930). Subsequently, attenuation of Asibi strain YFV was also achieved in cell culture with the modifications induced being attributed to the nature of the tissue used in the preparation of the growth media. Theiler and Smith, reported that serial passage of Asibi strain YFV in chick embryonic tissue, without the brain and spinal cord tissue, led to a substantial reduction in the neurotropic- and viscerotropic affinities of the virus (Theiler & Smith, 1937a). In 1937, Theiler and colleagues developed the live attenuated 17D vaccine prepared by serial passage of the wild-type Asibi strain in whole chick embryo (Theiler & Smith, 1937b). Around the same time the French neurotropic virus (FNV) vaccine, derived from the French viscerotropic virus (FVV) strain was prepared by serial passage in mouse brains. In 1980, production of the FNV vaccine was discontinued due to an abnormally high incidence of

vaccine-associated adverse events, especially encephalitis post-vaccination in children. Later the FNV vaccine-associated adverse events were attributed to the genomic instability of the vaccine strain virus due to the accumulation of changes at nucleotide level resulting in several amino acid substitutions. In mice, increase of the lethal dose $(LD)_{50}$ was also observed demonstrating a significant increase in the neurotropic affinity of the vaccine strain virus (Holbrook *et al.,* 2000).

Between 1960 and 1962 possibly the largest outbreak in yellow fever history was reported in Ethiopia. Initially, 15 000 deaths were attributed to yellow fever; however, after further investigation it was estimated that over 30 000 deaths and 200 000 cases were attributed to the outbreak (WHO, 1967). Later genetic studies revealed the possibility of the importation of the epidemic strain from the Democratic Republic of the Congo (formerly Zaire) (Lepineic *et al.*, 1994). Outbreaks in Africa have frequently been ascribed to the failure of vaccination schemes where a decline in immunisation coverage has occurred following absence of outbreaks in the preceding years. Subsequently, largely non-immune child populations existed in these areas, which caused the outbreaks mainly to affect children. Children often present with a less characteristic clinical picture as typically described for yellow fever leading to the delayed identification of these outbreaks (WHO, 1967).

Sequencing of the whole genome of the 17D strain YFV by Rice and colleagues in 1985 led to an increased understanding of YFV and the molecular basis for its virulence (Rice *et al.*, 1985). The complete genome sequence of the wild-type Asibi strain was obtained in 1987 by Hahn and colleagues. Comparative analysis of the wild-type Asibi strain and the 17D vaccine strain, derived from the Asibi strain, revealed 68 nucleotide differences throughout the YFV genome, which translated into 32 amino acid substitutions. The amino acid substitutions identified in the E protein, which may result in the alteration of receptor affinities, were implicated in the attenuation of the 17D strain as compared to the Asibi strain (Hahn *et al.*, 1987). In 2001, reports of vaccine-associated viscerotropic disease led to concern regarding the safety of the yellow fever vaccines. However, due to low rates of reporting of vaccine-associated viscerotropic disease, the high probability of contracting yellow fever in endemic areas and the highly efficacious nature of the vaccines the continuation of the yellow fever vaccines was warranted (Vasconcelos *et al.*, 2001b). YFV is still considered to be a major public health threat in yellow fever endemic areas, especially in West Africa with yellow fever outbreaks occurring annually (Stock *et al.*, 2013).

1.1.2 Yellow fever virus

YFV belongs to the genus *Flavivirus*, which was originally grouped within the *Togaviridae* family of viruses (Fenner, 1976); however, the genus *Flavivirus* was re-grouped into the family *Flaviviridae* (Calisher *et al.*, 1989). Flavivirus virions are small spherical enveloped virus particles, which are 37-50 nm in diameter and have icosahedral nucleocapsid symmetry (Schlesinger, 1980). YFV is a positive sense single stranded ribonucleic acid (RNA) virus approximately 11 kilobases (kb) in length that encodes a single polypeptide, which by co- and post-translational modification is translated into ten viral proteins. The encoded structural proteins include the capsid (C), membrane (M) and envelope (E) proteins and the non-structural (NS) proteins include the NS1, NS2A, NS2B, NS3, NS4A, NS4B and NS5 proteins (Rice *et al.*, 1985). The *Flavivirus* genome organisation is illustrated in Figure 1.1.

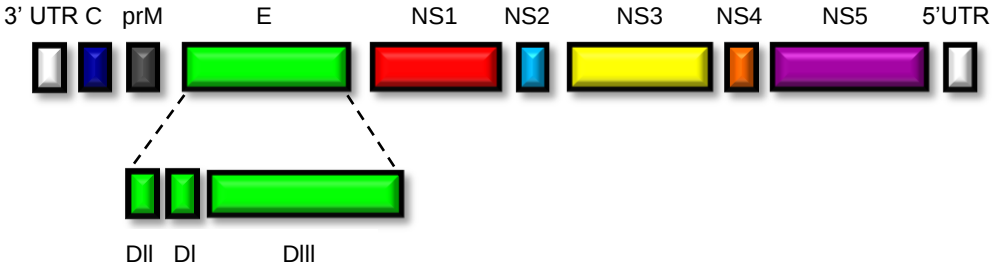

Figure 1.1: Representation of the *Flavivirus* genome organisation illustrating the encoded structural and non-structural proteins

The functions of all the encoded NS proteins have not been elucidated, but deductions as to the possible functions have been made based on mutagenesis, sequence homology and molecular modelling studies. The NS1 protein, localised in the perinuclear region, plays a role early in flavivirus RNA replication and pathogenesis with the glycosylation of the NS1 protein being essential to the functioning of the protein (Muylaert *et al.*, 1996). The NS1 protein has been shown to induce a protective response in non-human primates against fatal viral hepatitis (Schlesinger *et al.*, 1986). Although the function of the NS2A protein is not clear, the NS2A and NS3 proteins have been implicated in the assembly and/or release of infectious flavivirus particles, thus playing a role in virion maturation (Kümmerer & Rice, 2002). The NS2B and NS3 proteins have protease activity shown to be essential for viral replication. The dilution-insensitive cleavage of the NS2A-NS2B site is facilitated by the

protease activity of the NS2B protein, whereas the *cis*-acting site specific proteolysis of the NS2B-NS3 site is facilitated by the trypsin-like serine protease activity of the N-terminal functional domain of the NS3 protein (Gorbalenya *et al.*, 1989). The NS3 protein is divided into two functional domains, the N-terminal protease domain involved in the processing of NS viral proteins and the C-terminal helicase domain (Chambers *et al.*, 1990) involved in the unwinding of intermediates during RNA replication (Tan *et al.*, 1996). The NS4A protein may be essential for viral propagation due to its role in the stabilisation and localisation of the NS3 protein within the membrane. The levels of NS4A protein in infected cells regulate production of the NS5 protein, as well as the proteolytic processing of precursor protein. The NS4A protein has been shown to be essential for cleavage at the NS4B-NS5A site, but not cleavage at the NS5A-NS5B site (Tanji *et al.*, 1995). The NS4B protein is co-localised with the other NS proteins in the endoplasmic reticulum (ER) and is a component of the membrane-associated cytoplasmic replication complex (Hügle *et al.*, 2001). The NS5 protein is a nuclear phosphoprotein present in differentially phosphorylated states in virally-infected cells. The differential phosphorylation may play a role in the interaction observed between the NS3 and NS5 proteins and may also contribute to its function as part of the viral RNA replicase complex located in the ER membrane (Kapoor *et al.*, 1995). The NS5 protein can be divided into two functional domains, the N-terminal domain (NS5A) encoding a methyltransferase involved in viral RNA capping (Koonin, 1993) and the C-terminal domain (NS5B) encoding a RNA-dependent RNA polymerase. The NS3 and NS5 proteins have been shown to participate in flaviviral genome replication (Tan e*t al.*, 1996).

Virus particles are assembled from the expressed structural proteins and the C protein has been shown to be essential for virus packaging (Jones *et al.*, 2005). The E protein is the major antigenic protein of YFV (Vratskikh *et al.*, 2013) that elicits a protective neutralising antibody response (Brandriss *et al.*, 1990). Strain-, type- and Flavivirus group-specific epitopes have been identified on the E protein of YFV (Schlesinger *et al.*, 1984). The E protein accumulates in the nuclear-associated membrane (Ng *et al.*, 1983) and consists of three structural domains, designated domain I, II and III (Rey *et al.*, 1995), which corresponds to the three identified antigenic domains C, A and B, respectively (Mandl *et al.*, 1989). Domain III is an immunoglobulin (Ig)-like domain, which protrudes from the otherwise smooth surface and facilitates binding of flavivirus particles to host cell receptors (Rey *et al.*, 1995). All the major neutralising epitopes have been mapped to domain III of the E (ED-III) protein (Beasley & Barrett, 2002; Wu *et al.*, 2003; Sánchez *et al.*, 2005), which is the major antigenic domain of the E protein (Wu *et al.*, 2003) shown to be involved in receptor binding (Crill & Roehrig, 2001). Three epitopes have been identified within domain III as immunodominant epitopes targeted by T-cells post-immunisation with 17DD vaccine strain virus (de Melo *et*

al., 2013). Several studies of flavivirus ED-lll protein in mice have indicated the induction of both a cell-mediated and a humoral immune response, which protected immunised animals from a subsequent viral challenge. A predominantly T-helper (Th) 1 response characterised by interferon (IFN) γ and interleukin (IL) 2 release from stimulated cultured splenocytes and the production of IgG2a antibodies were elicited in response to immunisation with bacterially expressed West Nile virus (WNV) ED-lll protein. Furthermore, the immune response elicited was protective against a lethal WNV challenge and the antibodies were determined to have neutralising capability (Chu *et al.*, 2007). Chimeric tetravalent vaccines containing the ED-lll protein of dengue (DEN) serotypes 1, 2, 3 and 4 expressed in yeast and bacteria have proven effective at eliciting a tetravalent antibody response. However, the bacterially expressed chimeric protein elicited a moderate antibody response and was only partially protective against DEN-3 (Chen *et al.*, 2007; Etemad *et al.*, 2008). Cross-protection has been demonstrated in candidate vaccines developed against YFV and WNV using the E and ED-lll proteins, respectively. Brandriss and colleagues demonstrated protection against DEN-2 virus after immunisation with the YFV E protein thus illustrating the presence of cross-reactive antigenic determinants on the E protein with the potential to induce heterotypic neutralising antibodies (Brandriss *et al.*, 1990). Chu and colleagues demonstrated protection against Japanese encephalitis virus (JEV) after immunisation with WNV ED-lll protein thus illustrating that the cross-reactive antigenic determinants may be located on domain lll (Chu *et al.*, 2007).

1.1.3 Virus attachment, replication and release from yellow fever virus-infected cells

Cellular receptors are utilised by flavivirus particles to attach to host cells via the viral surface glycoprotein and gain entry into the host cell by receptor-mediated endocytosis. The interaction between heparan sulphate, a highly sulphated glycosaminoglycan, on the surface of target cells and the E protein of flavivirus particles have been shown to be essential for initial attachment and infectivity (Chen *et al.*, 1997). Antibody-mediated enhancement of viral replication in macrophages and macrophage-like cell lines that contain Ig Fc receptors has been demonstrated for flaviviruses. Including replication enhancement of 17D vaccine strain virus in the presence of the IgG fraction of serum obtained from 17D immunised individuals (Schlesinger & Brandriss, 1981). Antibody-mediated enhancement of viral replication has been shown to be caused by an increase in the efficiency of the internalisation process due to enhanced binding of virus to the cell surface, as well as the higher specific infectivity of antibody-opsonised virus particles (Gollins & Porterfield, 1984). Entry of single virus particles or aggregates of virus particles into the host cell is mediated by coated pits later identified as clathrin-coated pits, thus internalisation of flavivirus particles

occurs by the clathrin-mediated endocytic pathway (Gollins & Porterfield, 1985). Transport of the virus across the plasma membrane is facilitated by actin filaments and thereafter the virus is trafficked via the endosomal and lysosomal endocytic pathway with assistance from the microtubule network (Chu & Ng, 2004). Virus particles reside in uncoated pre-lysosomal vesicles prior to acid-catalysed membrane fusion brought on by the acidic environment. The acidic environment facilitates a conformational change resulting in the release of the viral nucleocapsid into the cytoplasm (Gollins & Porterfield, 1986b), which is subsequently trafficked to the ER (Chu & Ng, 2004). During the conformational change, the E protein present as heterodimers on the surface of virions will rearrange into a homotrimeric form (Stiasny *et al.*, 1996). The requirement for an acidic environment to facilitate the conformational change has been explained by the dependency on the protonation state of the E protein (Stiasny *et al.*, 2001). Fusion is dependent on the membrane composition, which will affect the pH facilitating membrane fusion (Gollins & Porterfield, 1986a). The flavivirus life cycle within an infected host cell is illustrated in Figure 1.2.

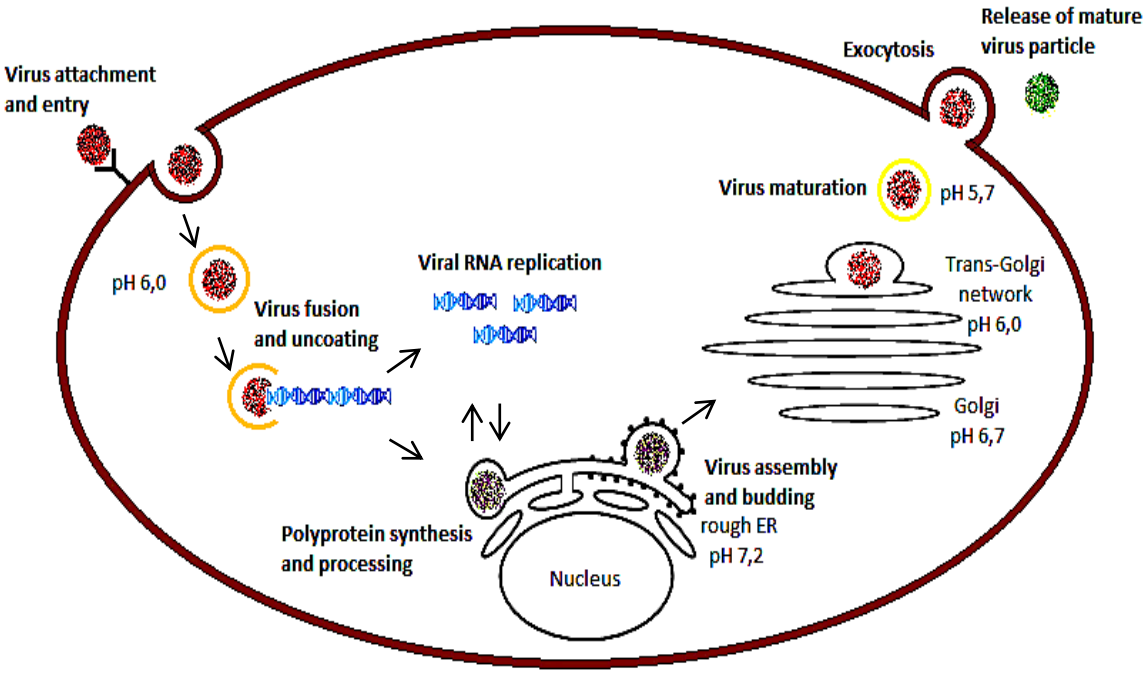

Figure 1.2: Illustration of the flavivirus life cycle within a host cell

Viral RNA synthesis and translation have been shown to occur in distinct areas of flavivirus-infected Vero cells (Ng *et al.*, 1983). Large virus specific proteins with molecular weights up to 250 000 kDa have been detected in the cell lysate of flavivirus-infected baby hamster

kidney (BHK) cells. The high molecular weight proteins were converted into smaller, more stable proteins, a process that was prevented by the inhibition of proteolysis, thus confirming the theory that large polypeptides are proteolytically cleaved into smaller functional proteins (Cleaves, 1985). Replication of flaviviruses occurs in the cytoplasm and is membrane-associated (Chu & Westaway, 1992). A semi-conservative asymmetric replication cycle is followed by flaviviruses, thus utilising a negative strand intermediate transcribed from the positive strand as a template for the production of additional positive strand viral RNA. Positive and negative strand synthesis occurs in parallel; however, the ratio of synthesised positive strand viral RNA to negative strand viral RNA increases throughout the course of infection (Lindenbach & Rice, 1997). The 3' untranslated region (UTR) consists of a conserved and a variable region with the conserved region playing an essential role in virus proliferation, virulence and viability (Mandl *et al.*, 1998). The infectivity of flaviviruses is affected by the efficiency of the translation of synthesised viral RNA (Edgil *et al.*, 2003). The viral replication complex is believed to consist of the NS1, NS2A, NS3, NS4A and NS5 proteins (Khromykh *et al.*, 2000), and is assembled at the cytoplasmic membrane in vesicle packets (Mackenzie *et al.*, 1996). Genome RNA contained in the viral core of flaviviruses has been shown to be directly accessible for translation (Koschinkski *et al.*, 2003).

Virus particles are assembled in the lumen of the rough ER and are transported to the Golgi-apparatus in individual vesicles via the secretory pathway facilitating virion maturation (Mackenzie & Westaway, 2001). The pre-membrane (prM) protein, the glycosylated precursor of the M protein, and the E protein associate to form immature intracellular virus particles (Wengler & Wengler, 1989). Immature virus particles are protected by the prM and E proteins from structural rearrangements during transport through the trans-Golgi network (Allison e*t al.*, 1995). During release, the prM protein undergoes proteolytic cleavage resulting in the dissociation of the heterodimers into three molecules with the E and M proteins remaining associated with the viral membrane (Wengler & Wengler, 1989). The conformational change into a homotrimeric form is induced by exposure to an acidic pH below 6,5 (Allison *et al.*, 1995). The conformational change has been hypothesised to facilitate fusion of the endosomal and viral membrane resulting in the formation of mature virus particles (Rey *et al.*, 1995). Cleavage of the prM protein during the release of virus increases the infectivity of virus particles, which is approximately 60-fold higher than the infectivity of immature virus particles (Wengler & Wengler, 1989). Furin, a component of the constitutive secretory pathway, mediates the cleavage of the prM protein, thereby facilitating the maturation of virus particles (Stadler *et al.*, 1997). Genome packaging is coupled to RNA replication (Khromykh *et al.*, 2001) and, in 17D vaccine virus infected Vero cells, newly synthesised nucleocapsids were located in the perinuclear region situated in inclusion

bodies. The host secretory pathway is utilised by nascent virus particles for maturation and subsequent release (Ishak *et al.*, 1988).

1.1.4 Genetic, antigenic and serological relatedness of yellow fever virus strains

Genetic characterisation of flaviviruses was initially performed using oligonucleotide fingerprinting, which facilitated the identification of distinct "topotypes" or geographical variants. Deubel and colleagues not only showed that YFV strains from Africa and South America were genetically distinct, but could also differentiate between West and East/Central African strains leading to the identification of two topotypes of YFV in Africa (Deubel *et al.*, 1986).

Subsequent genetic analysis by nucleotide sequence determination has revealed five genotypes in Africa, including the East and Central African genotype, West African genotypes I and II, the East African genotype and the Angola genotype (Deubel *et al.*, 1986; Chang *et al.*, 1995; Wang *et al.*, 1997; Mutebi *et al.*, 2001). The East and Central African genotype has been proposed to exist in an enzootic transmission cycle and circulates in the Central African Republic, the Democratic Republic of Congo, Ethiopia, Sudan and Uganda (Mutebi *et al.*, 2001). The West African genotype I circulates in Cameroon, Gabon, Ivory Coast, Nigeria and one strain circulates in Senegal, whereas West African genotype II circulates in Burkina Faso, Ghana, Guinea, Guinea-Bissau, Ivory Coast and Mali (Lepineic *et al.*, 1994; Mutebi *et al.*, 2001; Stock *et al.*, 2013). Strains belonging to West African genotype I were more heterogeneous compared to strains belonging to West African genotype II. The higher heterogeneity of the West African genotype I strains was attributed to regular human epidemics in the regions of circulation, whereas the West African genotype II has been proposed to exist in an enzootic transmission cycle (Mutebi *et al.*, 2001). West African genotypes I and II have been shown to co-circulate in Ivory Coast (Lepineic *et al.*, 1994; Stock *et al.*, 2013). The East African genotype circulates in Kenya and Uganda (Chang *et al.*, 1995), whereas the Angola genotype has only been found to circulate within Angola (Mutebi *et al.*, 2001). The Angola71 strain, within the Angola genotype, may have evolved independently as this strain is genetically highly divergent from other East and Central African strains of YFV. Despite the demonstration of extensive nucleotide divergence in strains of YFV in Africa the deduced amino acid sequences had a high degree of homology, ranging between 91,9 and 100%. Although the evolutionary rate for the different genotypes in Africa was shown to be similar, the genotypes were shown to have evolved independently in the respective geographical regions (Mutebi *et al.*, 2001).

In South America, two genotypes have been identified, including the South American genotypes I and II (Deubel *et al.*, 1986; Wang *et al.*, 1997). The South American genotype I mainly circulates in Brazil, Ecuador and Panama, whereas the South American genotype II mainly circulates in Peru and Trinidad (Wang *et al.*, 1997). The spread of predominantly South American genotype 1 strains throughout Central and South America occurred after introduction into Brazil, whereas South American genotype II has mostly remained confined to the western Brazilian Amazon, Bolivia and Peru (Nunes *et al.*, 2012). The number of YFV-specific repeat sequences (RYF's) located within the 3' non-coding region (NCR) were shown to be different for West African genotypes, South American genotypes and East and Central African genotypes. Differences in the RYF's between different genotypes were attributed to selective pressures; however, the selective advantages as yet are unknown (Wang *et al.*, 1997). Introduction of YFV into South America from West Africa has been genetically substantiated (Chang *et al.*, 1995; Wang *et al.*, 1996). High genetic stability has been observed for YFV strains with only minor variations occurring with time (Deubel *et al.*, 1986; Lepineic *et al.*, 1994; Stock *et al.*, 2013). These minor variations may be due to selection pressure by the host and/or vector (Deubel *et al.*, 1986).

The genus *Flavivirus* is divided into eight antigenic complexes, including the Japanese encephalitis, Ntaya, Tyuleniy, Uganda S, dengue, Modoc, Rio Bravo and tick-borne encephalitis antigenic complexes, based on serological cross-reactivity due to the sharing of closely related epitopes on the surface on the E glycoprotein. YFV was not assigned to an antigenic complex due to a lack of significant serological cross-reactivity with other flaviviruses (Calisher *et al.*, 1989). Although demonstrable antigenic differences have been identified between African and South American strains of YFV, viruses from each geographical type have been shown to maintain their antigenic identity. The antigenic diversity observed between YFV strains from Africa and South America may be related to the high degree of amino acid diversity between African and South American strains. Complete antigenic identity was maintained in the 17D- and FNV vaccine strains when compared to the Asibi- and FVV parent strains, respectively, indicating that the attenuation of vaccine strain virus did not affect the antigenic identity of the vaccine strain virus (Clarke, 1960). The slow evolutionary rate demonstrated by the genetic stability of the YFV genome may explain the antigenic stability of the virus.

1.1.5 Epidemiology, prevalence and transmission of yellow fever virus

YFV is endemic in the sub-tropical and tropical regions of Africa and South America, respectively (WHO, 1953). The yellow fever endemic region in Africa is inhabited by

approximately 500 million residents and is located 15° north to 15° south of the equator (Mutebi & Barrett, 2002). Areas at risk for yellow fever transmission are illustrated in Figure 1.3.

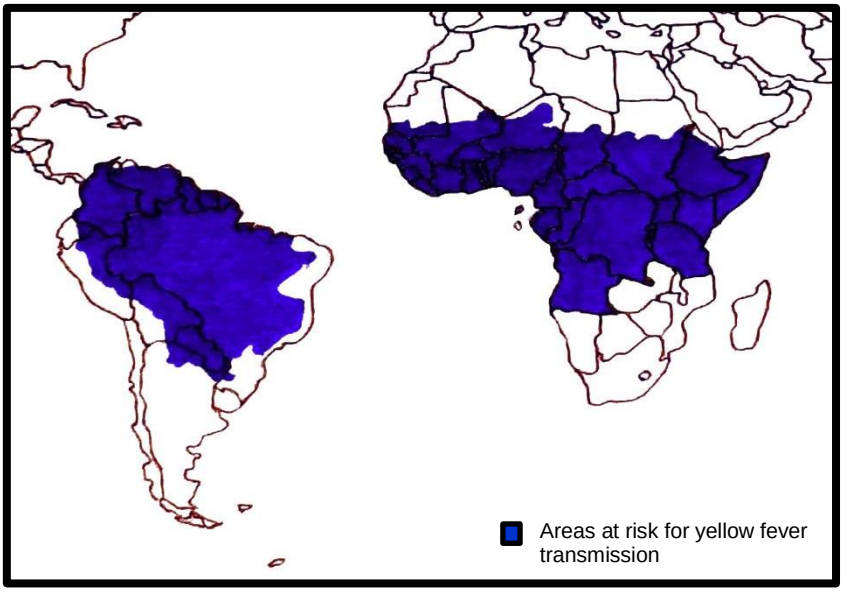

Figure 1.3: Map illustrating countries containing YFV endemic regions

In the 1990's, the World Health Organisation (WHO) estimated the annual prevalence of yellow fever to be 200 000 cases and 30 000 deaths (WHO, 1992); however, more recently YFV has been estimated to cause 51 000 to 380 000 severe cases and 19 000 to 180 000 deaths in Africa annually. The estimated prevalence of YFV in Africa for 2013 was 130 000 cases with fever and haemorrhage or jaundice and 78 000 deaths (Garske *et al.*, 2014). YFV generally has a fatality rate of 20% (Monath, 1999); however, higher fatality rates have been reported (Vasconcelos *et al.*, 2001c). Increases in the prevalence of yellow fever has been attributed to a substantial increase in urbanisation, deforestation, irrigation, ecological changes, a lack of piped water, proper water storage in homes, as well as the invasion of mosquito habitation by man (WHO, 1985). Seasonal changes including changes in the temperature and rainfall also affect the prevalence of yellow fever (Vasconcelos *et al.*, 2001a). However, recent mass vaccination campaigns initiated by the Global Alliance for Vaccines and Immunisation (GAVI) Alliance have contributed to a 27% decline in prevalence in Africa for 2013 (Garske *et al.*, 2014).

In 1942, the International Subcommittee on Viral Nomenclature endorsed the use of the term arbovirus, which refers to viruses maintained in nature due to the ability to proliferate in

arthropod vectors, which transmit the virus between vertebrate hosts. YFV is an arbovirus and transmission to humans, considered to be dead-end hosts, is mostly incidental. The geographical distribution of an arbovirus is dependent on the presence of competent insect vectors and vertebrate species with the ability to act as a reservoir for the virus in specific geographical areas (WHO, 1985). YFV is primarily transmitted by the bite of infected female *A. aegypti* mosquitoes (Reed & Carroll, 1902); however, several other mosquito species have also been implicated in the dissemination of YFV to human and non-human primates (Shannon *et al.*, 1938; Unknown, 1944). The three transmission cycles for YFV in Africa and South America are illustrated in Figure 1.4.

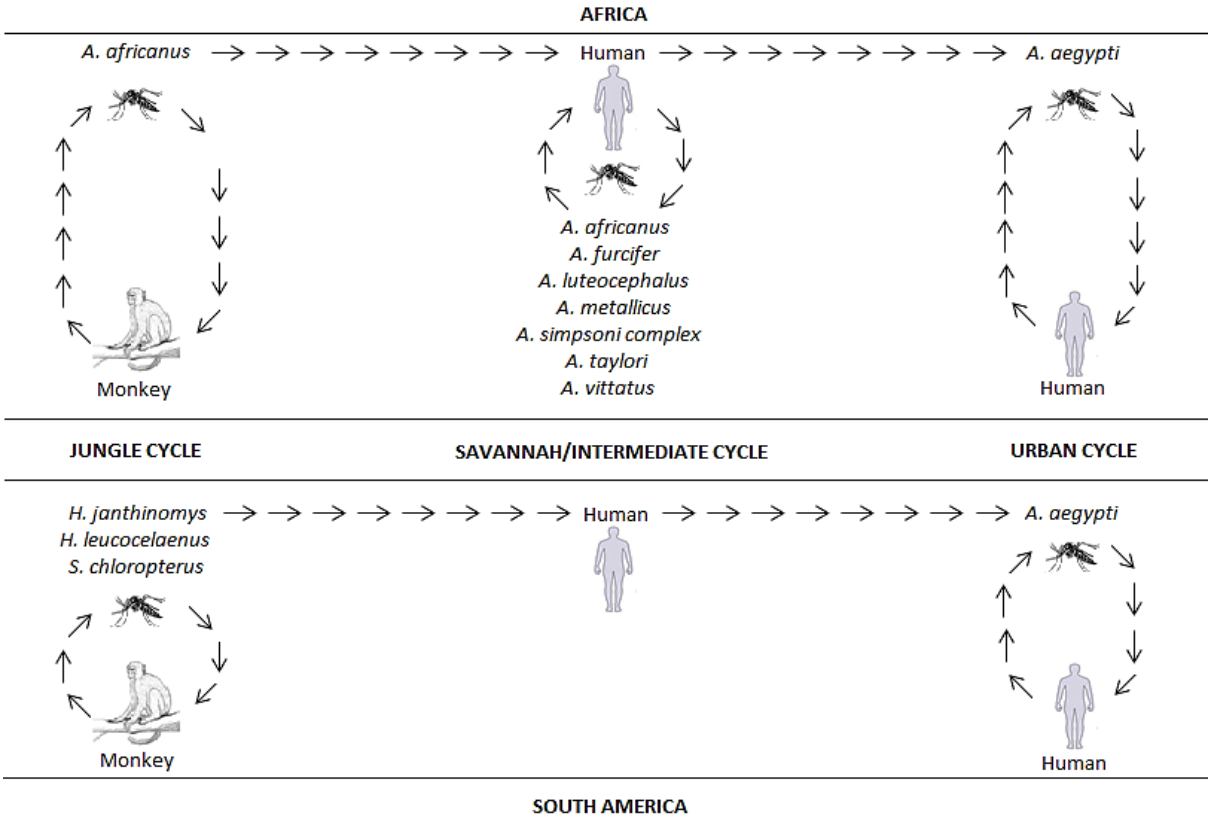

Figure 1.4: Transmission cycles of YFV in Africa and South America

Three transmission cycles have been identified for YFV, including the jungle-, savannah/intermediate- and the urban transmission cycle. Jungle yellow fever is primarily transmitted by *A. africanus* mosquitoes in the tropical jungles of Africa (Haddow *et al.*, 1948) and mosquito species of the *Hemagogus* and *Sabethes* genera in South America (Shannon *et al.*, 1938). Jungle yellow fever is transmitted in non-residential areas and is more

common in young men (Soper, 1936). The jungle cycle is maintained by transmission of YFV between mosquitoes and non-human primates (Haddow *et al.*, 1948). Interruption of the jungle cycle causes sporadic cases of yellow fever in humans and rarely leads to large outbreaks (Mutebi & Barrett, 2002). Antibodies to YFV have been isolated from opossums (*Didelphis marsupialis*) indicating that other small mammals may be involved in maintaining YFV in the jungle cycle (Unknown, 1944). Vaccination has proven to be moderately effective in controlling YFV in the jungle cycle (Monath, 1999). The savannah/intermediate transmission cycle is only present in the moist savannah of Africa in small villages and farmland.

In the savannah/intermediate transmission cycle, a high risk for yellow fever epidemics exists due to increased potential transmission to humans (Mutebi & Barrett, 2002). Mosquito vectors involved in the transmission of YFV in the savannah/intermediate cycle include *A. metallicus*, *A. luteocephalus*, *A. taylori*, *A. furcifer, A. vittatus* (Germain *et al.*, 1980), members of the *A. simpsoni complex* (Haddow *et al.*, 1948) and *A. opok* (Mutebi & Barrett, 2002).

In the urban transmission cycle, YFV is transmitted to humans by the bite of infected *A. aegypti* mosquitoes (Mutebi & Barrett, 2002) and effective mosquito control has proven to reduce the number of urban yellow fever cases (Soper, 1936). The potential risk for explosive outbreaks is greatest in the urban transmission cycle due to human to human transmission of YFV by the bite of an infected *A. aegypti* mosquito (Mutebi & Barrett, 2002). However, due to the low level viraemia experienced in humans, which is approximately a 100-fold less than in patients infected with DEN virus, a flavivirus also transmitted by infected *A. aegypti* mosquitoes, YFV is not efficiently transmitted by *A. aegypti* mosquitoes to other potential human hosts (Monath, 1999). In Africa, mosquito control measures are complicated due to the presence of *A. aegypti* mosquitoes in the jungle and not only in human housing (WHO, 1967).

Eradication of YFV is improbable due to the existence of non-human primates that serve as amplifying hosts of the virus, thus maintaining YFV in nature (Soper, 1936) and due to mosquitoes remaining infected life-long. Vaccination is the most effective strategy to prevent transmission of YFV; however, vaccination coverage of up to 90% may be required to establish herd immunity within a population and subsequently prevent transmission of YFV from human to human by mosquitoes (Monath, 1999).

1.1.6 Clinical presentation, diagnosis and treatment of yellow fever

Yellow fever may manifest in a spectrum of clinical presentations ranging from mild to severe infection, frequently characterised by jaundice, haemorrhage and renal failure (Jones & Wilson, 1972). A short period of remission generally on the third or fourth day after the onset of symptoms separates the two-phase development of yellow fever. Infection is initiated by the sudden onset of non-specific symptoms referred to as the "infectious" phase followed by hepatorenal dysfunction and haemorrhage referred to as the "toxic" phase (WHO, 1986; ter Meulen *et al.*, 2004). The two-phase development of yellow fever is illustrated in Figure 1.5.

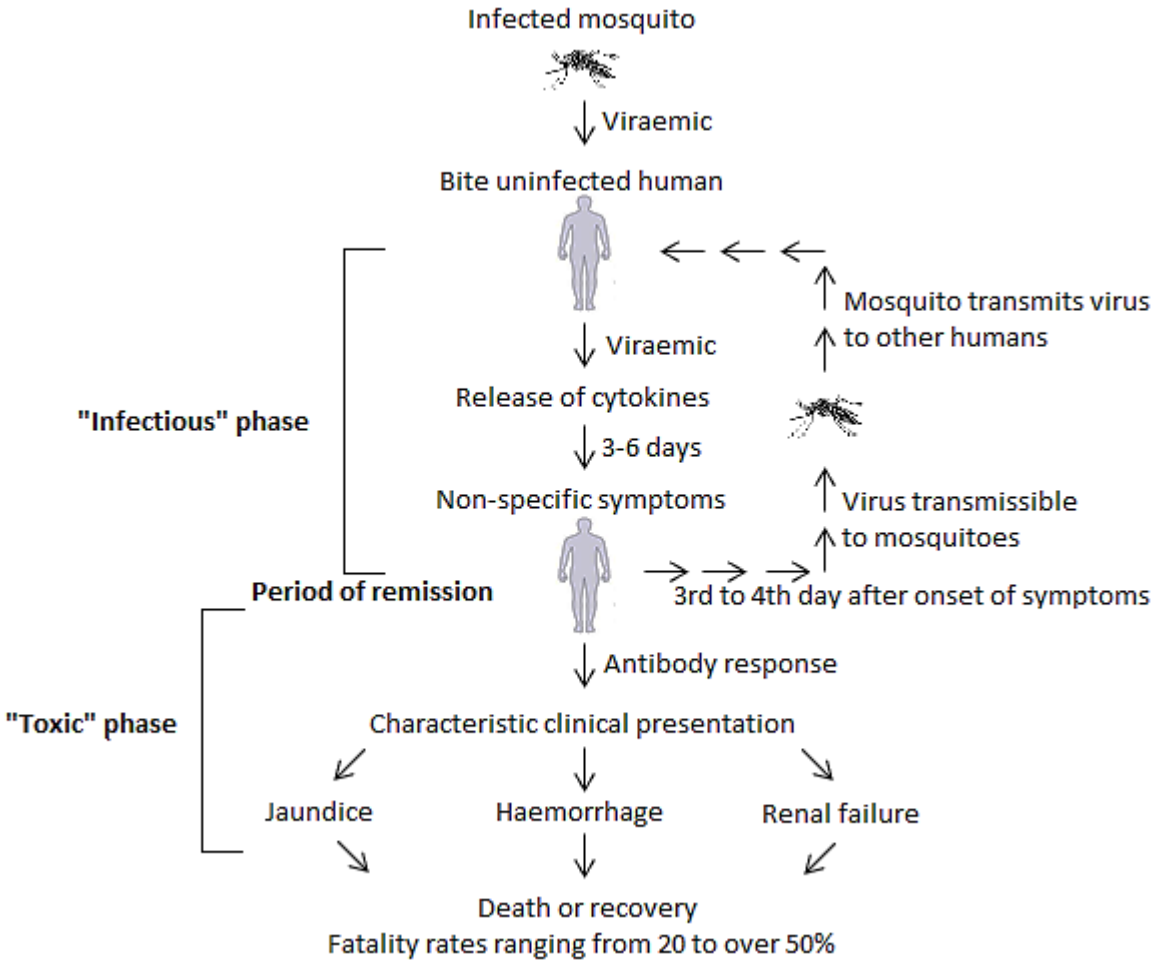

Figure 1.5: Two-phase development of yellow fever

During the "infectious" phase, YFV is present in the blood of infected individuals (WHO, 1986) and non-specific symptoms observed may be due to immune activation and the release of cytokines (ter Meulen *et al.*, 2004). After a short period of remission, approximately 15% of patients, progress to the "toxic" phase characterised by declining

viraemia and the appearance of virus-neutralising IgM antibodies. Exacerbation of disease in the "toxic" phase may be due to virus-antibody complexes, the release of cytokines and the activation of the complement and cytotoxic T-lymphocytes (CTL's) (Monath & Barrett, 2003). YFV generally has an incubation period of three to six days after the bite of an infected mosquito before the onset of symptoms (WHO, 1986). However, this incubation period may vary depending on the route of transmission, the amount of virus transmitted, host resistance, viral virulence and the degree of immunity of the host (Smetana, 1962).

During a large outbreak in Nigeria in 1969 the average duration of illness was determined to be 6,4 days for fatal cases and 17,8 days for non-fatal cases. The most common symptoms of yellow fever during this outbreak were fever, jaundice, haemorrhage, headaches, haematemesis (black vomit), abdominal pain, agitation and lower back pain. Whereas the less common symptoms included diarrhoea, hiccoughs, melaena, bleeding gums and epistaxis. Scleral icterus and bile pigments in the urine were noted in 95% of patients. Symptoms most commonly associated with fatal cases of yellow fever, included haemorrhage which led to haematemesis (black vomit), melaena, bleeding from intravenous (IV) infusions and haematomata in the deltoid muscles, as well as anuria, hiccoughs, renal failure and central nervous system involvement (Jones & Wilson, 1972).

An accurate diagnosis is difficult to make based on the clinical presentation of yellow fever infection due to many non-specific symptoms (Smetana, 1962) and similar symptoms caused by other microbiological agents. The differential diagnosis includes typhoid fever, influenza, rickettsial infection and other arboviral fevers that present with symptoms similar to yellow fever without jaundice. Special consideration should be given to the differentiation between yellow fever with jaundice and other diseases with hepatorenal dysfunction and/or other haemorrhagic manifestations, which may include malaria, viral hepatitis, other viral haemorrhagic fevers (Lassa fever, Marburg and Ebola virus disease, Rift Valley fever and Crimean-Congo haemorrhagic fever), infectious mononucleosis with jaundice and leptospirosis (WHO, 1986). Histopathological examination on liver biopsy is performed to determine the presence of diagnostic markers of damage to the liver during autopsy; however, needle biopsies of the liver combined with fluorescent antibody detection of viral antigen may be more useful for early detection of YFV (Smetana, 1962). Immunocytochemical staining of fixed human liver sections can be used to detect yellow fever antigens in post-mortem examination by using monoclonal anti-E protein antibodies; however, ante-mortem diagnosis is preferable. During the viraemic phase viral RNA can be detected in patient sera by reverse-transcriptase polymerase chain reaction (RT-PCR) or virus can be isolated in cell culture; however, if serum samples weren't stored correctly virus isolation may be compromised. The use of semi-nested polymerase chain reaction (PCR)

has been shown to improve the specificity and sensitivity for the detection of YFV viral RNA (Deubel *et al.*, 1997). Serodiagnosis of IgG and IgM antibodies against YFV can be accomplished by an indirect immunofluorescence assay (IFA), an enzyme-linked immunosorbent assay (ELISA) and neutralising antibodies can be detected by a plague reduction neutralisation test (PRNT) (Niedrig *et al.*, 2008; Vázquez *et al.*, 2003).

The treatment for yellow fever consists of supportive care by the replacement of fluid, electrolytes and the acid-base balance (Monath, 2005), as well as the administration of prophylactic antibiotics to prevent the development of pneumonia, which is common in yellow fever patients (Jones & Wilson, 1972). Treatment for hypotension and shock should also be administered (Monath, 2005). The antiviral activity of various agents against YFV has been determined in YFV-infected cell culture, hamsters and rhesus monkeys. However, the majority of agents with anti-YFV properties require administration prior to virus adsorption to host cells, thus limiting the efficacy of these agents for treatment of yellow fever patients (Neyts *et al.*, 1996; Ono *et al.*, 2003).

1.1.7 Yellow fever virus vaccines and adverse events

YFV is considered to be a major public health threat in endemic areas despite the availability of live attenuated vaccines. The 17D yellow fever vaccine was prepared in 1937 by serial passage of wild-type YFV Asibi strain in chick embryo (Theiler & Smith, 1937b) and is still in use today. In 1987, the complete genome sequences obtained from the 17D vaccine strain and the wild-type Asibi strain were compared. Sixty-eight nucleotide substitutions were identified that resulted in 32 non-synonymous amino acid substitutions. Most of the non-synonymous amino acid substitutions were located within the NS2A and NS2B coding regions that resulted in 3% and 2,3% amino acid divergence, respectively. The E protein coding region had an amino acid divergence of 2,4% as compared to the wild-type Asibi strain virus. Amino acid substitutions within the E protein were considered to influence attenuation of the 17D vaccine strain virus. The changes may affect the binding of virus to host cell receptors, which in turn may account for a reduction in the neuro- and viscerotropism of the 17D vaccine strain virus (Hahn *et al.*, 1987). Viscerotropic attenuation of the 17D vaccine strain virus due to enhanced glycosaminoglycan binding, as well as virus dissemination and virulence have been attributed to changes in domain lll of the E protein (Lee & Lobigs, 2008).

The simultaneous initiation of the activation and modulation pathways associated with the cell-mediated and humoral immune responses, thought to play a role in preventing adverse events and death associated with vaccination, has been demonstrated in 17DD vaccinated

individuals (Martins *et al.*, 2007). Individuals vaccinated with the 17D vaccine strain virus experience low viraemia followed by a long lasting immune response characterised by yellow fever specific T-cell and neutralising antibody responses (Reinhart *et al.*, 1998; ter Meulen *et al.*, 2004; Barba-Spaeth e*t al.*, 2005). Post-immunisation, increased markers of T-cell activation and activation of $CD8^+$ T-cells have been reported (Reinhart *et al.*, 1998; ter Meulen *et al.*, 2004), and may play a role in viral suppression early in infection (Reinhart *et al.*, 1998; Gaucher *et al.*, 2008). In addition, the release of tumour necrosis factor (TNF)-α (Hacker *et al.*, 1998), likely facilitates the maturation of dendritic cells (DC's), a process that protects cells from infection by YFV (Barba-Spaeth e*t al.*, 2005). Neutralising antibodies elicited in response to vaccination with the 17D vaccine have been demonstrated to persist for 30 years and longer (Poland *et al.*, 1981). Neutralising antibodies have been determined to be the correlate of protection against yellow fever infection and a neutralising antibody titre of 40 or more as determined by a $PRNT_{50}$ has been determined to confer protection against a lethal YFV challenge in mice (Julander *et al.*, 2011). Antibodies elicited by the 17D vaccine strain virus have been shown to rarely cross-react with DEN-1 (Reinhart *et al.*, 1998).

Recently, possible transmission by breastfeeding was reported for the live attenuated yellow fever vaccines after the identification of vaccine strain virus in two infants with meningoencephalitis post-vaccination. However, breast milk was not available for testing (CDC, 2010b; Kuhn *et al.*, 2011). West Nile viral RNA, as well as WNV-specific IgM and IgG antibodies have been detected in breast milk (CDC, 2002). Therefore, vaccination has been contraindicated in lactating women by the Advisory Committee on Immunisation Practices (ACIP) except when travel to high risk yellow fever endemic areas cannot be circumvented (Cetron *et al.*, 2002). Transmission of yellow fever vaccine virus through blood transfusion has also been confirmed (CDC, 2010a). The administration of yellow fever vaccines are contraindicated in immunocompromised individuals, pregnant and lactating women, individuals with hypersensitivity to eggs (Cetron *et al.*, 2002) or chicken (Staples *et al.*, 2010), infants younger than 6 months of age (WHO, 1998), individuals with thymic disorders or that had a thymectomy (Barwick & Yellow Fever Vaccine Safety Working Group, 2004), individuals with human immunodeficiency virus (HIV) or acquired immunodeficiency syndrome (AIDS), individuals on immunosuppressive therapies (Staples *et al.*, 2010) and the elderly, including individuals older than 65 years of age (Martin *et al.*, 2001b).

Adverse events have been associated with the administration of yellow fever vaccines, including the most common serious adverse event, vaccine-associated neurotropic disease (CDC, 2002) and the more recent rare vaccine-associated viscerotropic disease (Chan *et al.*, 2001; Doblas *et al.*, 2006; Gerasimon & Lowry, 2005; Martin *et al.*, 2001a; Vasconcelos *et*

al., 2001b). Due to the risk of developing encephalitis or vaccine-associated neurotropic disease, vaccination in infants younger than 9 months of age has been contraindicated by the Food and Drug Administration (FDA) (Cetron *et al.*, 2002). Rare vaccine-associated viscerotropic disease is a serious, frequently fatal, multisystemic disease, which typically develops within 2-5 days of vaccination independent of the vaccine strain or manufacturer (Martin *et al.*, 2001a; Vasconcelos *et al.*, 2001b). Vaccine-associated viscerotropic disease is characterised by dysfunction of the lungs, liver, kidneys and the central nervous system, as well as thrombocytopaenia (Martin *et al.*, 2001a; Vasconcelos *et al.*, 2001b). Some typical characteristics associated with wild-type yellow fever infection are absent or altered during vaccine-associated viscerotropic disease, including the absence of bradycardia, leucopaenia or neutropaenia, only mildly raised urine protein and hepatic aminotransferase concentration and less prominent haemorrhage (Martin *et al.*, 2001a). Several risk factors for the development of vaccine-associated adverse events have been identified, including advanced age and autoimmune disease (Martin *et al.*, 2001b; Seligman *et al.*, 2014).

Martin and colleagues suggested that yellow fever virions of altered virulence may be the cause of the vaccine-associated neurotropic- and viscerotropic disease due to the presence of minor virion subpopulations or quasispecies of YFV in the vaccine virus. The minor virion subpopulations or quasispecies may have the ability to replicate within the host thereby revealing the neurotropic- and viscerotropic potential of the parent virus (Martin *et al.*, 2001a). However, these subpopulations have not been detected to a significant extent in investigated cases of viscerotropic disease post-vaccination (Whittembury *et al.*, 2009). Susceptibility of the host may also play a role in the development of these adverse events (Martin *et al.*, 2001a) and increased susceptibility may be attributed to a genetic predisposition conferred by a single genetic variation or a combination of genetic variations (Whittembury *et al.*, 2009). Possible involvement of the 2'-5' oligoadenylate synthetase (Oas) 1 gene at increasing the risk of developing vaccine-associated viscerotropic disease was investigated by Belsher and colleagues due to the association of the Oas1b gene with the susceptibility of mice to flaviviruses (Perelygin *et al.*, 2002). Belsher and colleagues isolated and sequenced selected genes in the patient genomes and determined that p46 will be produced (Belsher *et al.*, 2007). Through computer modelling (Torshin, 2005), p46 was predicted to have impaired enzymatic function, thus possibly reducing the ability to inhibit replication of RNA viruses and allowing the virus to reach high levels within the host. However, this conclusion has not been supported by experimental data (Belsher *et al.*, 2007) and no abnormalities in the Oas1 or Oas2 genes were found in another case patient (Pulendran *et al.*, 2008). An additional unexpected characteristic in various patients that developed vaccine-associated viscerotropic disease were abnormally high neutralisation

titres, which reached as high as 10 240, exceeding neutralising antibody titres associated with vaccination, which rarely reaches 320 (Martin *et al.*, 2001a; Pulendran *et al.*, 2008). The robust adaptive immune response was attributed to persistent viraemia and the development of vaccine-associated viscerotropic disease could therefore not be attributed to an insufficient adaptive immune response, which included antigen-specific B- and T-cell responses (Pulendran *et al.*, 2008). Sequence analysis of vaccine strain virus in cases of vaccine-associated viscerotropic disease has not substantiated reversion to virulence (Galler *et al.*, 2001; Martin *et al.*, 2001a; Whittembury *et al.*, 2009). Low rates of reporting of serious adverse events have been described for the 17D and 17DD yellow fever vaccines (Thomas *et al.*, 2013), which may be attributed to the restricted replication noted in vaccine strains. Martin and colleagues suggested that the prevalence of the adverse events may be underestimated due to difficulty with adverse events surveillance and masking of adverse events by wild-type yellow fever in yellow fever endemic areas (Martin *et al.*, 2001a), especially considering that vaccine-associated viscerotropic disease resembles wild-type yellow fever infection (Vasconcelos *et al.*, 2001b). In a study to determine the genetic divergence and distribution of YFV strains throughout Brazil by nucleotide sequence determination, vaccine strain virus was detected in a patient previously considered to have died from wild-type yellow fever infection in 1975. This patient was vaccinated five days prior to the onset of symptoms (Vasconcelos *et al.*, 2004). The isolated strain, designated Brazil75, was further analysed to identify any virus-related factors that may contribute to the development of vaccine-associated viscerotropic disease. Many of the amino acid substitutions identified were conserved among the yellow fever vaccine strains. However, two unique amino acids substitutions M-49 (isoleucine (I) → leucine (L)) and NS4B-240 (tyrosine (Y) → phenylalanine (F)) were identified, which were not conserved in yellow fever vaccine or wild-type strains. Phenotypically the Brazil75 and 17DD vaccine strain, most closely related to Brazil75 strain, were identical with no alterations observed *in vitro* in cell culture or *in vivo* in hamsters (*Mesocricetus auratus*) (Engel *et al.*, 2006).

An inactivated candidate vaccine against YFV, designated XRX-001, has been prepared by inactivation of 17D vaccine strain virus using β-propiolactone. Inactivated virus was subsequently adsorbed to aluminium hydroxide and administered by the intramuscular (IM) or subcutaneous routes. XRX-001 was highly immunogenic in mice, hamsters and cynomolgus macaques with the induction of a neutralising antibody response. Hamsters immunised with a single dose of XRX-001 were protected from a lethal challenge (Monath *et al.*, 2010). Subsequently, a double-blind, placebo-controlled, dose-escalation, phase 1 trial was initiated in healthy human volunteers. All subjects were immunised by the IM route with a higher 4,8µg or a lower 0,48µg dose of antigen. All subjects immunised with a higher dose

of inactivated vaccine developed neutralising antibody, and a positive correlation between the dose administered and the neutralising antibody titre was observed. However, a high number of individuals reported injection-site adverse events post-immunisation, which primarily included tenderness, mild pain and itching at the site of injection. One patient immunised with the higher vaccine dose developed utricaria three days post-immunisation. The high rate of adverse events may be related to the co-administration of aluminium hydroxide, an adjuvant (Monath *et al.*, 2011).

1.1.8 DNA vaccines

Although there have been numerous vaccination strategies explored thoughout history within the scopy of this study attention will given to deoxyribonucleic acid (DNA) vaccines. Immunisation strategies with DNA were first explored after the demonstration that protein expression occurred in muscle cells after immunisation with RNA and DNA constructs (Wolff *et al.*, 1990). Plasmid DNA encoding an influenza viral protein has been shown to elicit CTL responses (Ulmer *et al.*, 1993), which have been shown to play an essential role in the clearance of a viral infection (Matloubian *et al.*, 1994). CTL responses are generally elicited due to endogenous expression of an antigen, similar to that observed in virus infection, thus DNA immunisation mimics natural infection with regards to the intracellular expression of the encoded antigen (Ulmer *et al.*, 1993). Fynan and colleagues evaluated the efficiency of different routes of inoculation at eliciting immune responses in mice using DNA plasmids encoding the influenza virus haemagglutinin (H) glycoproteins H1 and H7. Administration of plasmid DNA by the IM and IV routes was shown to be the most effective parenteral routes of inoculation. DNA drops administered to the nares and trachea of mice were shown to be effective at eliciting an immune response, thus also enabling vaccination by mucosal routes against respiratory pathogens. The most efficient DNA immunisations were achieved by gene gun delivery of DNA-coated gold beads to the epidermis of mice. The routes of inoculation with the highest survival rates in mice were immunisation by the IM route and gene gun administration of DNA (Fynan *et al.*, 1993). In 1995, the first human trial for a DNA vaccine was initiated and the DNA vaccine against HIV elicited CTL and antibody responses with no reported adverse events. However, the magnitude of the immune response elicited was not satisfactory (MacGregor *et al.*, 1998). DNA vaccines against several intracellular pathogens have been shown to have the ability to elicit a major histocompatibility complex (MHC) class l restricted CTL memory response in humans (Calarota *et al.*, 1998; MacGregor *et al.*, 1998; Wang *et al.*, 1998). The weak immunogenicity in humans compared to smaller animal models have been attributed to insufficient hydrostatic pressure in muscle cells due to the relative volume of the inoculum compared to the mass of the muscle. In other words,

the volume of inoculum is large compared to the small tibialis anterior muscle of a mouse, whereas the volume of inoculum is small compared to the large muscle of a human (Dupuis *et al.*, 2000). A DNA vaccine against influenza virus with the ability to elicit a high level of protein expression have been shown to protect against a lethal viral challenge (Montgomery *et al.*, 1993), therefore several approaches were examined to enhance the expression of protein after immunisation. The most efficacious approaches included modification of the heterologous gene, polyadenylation and transcriptional termination sequences, as well as plasmid backbone elements (Hartikka *et al.*, 1996). Neonates are more susceptible to infection due to the inability to mount a strong T-cell response; however, DNA vaccines targeting a Sendai viral protein and a truncated tetanus toxin have been shown to elicit Th1 and Th1/Th2 responses, respectively, and a CTL response in puppies (Martinez *et al.*, 1997). DNA-based vaccines have also been shown to confer protective immunity against hepatitis B virus in new born chimpanzees (Prince *et al.*, 1997).

In an attempt to increase the immunogenicity of DNA vaccines, DNA-launched replicon vaccines have been prepared using virus NS genes to facilitate replication of a DNA construct within a transfected host cell. However, the absence of the structural viral genes of the virus used for preparation of the DNA construct prevents the formation of infectious particles, thereby ensuring safe vaccination. The DNA-launched replicon vaccines, also referred to as replicon-based DNA vaccines, have demonstrated high expression levels of HIV viral proteins (Ljungberg *et al.*, 2007) and a more robust immune response compared to conventional DNA vaccines against herpes simplex virus, HIV and canine parvovirus (Hariharan *et al.*, 1998; Ljungberg *et al.*, 2007; Dahiya *et al.*, 2012). Strong humoral and/or cell-mediated immune responses have been elicited by the DNA-launched replicon vaccines developed against herpes simplex virus (Hariharan *et al.*, 1998), HIV (Ljungberg *et al.*, 2007), swine vesicular disease virus (Sun *et al.*, 2007), rabies virus (Saxena e*t al.*, 2008) and canine parvovirus (Dahiya *et al.*, 2012). Protective immune responses in some or all of the immunised animals have also been reported post-immunisation with DNA-launched replicon vaccines (Hariharan *et al.*, 1998; Sun *et al.*, 2007; Saxena e*t al.*, 2008; Pujhari e*t al.*, 2013).

1.2 Problem identification

YFV, a re-emerging mosquito-borne positive sense single stranded RNA virus, first isolated in 1927, is still considered to be a public health threat in yellow fever endemic areas. Yellow fever disease characterised by renal failure, jaundice and/or haemorrhage has reported fatality rates ranging from 20% (Monath, 1999) to over 50% (Vasconcelos *et al.*, 2001c).

Despite the availability of highly efficacious live attenuated vaccines against YFV, the estimated prevalence of yellow fever in Africa for 2013 was 130 000 severe cases and 78 000 deaths (Garske *et al.*, 2014). The re-emergence and high prevalence in Africa are attributed to failing vaccination programs with approximately 90% of reported cases occurring in Africa (Mutebi & Barrett, 2002). Furthermore, the available live attenuated vaccines against YFV have been contraindicated for use in immunocompromised individuals, as well as individuals with hypersensitivity to eggs and/or chicken.

Vaccine-associated adverse events have been reported for the live attenuated yellow fever vaccines, including vaccine-associated neurotropic- and viscerotropic adverse events. Reports of vaccine-associated viscerotropic adverse events resembling wild-type yellow fever led to concerns with regard to the safety of the live attenuated vaccines. Although the incidence of vaccine-associated viscerotropic adverse events has been reported to be 0,013 per 100 000 cases (Breugelmans *et al.*, 2013), the incidence might be higher due to adverse events being mistaken for wild-type yellow fever infection in yellow fever endemic areas (Martin *et al.*, 2001a). Investigation of alternative vaccines to complement the live attenuated vaccines is warranted for immunocompromised patients and individuals with risk factors associated with vaccine-associated adverse events, thereby improving vaccine coverage in endemic areas, as well as improving the safety of vaccination for the at-risk population. In this study, the use of a DNA-launched replicon vaccine was investigated as a model to establish the immune responses induced by the YFV ED-lll protein and to determine the immune responses induced using a DNA-launched vaccine approach.

1.3 Aim

Evaluation of the immunogenicity of a prepared DNA-launched Sindbis replicon encoding the YFV ED-lll protein in a mouse model.

1.4 Objectives

1. Preparation of a DNA-launched Sindbis replicon containing the gene encoding the YFV ED-lll protein.
2. Characterisation of the expressed YFV ED-lll protein in mammalian cell lines.
3. Evaluation of the immunogenicity of the prepared DNA-launched Sindbis replicon containing the gene encoding the YFV ED-lll protein in mice.

CHAPTER 2: Preparation of a DNA-launched Sindbis replicon containing the gene encoding the envelope domain lll protein of yellow fever virus

2.1 Introduction

DNA vaccines were first prepared after demonstration by Wolff and colleagues that DNA and RNA constructs taken up by muscle cells expressed the encoded proteins (Wolff e*t al.*, 1990) and were subsequently shown to have the ability to induce a memory MHC class l restricted CTL response in humans (Calarota *et al.*, 1998; MacGregor *et al.*, 1998; Wang *et al.*, 1998). However, conventional DNA vaccines were weakly immunogenic in larger mammals and therefore attempts were made to enhance the immunogenicity of DNA vaccines, including the preparation of DNA-launched replicon vaccines. DNA-launched replicon vaccines are prepared by inclusion of the virus NS genes, frequently from viruses belonging to the genus *Alphavirus*, within a DNA construct; however, the virus structural genes are not included preventing the formation of infectious particles (Pushko *et al.*, 1997). Alphaviruses utilised for DNA-launched replicon vaccine preparation include Venezuelan equine encephalitis virus (VEE) (Ljungberg *et al.*, 2007), Semliki Forest virus (SFV) (Sun *et al.*, 2007) and Sindbis virus (SINV) (Hariharan e*t al.*, 1998; Saxena e*t al.*, 2008). Gene expression has been shown to be efficient and rapid for SINV vectors for a broad host range including avian, insect and mammalian cells (Xiong *et al.*, 1989).

A DNA-launched Sindbis replicon containing a gene encoding the green fluorescent protein (GFP), designated pSinGFP, was developed and provided by Prof. Mark Heise from the University of North Carolina in the United States of America (USA). DNA vaccines contain elements that play an essential role in the expression of the encoded protein and the subsequent induction of an immune response. Expression of the encoded protein has been shown to be significantly influenced by the regulatory elements contained within a DNA construct (Manthorpe *et al.*, 1993). The pSinGFP DNA-launched replicon (Figure 2.1) contains a human cytomegalovirus (hCMV) immediate-early promoter/enhancer element, consisting of a strong constitutive promoter and an enhancer element, essential for eukaryotic expression (Boshart *et al.*, 1985). The hCMV immediate-early promoter/enhancer element will facilitate initiation of expression of the encoded SINV NS and heterologous proteins in a eukaryotic host cell. The hCMV immediate-early promoter/enhancer element was determined in cell culture to be a strong broadly active element with the ability to drive the transcription of heterologous genes. However, the activity of the promoter/enhancer element was greatly reduced when stably integrated into the cellular genome (Koedood *et al.*, 1995). The reduction in activity observed in cells upon stable integration of the promoter/enhancer element should not have a negative impact on the level of protein

expression in transfected host cells as the DNA-launched Sindbis replicon is not dependent on integration into the host cellular genome for expression of the encoded proteins.

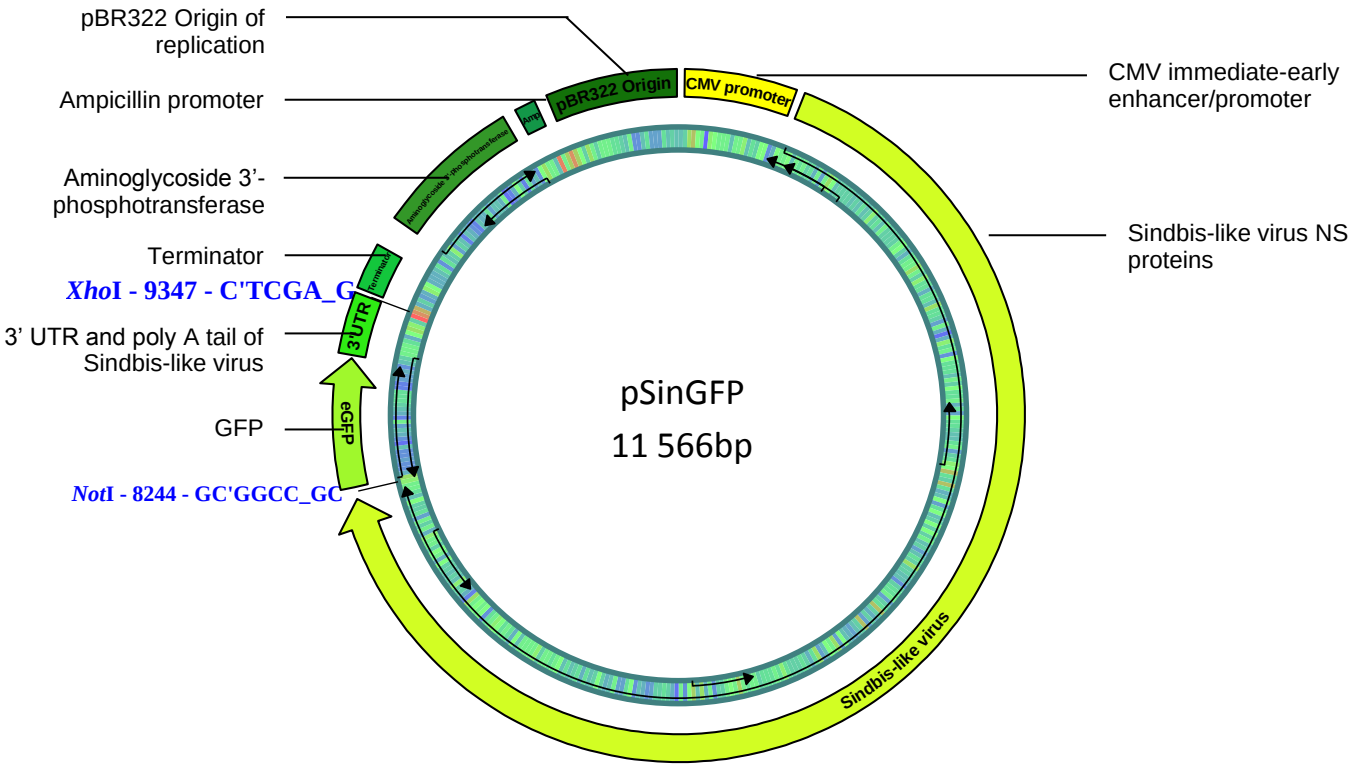

Figure 2.1: Vector map of pSinGFP

The encoded SINV NS proteins will facilitate replication of the DNA-launched replicon within transfected host cells; however, both the 5' and 3' UTR's have been shown to be essential for the initiation of viral replication in SINV-infected cells. The 5' UTR of SINV has also been shown to contain distinct core promoter elements (Frolov *et al.*, 2001). Therefore, both the 5' and 3' UTR's were included within the DNA-launched replicon construct. The 5' UTR immediately precedes the genes encoding the SINV NS proteins, whereas the 3' UTR and polyadenylation (poly A) signal were inserted at the 3' end of the heterologous gene. A bovine growth hormone (BGH) transcriptional terminator is present at the 3' end of the poly A signal, which facilitates the termination of transcription and protects the messenger (m)-RNA from degradation by the addition of a poly A tail. The CMV/BGH promoter/terminator

combination has been shown to facilitate a high level of protein expression (Montgomery *et al.*, 1993). The DNA-launched replicon also contains a bacterial origin of replication to facilitate high yield production of the replicon in the bacterial host, *Escherichia coli.* The Neokan promoter serves as a dual promoter for neomycin and kanamycin resistance, which drives expression of a gene encoding the Neo/Kan selectable marker for bacterial and eukaryotic expression. The encoded aminoglycoside 3'- phosphotransferase confers resistance against kanamycin and neomycin for bacterial and eukaryotic antibiotic selection, respectively (Yenofsky *et al.,* 1990).

Modification of the heterologous gene has been shown to be one of the most efficacious approaches to enhance protein expression (Hartikka *et al.*, 1996). Modification by codon-optimisation has been shown to enhance the expression of encoded viral genes in mammalian expression systems, subsequently also enhancing the immune responses elicited by the administered DNA vaccines (André *et al.*, 1998; zur Megede *et al.*, 2000; Deml *et al.*, 2001; Cid-Arregui *et al.*, 2003; Gao *et al.*, 2003; zur Megede *et al.*, 2003; Ternette *et al.*, 2007; Carnero *et al.*, 2009). The gene encoding the YFV ED-lll protein was codon-optimised in an attempt to optimise protein expression and immunogenicity of the DNA-launched replicon in a mammalian system. Codon-optimisation requires the alteration of the nucleotide sequence of a gene to optimise for the transfer (t)-RNA availability within a specific host, thus facilitating the expression of a heterologous gene; however, not resulting in the alteration of the encoded amino acid sequence. The mechanisms of codon-optimisation resulting in increased heterologous protein expression have been hypothesised to be increased rates of exportation of m-RNA to the cytoplasm, increased stability of m-RNA due to increased GC content of the m-RNA transcripts and/or increased translational efficiency due to the availability of the required t-RNA within the host (Narum *et al.*, 2001). For the expression of heterologous genes, the codon usage must be adjusted to coincide with the codon usage of the host organism as to maximise the expression of the heterologous gene. The codon adaptation index (CAI) ranging from 0 to 1,0 is a measurement of codon usage bias in a specific organism and is useful for prediction of the level of expression of a gene, the probability of heterologous protein expression within a specific host, as well as the comparison of the codon usage in different organisms. The level of gene expression has been shown to be directly proportional to the CAI value. The CAI value therefore facilitates the prediction of the suitability of the translational system of a host for a specific gene (Sharp & Li, 1987). Differences in the usage of codons exist between different species regarding the preference for specific degenerate bases encoding the same amino acids (Grantham *et al.*, 1980). A correlation, which is not precisely proportional, exists between the translational efficiency in mammalian cells and the level of

codon-optimisation for a specific gene. A study performed by Nagata and colleagues, suggested that higher levels of codon-optimisation expressed as the CAI value correlated to higher expression levels of the encoded polypeptide, subsequently leading to the induction of a stronger immune response (Nagata *et al.*, 1999).

The aim of this chapter was to prepare a DNA-launched Sindbis replicon encoding the YFV ED-lll protein and to confirm and characterise expression of YFV ED-lll protein in a mammalian expression system.

2.2 Methods and materials

2.2.1 Preparation of replicon DNA for ligation using pSinGFP replicon DNA

The DNA-launched Sindbis replicon encoding the GFP, designated pSinGFP, purified from a bacterial preparation using the NucleoBond® Xtra Midi Plus EF (Machery-Nagel, Düren, Germany) plasmid purification kit was obtained at a DNA concentration of 700ng/µl as determined using the Nanodrop™ 2000 (Thermo Fisher Scientific, Wilmington, USA). Glycerol stocks, designated pSinGFP glycerol stock, were obtained and stored at -80°C.

The gene encoding GFP was excised from pSinGFP replicon DNA by double restriction digestion using *Not*I (Promega, Wisconsin, USA) and *Xho*I (Promega, Wisconsin, USA) restriction endonucleases, rendering the linearised replicon with 5' *Not*I and 3' *Xho*I sticky ends. The double restriction digestion reaction mixture (Table 2.1) was incubated at 37°C for 2 hours. Two control reactions were included to confirm the endonuclease activity of the *Not*I and *Xho*I restriction endonucleases, as well as a negative control of uncleaved pSinGFP DNA.

Table 2.1: Composition of double restriction digestion reaction mixture for linearisation of pSinGFP replicon DNA

Components:	*Not*I control reaction	*Xho*I control reaction	pSinGFP reaction	pSinGFP reaction
	Volume (µl):	Volume (µl):	Volume (µl):	Volume (µl):
10X Buffer D	2,0	2,0	2,0	2,0
pSinGFP DNA (720,6 ng/µl)	0,5	0,5	0,5	1,0
*Not*I (10 units/µl)	1,0	-	1,0	1,0
*Xho*I (10 units/µl)	-	1,0	1,0	1,0
Nuclease-free water	16,5	16,5	15,5	15,0
Total reaction volume	20,0	20,0	20,0	20,0

The DNA fragments were separated by electrophoresis at 80V for 60 minutes using a 1% SeaKem® LE agarose gel (Lonza, Maine, USA) in trisaminomethane (tris)-acetate-ethylenediaminetetraacetic acid (EDTA) (TAE) buffer (refer to appendix F for buffer composition) and were visualised using ethidium bromide (Sigma, Missouri, USA) to a final concentration of 0,6 µg/ml on a UviPro UV transilluminator (UVItec, Cambridge, UK). The O'GeneRuler™ DNA Ladder Mix #SM1173 (Fermentas, Illinois, USA) molecular weight marker with a range of DNA fragments from 100 - 10 000 bp was used for estimating the size of the DNA digestion products. Bands of approximately 10 456 bp corresponding to the predicted size of linearised replicon were excised and gel purified using the Wizard® SV Gel and PCR Clean-Up System (Promega, Wisconsin, USA) according to the manufacturer's instructions. Briefly, gel purification was performed by the addition of 1 µl per mg membrane binding solution to the excised gel and was subsequently dissolved at 65°C. DNA was bound to a silica membrane on the Wizard® SV Minicolumn and washes were performed with 700 µl and 500 µl aliquots of membrane wash solution with centrifugation at 16 000 x *g* between each subsequent wash. DNA was eluted in nuclease-free water and the DNA concentration was determined using the Nanodrop™ 2000.

2.2.2 Design of gene encoding the YFV ED-III protein for synthesis

The gene encoding the wild-type Asibi strain YFV ED-III protein (GenBank Accession number: KF769016.1) was codon-optimised for expression in *Mus musculus* (house mouse) using the JAVA Codon Adaptation Tool (JCat) (Grote *et al.*, 2005). Codon-optimisation was performed in an attempt to optimise the expression and immunogenicity of the YFV ED-III protein in mice (refer to appendix A for codon-optimisation of the YFV ED-III gene). Higher expression levels of encoded proteins have been shown to induce a stronger immune response (Nagata *et al.*, 1999). The synthesised gene encoding the YFV ED-III protein is illustrated in Figure 2.2.

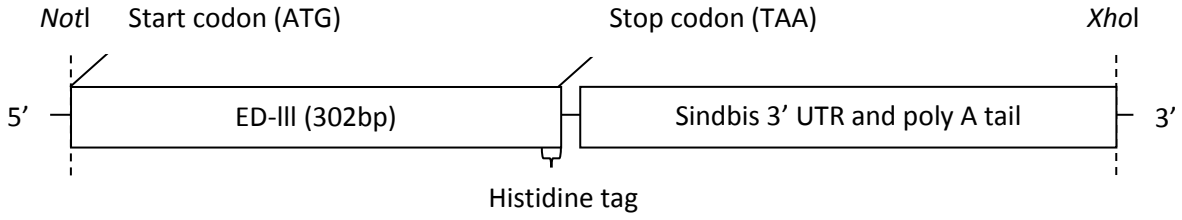

Figure 2.2: Illustration of the gene encoding the YFV ED-III protein

The gene synthesised for preparation of the vaccine construct, included the nucleotide sequence encoding the YFV ED-III protein and features that facilitated gene expression and the ligation process, and the sequence encoding a histidine tag to facilitate detection of expressed protein. The gene synthesised by GenScript was flanked with a *Not*I restriction site at the 5' end and a *Xho*I restriction site at the 3' end facilitating directional cloning of the gene encoding the YFV ED-III protein into the replicon by utilising the complementary sticky ends yielded by restriction digestion. A start codon was inserted at the 5' end of the gene encoding the YFV ED-III protein. At the 3' end of the gene encoding the YFV ED-III protein, a histidine tag was inserted to facilitate detection of the expressed YFV ED-III protein using anti-His_6 mouse monoclonal antibody. The histidine tag was followed by a stop codon (TAA) to facilitate termination of translation. The 3' UTR and poly A tail of SINV were included within the synthesised gene as excision of the gene encoding the GFP from pSinGFP replicon DNA resulted in excision of the replicon elements. These elements have been shown to be essential for replication mediated by the SINV NS proteins in SINV infection (Hardy & Rice, 2005).

2.2.3 Isolation and purification of the gene encoding the YFV ED-III protein from pUC57/ED-III

The gene synthesised by GenScript was supplied in pUC57 and designated pUC57/ED-III (refer to appendix B for pUC57/ED-III vector map). Competent *E. coli* XL10-Gold® cells (Stratagene, La Jolia, USA) with a transformation efficiency of 3 x 10^7 colony forming units (cfu)/µg were transformed with pUC57/ED-III plasmid DNA using the heat shock method. After the addition of 416,2 ng pUC57/ED-III plasmid DNA to a 100 µl aliquot of competent XL10-Gold® *E. coli* cells, cells were incubated on ice for 20 minutes, heat shocked at 42°C for 50 seconds and incubated on ice for 2 minutes. After the addition of 900 µl Super Optimal broth with Catabolite repression (SOC) (refer to appendix F for media composition) at room temperature, the transformation mixture was incubated at 37°C for 90 minutes with shaking at 200 rotations per minute (rpm). The transformation mixture was plated on Luria-Bertani (LB) (refer to appendix F for media composition) plates containing ampicillin (Roche, Mannheim, Germany) to a final concentration of 100 µg/ml (LB/amp), 5-bromo-4-chloro-3-indolyl-β-D-galactopyranoside (X-gal) (Fermentas, Gauteng, RSA) (refer to appendix F for preparation of X-gal) to a final concentration of 40 µg/ml and isopropyl β-D-1-thiogalactopyranoside (IPTG) (Melford Laboratories Ltd, Suffolk, UK) (refer to appendix F for preparation of IPTG) to a final concentration of 0,2 mM.

The addition of X-gal and IPTG to LB/amp plates facilitated blue/white screening for the selection of positively transformed colonies. Three white colonies, designated colony 1, 2 and 3, were streaked on fresh LB/amp plates. Three aliquots of 5 ml LB/amp broth were inoculated with each of the freshly streaked colonies and incubated at 37°C overnight (o/n) with shaking at 200 rpm. Plasmid DNA was purified from 3 ml o/n culture prepared for each colony using the PureYield™ Plasmid Miniprep System (Promega, Wisconsin, USA) according to the manufacturer's instructions. Briefly, a 3 ml aliquot of the o/n culture was pelleted by centrifugation at 16 000 x *g*. After re-suspension of the bacterial pellet in 600 µl deionised water, bacterial cells were lysed using alkaline lysis and the reaction was stopped by the addition of a pre-chilled neutralisation buffer. After centrifugation at 16 000 x *g*, DNA in the cell lysate was bound to the silica membrane in the PureYield™ minicolumn. The silica membrane was subsequently washed with endotoxin removal wash and column wash solution with centrifugation at 16 000 x *g* after each wash. The plasmid DNA was eluted in nuclease-free water and the DNA concentration was determined using the Nanodrop™ 2000. Glycerol stocks were prepared for each colony by the addition of glycerol to a final concentration of 15% to the remaining 2 ml o/n culture and were stored at -80°C.

To confirm positive transformants, a double restriction digestion was performed using *Not*I (Promega, Wisconsin, USA) and *Xho*I (Promega, Wisconsin, USA) restriction endonucleases. The reaction mixture (Table 2.2) was incubated at 37°C for 2 hours.

Table 2.2: Composition of double restriction digestion reaction mixture for confirmation of pUC57/ED-lll positive transformants

Components:	Colony 1 DNA concentration 434,4 ng/µl	Colony 2 DNA concentration 414,2 ng/µl	Colony 3 DNA concentration 284,3 ng/µl
	Volume (µl):	Volume (µl):	Volume (µl):
10X Buffer D	2,0	2,0	2,0
pUC57/ED-lll DNA	0,5	0,5	0,5
*Not*I (10 units/µl)	1,0	1,0	1,0
*Xho*I (10 units/µl)	1,0	1,0	1,0
Nuclease-free water	15,5	15,5	15,5
Total reaction volume	20,0	20,0	20,0

DNA fragments were analysed by electrophoresis as described in section 2.2.1. Predicted DNA fragments from positive transformants include a 2 710 bp fragment representing the pUC57 plasmid and a 696 bp fragment representing the synthesised insert encoding the

codon-optimised YFV ED-III protein. Glycerol stocks, designated pUC57/ED-III glycerol stock, prepared from colony 1 were selected for use in this project.

The gene encoding the YFV ED-III protein was obtained by double restriction digestion using *Not*I and *Xho*I restriction endonucleases. The reaction mixture (Table 2.3) was incubated at 37°C for 2 hours.

Table 2.3: Composition of reaction mixture for double restriction digestion with *Not*I and *Xho*I to obtain the gene encoding the YFV ED-III protein

Components:	Volume (µl):
10X Buffer D	2,0
pUC57/ED-III DNA (434,4 ng/µl)	1,0
*Not*I (10 units/µl)	1,0
*Xho*I (10 units/µl)	1,0
Nuclease-free water	15,0
Total reaction volume	20,0

DNA fragments were analysed using electrophoresis as described in section 2.2.1. Bands of 696 bp in length representing the gene encoding the YFV ED-III protein were excised and gel purified using the Wizard® SV Gel and PCR Clean-Up System according to the manufacturer's instructions. In the final step, the DNA was eluted in a final volume of 30 µl of nuclease-free water and the DNA concentration was determined using a Nanodrop™ 2000. Double restriction digestion using *Not*I and *Xho*I restriction endonucleases of the gene encoding the YFV ED-III protein yielded complementary 5' and 3' sticky ends facilitating ligation into replicon DNA.

2.2.4 Preparation and characterisation of the pSinED-III replicon

Agarose gel electrophoresis was utilised to confirm the integrity of the DNA and subsequently the gene encoding the YFV ED-III protein was ligated into the linearised replicon DNA using the complementary sticky ends generated by restriction digestion. The ligation reaction mixture (Table 2.4) prepared using the pGem®-T vector system I kit (Promega, Wisconsin, USA) was incubated o/n at 4ºC.

Table 2.4: Composition of reaction mixture for ligation of the gene encoding the YFV ED-III protein into the replicon

Components:	Volume (µl):
10X Ligation Buffer	1,0
T4 Ligase (1 units/µl)	1,0
Linearised pSinGFP DNA (68,2 ng/µl)	1,0
YFV ED-III insert DNA (16,0 ng/µl)	7,0
Total reaction volume	10,0

A 100 µl aliquot of OverExpress™ *E. coli* BL21 (DE3) cells (Lucigen Corporation, Wisconsin, USA) with a transformation efficiency of 3 x 10^7 cfu/µg were transformed with the ligation reaction mixture by the heat shock method. The cells were incubated on ice for 20 minutes, followed by heat shock for 50 seconds at 42ºC and incubation on ice for 2 minutes. After the addition of 900 µl of SOC broth at room temperature, the transformation mixture was incubated at 37°C for 90 minutes with shaking at 200 rpm. Thereafter, the transformation mixture was plated on 2X tryptone yeast (2X TY) (refer to appendix F for media composition) plates containing kanamycin (Sigma, Missouri, USA) to a final concentration of 50 µg/ml (2X TY/kan) and was incubated at 37°C o/n.

Seven colonies were selected and streaked on 2X TY/kan plates. Positive transformants were confirmed by performing a PCR using GoTaq® polymerase (Promega, Wisconsin, USA) on individual selected colonies using primers designed from sequence data as shown in Table 2.5. The primers, designated FW-pSin and RV-pSin, were designed to target the regions flanking the site of insertion, thus facilitating the amplification of the inserted gene.

Table 2.5: Primers for confirmation of positive transformants and sequencing

Primer:	Primer sequence:	Sequence length:	Tm of primer (°C):	Position of primer relative to pSinED-III:
FW-pSin	5'-AAA TAG TCA GCA TAG TAC ATT-3'	21	46,5	8 199 - 8 219
RV-pSin	5'-TGC AAT TTC CTC ATT TTA TTA-3'	21	45,6	9 089 – 9 069

The cycling conditions used for the confirmation of positive transformants were an initial denaturation step at 95°C for 2 minutes, denaturation at 95°C for 1 minute, annealing at 44°C for 1 minute and extension at 72°C for 1 minute for 25 cycles. A final extension step at 72°C was performed for 5 minutes and tubes held at 4°C using the GeneAmp® PCR system

9700 (Applied Biosystems, London, England). PCR products were separated by agarose gel electrophoresis as described in section 2.1.1.

Two positive transformants, colonies 3 and 5, confirmed by PCR were inoculated in 5 ml 2X TY/kan broth and incubated at 37°C o/n with shaking at 200 rpm. The PureYield™ Plasmid Miniprep System was used according to the manufacturer's instructions to purify pSinED-lll plasmid DNA from a 3 ml aliquot of o/n culture for each colony. DNA purified from each colony was used for sequence determination at the site of insertion. The DNA concentration was determined using a Nanodrop™ 2000. Glycerol stocks, designated pSinED-lll glycerol stock, were prepared by the addition of glycerol to a final concentration of 15% and stored at -80°C.

The nucleotide sequence of the DNA construct at the site of insertion was determined using the BigDye® Terminator V3.1 Ready Reaction Cycle Sequencing kit (Applied Biosystems, London, England) to confirm the sequence encoding the YFV ED-lll protein remained unaltered during the cloning process. The sequencing reaction mixture (Tables 2.6 and 2.7) was subjected to the following cycling conditions: an initial denaturation step at 96°C for 1 minute, followed by 25 cycles of denaturing at 96°C for 10 seconds, annealing at 44°C for 5 seconds, extension at 60°C for 4 minutes and tubes were held at 4°C using the GeneAmp® PCR system 9700. The FW-pSin and RV-pSin primers were used for bidirectional sequencing to allow base calling if discrepancies were to exist for certain nucleotide positions.

Table 2.6: Reaction mixture to determine the nucleotide sequence of the gene encoding the YFV ED-lll using BigDye® Terminator V3.1 Ready Reaction Cycle Sequencing

Component:	DNA purified from colony 3	DNA purified from colony 3	DNA purified from colony 5	DNA purified from colony 5
	Volume (µl):	Volume (µl):	Volume (µl):	Volume (µl):
Ready Reaction	1,0	1,0	1,0	1,0
FW-pSin primer (0,8 pmol/µl)	4,0	-	4,0	-
RV-pSin primer (0,8 pmol/µl)	-	4,0	-	4,0
5X Sequencing buffer	2,0	2,0	2,0	2,0
DNA from colony 3 (361,9 ng/µl)	2,0	2,0	-	-
DNA from colony 5 (601,3 ng/µl)	-	-	1,0	1,0
Nuclease-free water	1,0	1,0	2,0	2,0
Total Reaction Volume	10,0	10,0	10,0	10,0

Table 2.7: Reaction mixture for determination of the control DNA sequence using BigDye® Terminator V3.1 Ready Reaction Cycle Sequencing

Component:	Volume (µl):
Ready reaction	1,0
M13 primer (0,8 pmol/µl)	4,0
5X Sequencing buffer	2,0
pGEM3Zf(+) (0,2 µg/µl)	1,0
Nuclease-free water	5,0
Total Reaction Volume	10,0

A post-reaction sequencing clean-up was performed by EDTA/ethanol precipitation. The volume of the sequencing reaction was adjusted to a final volume of 20 µl with nuclease-free water. Thereafter, the 20 µl reaction mixture was transferred to a clean 1,5ml tube, containing 5 µl 125 mM EDTA (refer to appendix F for preparation of EDTA) and 60 µl absolute ethanol. Samples were vortexed facilitating mixture of the content and incubated at room temperature for 15 minutes for DNA precipitation to occur. Thereafter, samples were subjected to centrifugation at 14 000 x *g* for 10 minutes at 4°C. After completely aspirating the supernatant, 500 µl of 70% ethanol was added and the samples were centrifuged at 14 000 x *g* for 10 minutes at 4°C. Thereafter, the supernatant was completely aspirated and any residual ethanol was allowed to evaporate by incubation at 37°C for 2 hours. The samples were stored at 4°C in the dark, until submission for electrophoresis. The nucleotide sequence was determined using the ABI PRISM® 3130XL-16 capillary genetic analyser (Applied Biosystems, California, USA) by the Department of Microbial, Biochemical and Food Biotechnology, University of the Free State.

Sequencing data was analysed with ChromasPro version 1.6 (Technelysium, South Brisbane, Australia). The open reading frame (ORF) was identified using ORF finder (Rombel *et al.*, 2002) and was translated into the amino acid sequence using the Expasy translation tool (Gasteiger e*t al.*, 2003). Thereafter, the nucleotide and amino sequences for the codon-optimised gene encoding wild-type YFV ED-lll were aligned with the sequence data and translated sequence data obtained to confirm that complete nucleotide and amino acid sequence identity were maintained. Alignments were performed using ClustalW (Larkin *et al.*, 2007) and Clustal Omega (Sievers *et al.*, 2011).

Transfection grade DNA was prepared from bacterial cultures using the QIAGEN® Plasmid *Plus* Midi kit (Qiagen, Hilden, Germany) according to the manufacturer's instructions. Briefly, a 5 ml starter culture was prepared using pSinED-lll glycerol stock. A 1:250 dilution of the starter culture was prepared by the addition of 100 µl of culture to 25 ml of pre-

warmed 2X TY/kan broth. The culture was incubated at 37°C for approximately 8 hours with shaking at 200 rpm. Thereafter, the pellet was harvested by centrifugation at 6 000 x *g* for 15 minutes at 4°C and was re-suspended in a re-suspension buffer. Alkaline lysis was performed for 3 minutes at room temperature and was stopped by the addition of a pre-chilled neutralisation buffer. The lysate was filtered using a QIAfilter Cartridge and after the addition of buffer BB, a binding buffer, the lysate was transferred to a QIAGEN® Plasmid *Plus* spin column. A vacuum was applied to drain the lysate through the spin column and subsequent washes with buffer ETR, an endotoxin removal buffer, and buffer PE, a wash buffer, were performed. Any residual wash buffer was removed by centrifugation at 10 000 x *g* for 1 minute and DNA was eluted in 200 µl nuclease-free water. The DNA concentration was determined using the Nanodrop™ 2000.

2.2.5 Confirmation of protein expression in selected mammalian cell lines

BHK-21 (American Type Culture Collection (ATCC) number CCL-10 passage 6) cells were propagated in Dulbecco's Modified Eagle Medium (DMEM) (Lonza, Verviers, Belgium) supplemented with 5% foetal bovine serum (FBS) (BiochromAG, Berlin, Germany), 100 units per ml (U/ml) penicillin and streptomycin (pen/strep) (Lonza, Verviers, Belgium), L-glutamine (L-glu) (Lonza, Verviers, Belgium) to a final concentration of 2 mM and non-essential amino acids (NEAA's) (Lonza, Verviers, Belgium) at 37ºC and were passaged when 95% confluent. CV-1 in Origin carrying SV40 (COS)-7 (ATCC number CRL-1651 passage 46) and human embryonic kidney (HEK)-293 (ATCC number CRL-1573 passage 39) cells were propagated in DMEM supplemented with 5% heat-inactivated FBS (BiochromAG, Berlin, Germany), 100 U/ml pen/strep, L-glu to a final concentration of 2 mM and NEAA's at 37°C in 5% CO_2 and were passaged when 95% confluent. Vero-76 (ATCC number CRL-1587 passage 29) cells were propagated in Eagle's Minimal Essential Medium (EMEM) (Lonza, Verviers, Belgium) supplemented with 10% heat-inactivated FBS, 100 U/ml pen/strep, L-glu to a final concentration of 2 mM and NEAA's at 37°C and were passaged when 95% confluent. The BHK-21, HEK-298 and Vero-76 cells were kindly provided by Dr. Caroline Knox from Rhodes University and the COS-7 cells were kindly provided by Dr. Trudi O'Neill from the University of the Free State. Cells were passaged by discarding the growth media, washing the cells with phosphate buffered saline (PBS) (Lonza, Verviers, Belgium) at a pH of 7,4 and dissociation of cells with the appropriate volume of trypsin (Lonza, Verviers, Belgium) depending on the cell line and flask size. The cells were re-suspended in an appropriate volume of growth media and seeded according to the cell line and flask size.

Prior to performing a mouse immunisation study, expression of the encoded YFV ED-lll protein was confirmed by transfection of mammalian cells. Protein expression was evaluated in selected mammalian cell lines, including the BHK-21, COS-7, HEK-293 and Vero-76 cell lines. Each cell line was seeded at the appropriate seeding density (Table 2.8) in separate 24-well plates (Corning, New York, USA) to obtain a confluency of approximately 80% on the day post-seeding. Prior to seeding cells, round glass slips 12 mm in diameter, were added to each well to facilitate immunofluorescence staining post-attachment of cells. Cells were re-suspended in the appropriate growth media and counted using the trypan blue exclusion method in 0,4% trypan blue (Merck, Darmstadt, Germany) in PBS at a pH of 7,4 (refer to appendix F for buffer composition). Briefly, cells were diluted in trypan blue to allow differentiation of viable cells from non-viable cells. The tryphan blue exclusion method is based on the uptake of a dye, trypan blue, by non-viable cells due to the integrity of the cell membrane being compromised. Therefore, non-viable cells will have a blue cytoplasm, whereas viable cells will have a clear cytoplasm (Strober, 2001). Thereafter, the viable cells are counted to estimate the number of cells per millilitre in the cell suspension.

Table 2.8: Seeding densities for selected mammalian cell lines in a 24-well plate

Cell line:	Seeding density (cells/well):
BHK-21	1×10^5
COS-7	7×10^4
HEK-293	2×10^5
Vero-76	8×10^4

Cells were transfected when approximately 80% confluent using 3 µl Lipofectamine® 2000 (Invitrogen, California, USA) diluted in 50 µl Opti-minimum essential media (MEM) reduced serum medium (Gibco, Paisley, UK) for each well. The diluted Lipofectamine® 2000 was incubated for 20 minutes at room temperature prior to the addition of diluted DNA. For each transfection 2 µg replicon DNA was diluted in 50 µl Opti-MEM reduced serum medium and was incubated for 5 minutes. The DNA/Opti-MEM mixture was combined with the Lipofectamine® 2000/Opti-MEM mixture and incubated for 20 minutes at room temperature facilitating the formation of DNA/Lipofectamine complexes. The growth media was aspirated and replaced with transfection medium consisting of DMEM supplemented with 5% FBS and L-glu to a final concentration of 2 mM. Subsequently, the DNA/Lipofectamine complexes were added to the respective wells and incubated at 37°C in a humid 5% CO_2 atmosphere. For all transfection reactions untransfected cells served as a negative control and cells transfected with the pSinGFP replicon served as a positive control.

Protein expression in transfected cells was confirmed 24 hours post-transfection. Cells were fixed to the glass cover slips using a 1:1 solution of cold methanol (Merck, Darmstadt, Germany) and acetone (Merck, Darmstadt, Germany) at -20°C for 20 minutes. Cells transfected with pSinGFP replicon DNA were visualised directly for expression of the GFP using an OPTIPHOT fluorescence microscope (Nikon, Tokyo, Japan). To visualise expression of the YFV ED-III protein an indirect IFA was performed. After fixation, untransfected cells and cells transfected with pSinED-III replicon DNA were blocked with 10% sucrose and 0,5% Triton X-100 (Promega, Wisconsin, USA) in PBS at a pH of 7,4 for 20 minutes at room temperature to prevent non-specific binding of antibody. Thereafter, residual blocking solution was removed and anti-His_6 mouse monoclonal antibody (Roche, Indianapolis, USA) diluted 1:10 in blocking solution was applied. Cells were incubated at 37°C for 90 minutes in a humid container. The expressed protein was detected using anti-His_6 mouse monoclonal antibody specific for the C-terminal histidine tag added to the YFV ED-III protein coding sequence. Unbound antibody was removed by washing with 1% Tween® 20 (Promega, Wisconsin, USA) in PBS. Goat anti-mouse IgG fluorescein isothiocyanate (FITC) (KPL, Maryland, USA) diluted at 1:40 in 0,1% Evans blue (Merck, Darmstadt, Germany) in PBS was used to detect bound anti-His_6 mouse monoclonal antibody. Slides were incubated at 37°C for 30 minutes in a humid container and subsequently unbound antibody was removed by washing with 1% Tween® 20 in PBS. Transfected cells were visualised by fluorescence microscopy and the transfection efficiency was estimated based on the number of fluorescing cells observed in two to three fields of vision.

2.2.6 Characterisation of the expressed YFV ED-III protein in mammalian cells using anti-YFV ED-III antibody

The BHK-21 cell line was chosen for characterisation of the expressed YFV ED-III protein as this cell line had the highest transfection efficiency during transfection experiments using pSinED-III replicon DNA when compared to the other mammalian cell lines evaluated. To facilitate high transfection efficiency X-tremeGENE™ HP (Roche, Indiana, USA) DNA transfection reagent was compared to Lipofectamine® 2000.

BHK-21 cells in the log growth phase were seeded at 1 x 10^5 cells/well in a 24-well plate containing growth media and a round glass slip in each seeded well. Cells were transfected 24 hours post-seeding when approximately 80% confluent. Transfection complexes were prepared by the dilution of 2 µg pSinGFP (positive control) and pSinED-III replicon DNA in 50 µl Opti-MEM for each reaction. Thereafter, 2 µl X-tremeGENE™ HP was added to each

pSinGFP control reaction and 4 µl X-tremeGENE™ HP was added to each pSinED-lll reaction. The prepared transfection mixtures were incubated for 15 minutes at room temperature to facilitate the formation of DNA/X-tremeGENE complexes. Thereafter, the transfection complexes were added to the respective wells and incubated for 24 hours at 37°C in a humid 5% CO_2 atmosphere.

To facilitate detection of the expressed YFV ED-lll protein cells were fixed using a 1:1 methanol and acetone solution at -20°C o/n. Cells transfected with pSinGFP replicon DNA were visualised directly by fluorescence microscopy to confirm expression of the encoded GFP. Thereafter, untransfected cells and cells transfected with the pSinED-lll replicon were blocked with 10% sucrose and 0,5% Triton X-100 in PBS at a pH of 7,4 for 20 minutes at room temperature. Anti-YFV ED-lll antibody raised in a mouse by immunisation with bacterially expressed recombinant 17D YFV ED-lll protein was used for the characterisation of the expressed YFV ED-lll protein. The mouse immune serum has previously been confirmed to contain anti-YFV ED-lll antibody by indirect ELISA in an unrelated study (Smouse, 2013). After incubation, anti-YFV ED-lll antibody diluted 1:10 in blocking solution was applied and incubated at 37°C for 90 minutes in a humid container. Thereafter, unbound antibody was removed by washing with 1% Tween® 20 in PBS and cells were incubated at 37°C for 30 minutes in a humid container with goat anti-mouse IgG FITC diluted at 1:40 in 0,1% Evans blue in PBS. Subsequently, unbound antibody was removed by washing with 1% Tween® 20 in PBS and transfected cells were visualised by fluorescence microscopy. The transfection efficiency was estimated based on the number of fluorescing cells observed in two to three fields of vision.

2.3 Results

2.3.1 Preparation of replicon DNA for ligation using pSinGFP replicon DNA

The pSinGFP replicon was linearised by restriction digestion using *Not*I and *Xho*I restriction endonucleases. The gene encoding the GFP was excised by restriction digestion generating complementary ends facilitating ligation of the gene encoding the YFV ED-lll protein flanked by *Not*I and *Xho*I restriction sites. Control single digestion reactions using *Not*I and *Xho*I restriction endonucleases were included to establish the activity of the *Not*I and *Xho*I restriction endonucleases. The control reactions in lanes 3 and 4 confirmed that the *Not*I and *Xho*I restriction endonucleases were functioning, thus rendering linearised DNA as compared to the uncut pSinGFP DNA in lane 2, which consists of supercoiled and nicked replicon DNA as illustrated in Figure 2.3. The bands in lanes 5 and 6 corresponding to an

approximately 10 456 bp DNA fragment were excised, gel purified and the concentration was determined to be 68,2 ng/µl.

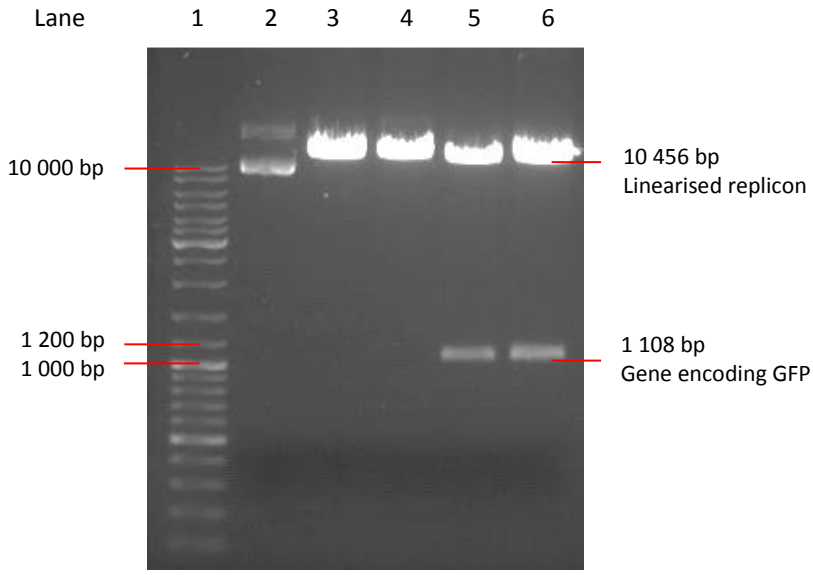

Figure 2.3: Agarose gel electrophoretic analysis of the restriction digestion product of pSinGFP

Lane 1 – O'GeneRuler™ molecular weight marker; Lane 2 – Undigested pSinGFP replicon; Lane 3 – pSinGFP digested with *Not*I; Lane 4 – pSinGFP digested with *Xho*I; Lane 5 – pSinGFP double digested with *Not*I and *Xho*I (0,5 µl reaction); Lane 6 - pSinGFP double digested with *Not*I and *Xho*I (1,0 µl reaction).

2.3.2 Isolation and purification of the gene encoding the YFV ED-lll protein from pUC57/ED-lll

The reconstituted pUC57/ED-lll DNA determined to have a DNA concentration of 416,2 ng/µl was used for the transformation of XL10-Gold® *E. coli* cells. Blue/white selection allowed easy differentiation between positive transformants and satellite colonies. Blue/white selection is based on α-complementation using the α-peptide of the gene encoding β-galactosidase, designated lacZ, subsequently facilitating the production of functional β-galactosidase from a truncated lacZ gene within a suitable host organism (Langley *et al.*, 1975). Positive transformants were identified based on the colour of the colonies. Colonies harbouring plasmid without a DNA insert within the multiple cloning site (MCS), located within the encoded α-peptide, will lead to the production of the α-peptide. Subsequently, leading to the production of functional β-galactosidase, which will convert the X-gal contained within the agar into a blue product. In positive transformants, the α-peptide would not be produced due to the disruption of the gene with a DNA insert and subsequently

functional β-galactosidase cannot be produced leading to a colony that is white in colour. All colonies post-transformation were white in colour suggesting the presence of an insertion within the encoded α-peptide, thus potentially identifying positive transformants.

Table 2.9: Concentration of DNA purified from selected colonies for confirmation of positive transformants

Colony:	DNA concentration (ng/µl):
1	434,3
2	414,2
3	284,3

DNA purified from selected colonies (Table 2.9) was used for the confirmation of positive transformants by restriction digestion analysis using *Not*I and *Xho*I restriction endonucleases. Analysis of the restriction digestion product was performed by agarose gel electrophoresis.

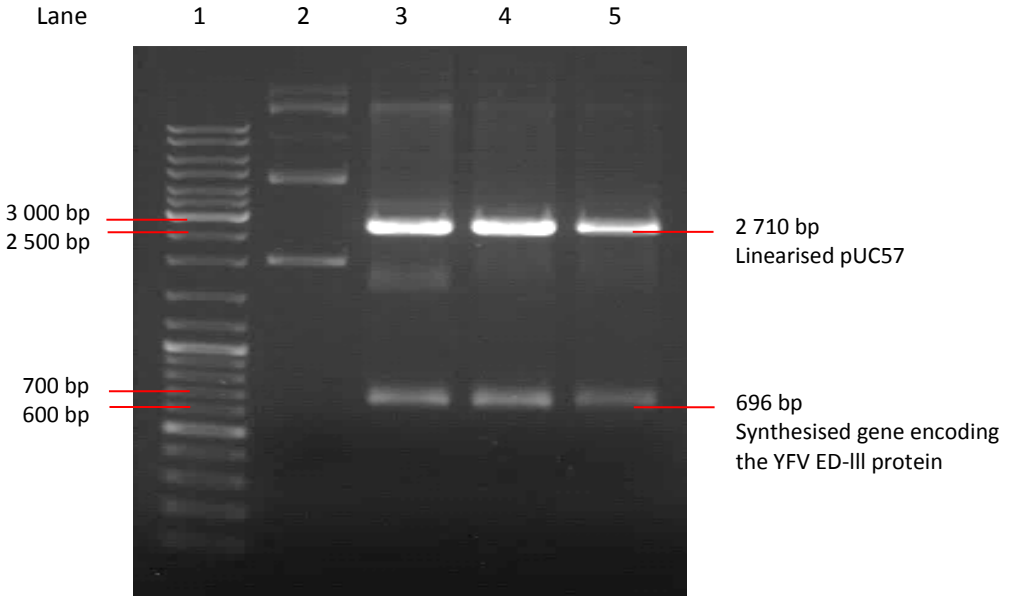

Figure 2.4: Agarose gel electrophoretic analysis of the restriction digestion product of pUC57/ED-III

Lane 1 – O'GeneRuler™ molecular weight marker; Lane 2 – Undigested pUC57/ED-III; Lane 3 - pUC/ED-III double digested with *Not*I and *Xho*I from colony 1; Lane 4 - pUC/ED-III double digested with *Not*I and *Xho*I from colony 2; Lane 5 - pUC/ED-III double digested with *Not*I and *Xho*I from colony 3.

A DNA fragment of 2 710 bp in length represents the pUC57 vector and a DNA fragment of 696bp in length represents the synthesised gene encoding the YFV ED-III protein. Thus, the presence of both a 2 710 bp fragment and a 696 bp fragment would indicate a positive transformant, whereas the presence of only a 2 710bp fragment would indicate a transformant containing the pUC57 vector without the synthesised gene encoding the YFV ED-III protein. All selected colonies were positive transformants as confirmed by the presence of a band corresponding to a 696 bp fragment in lanes 3 to 5 as illustrated in Figure 2.4. Subsequently, the gene encoding the YFV ED-III protein was obtained by restriction digestion using *Not*I and *Xho*I restriction endonucleases yielding complementary ends to facilitate ligation into replicon DNA. The bands corresponding to a 696 bp DNA fragment were excised, pooled and gel purified. The DNA concentration of the purified gene encoding the YFV ED-III protein was determined to be 16,0 ng/µl.

2.3.3 Preparation and characterisation of the pSinED-III replicon

Prior to ligation, 1 µl purified linearised replicon DNA and 1 µl purified gene encoding the YFV ED-III protein were analysed by agarose gel electrophoresis to establish the integrity of the DNA.

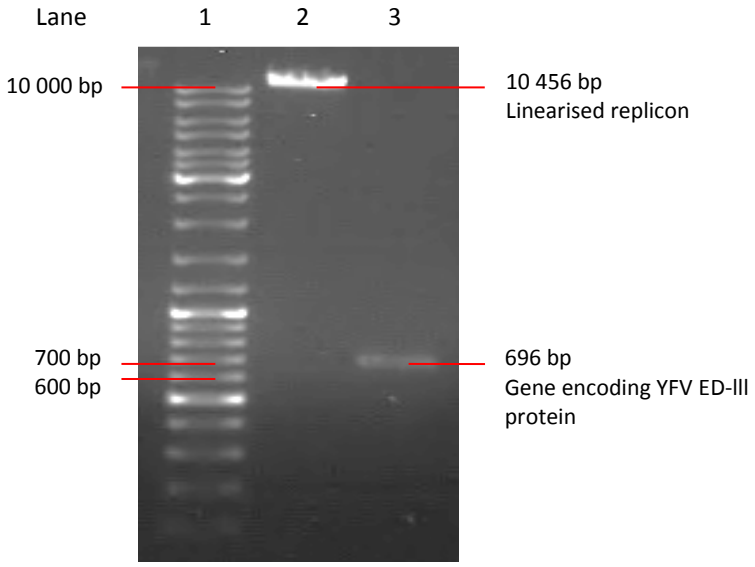

Figure 2.5: Agarose electrophoretic analysis to establish the integrity of purified replicon DNA and the purified gene encoding the YFV ED-III protein

Lane 1 – O'GeneRuler™ molecular weight marker; Lane 2 – Purified linearised replicon DNA; Lane 3 – Purified gene encoding the YFV ED-III protein.

As illustrated in Figure 2.5, a single band corresponding to a 10 456 bp fragment was present in lane 2, thus only the linearised replicon DNA. In lane 3, a single band corresponding to a 696 bp fragment was present representing the gene encoding the YFV ED-III protein. After ligation, OverExpress™ *E. coli* cells were transformed with the ligation reaction mixture facilitating amplification of replicon DNA in *E. coli*. The selection of positive transformants was facilitated by the addition of kanamycin antibiotic to the growth media, thus selecting for colonies containing the kanamycin resistance encoded within the replicon. However, since partial restriction digestion and subsequent re-ligation can result in colonies containing the pSinGFP replicon, confirmation of positive transformants was required to distinguish between true positive transformants and satellite colonies containing the pSinGFP replicon. Therefore, a single set of primers targeting the regions flanking the site of insertion was designed to facilitate PCR amplification of replicon containing the gene encoding the GFP and the YFV ED-III protein. Replicon containing the gene encoding the GFP, designated pSinGFP, has a predicted amplicon size of 1 307 bp, whereas the pSinED-III replicon has a predicted amplicon size of 893 bp. The difference in amplicon size facilitated differentiation between colonies containing the pSinGFP and pSinED-III replicon as illustrated in Figure 2.6.

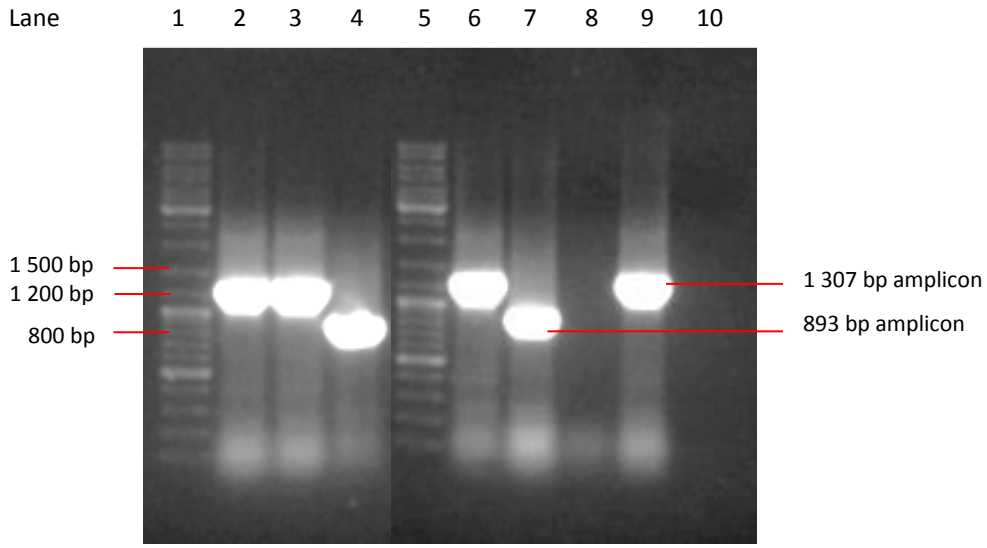

Figure 2.6: Agarose electrophoretic analysis of PCR product for confirmation of positive transformants

Lane 1 – O'GeneRuler™ molecular weight marker; Lane 2 – PCR product for colony 1; Lane 3 – PCR product for colony 2; Lane 4 – PCR product for colony 3; Lane 5 – O'GeneRuler™ molecular weight marker; Lane 6 – PCR product for colony 4; Lane 7 – PCR product for colony 5; Lane 8 – PCR product for colony 6; Lane 9 – PCR product for colony 7; Lane 10 – Negative control.

The presence of a band corresponding to a 1 307 bp fragment in lanes 2, 3, 6 and 9 confirmed that the selected colonies were likely transformed with pSinGFP suggesting that partial digestion of the pSinGFP replicon occurred during the double restriction digestion reaction allowing some re-ligation of the GFP encoding replicon. The presence of a band corresponding to an 893 bp fragment in lanes 4 and 7 confirmed that colonies 3 and 5 were transformed with the pSinED-lll replicon. The nucleotide sequence at the site of insertion was determined using DNA purified from o/n cultures of colonies 3 and 5 (Table 2.10).

Table 2.10: DNA concentration obtained from positive transformants

Colony:	DNA concentration (ng/µl):
3	361,9
5	601,3

Analysis of the sequence data confirmed that complete nucleotide identity of the gene encoding the YFV ED-lll protein was retained in both constructs. Glycerol stocks prepared from a culture of colony 5, designated pSinED-lll glycerol stock, were selected for continued work (refer to appendix C for sequencing data).

2.3.4 Confirmation of protein expression in selected mammalian cell lines

BHK-21, COS-7, HEK-293 and Vero-76 cells were transfected with the pSinGFP and pSinED-lll replicon constructs to confirm the expression of the encoded GFP and YFV ED-lll proteins, respectively. Negative controls were included for all transfection reactions. Expression of the YFV ED-lll protein was initially confirmed by detection of the C-terminal histidine tag fused to the YFV ED-lll protein using mouse monoclonal anti-His_6 antibody. The GFP and YFV ED-lll proteins were expressed in BHK-21 cells, COS-7 cells, HEK-293 cells and Vero-76 cells post-transfection with the pSinGFP and pSinED-lll replicons, respectively, as illustrated in Figure 2.7.

The transfection efficiency, based on visual observation of cells and estimation of fluorescent positive cells to non-fluorescing cells, differed between the different mammalian cell lines evaluated.

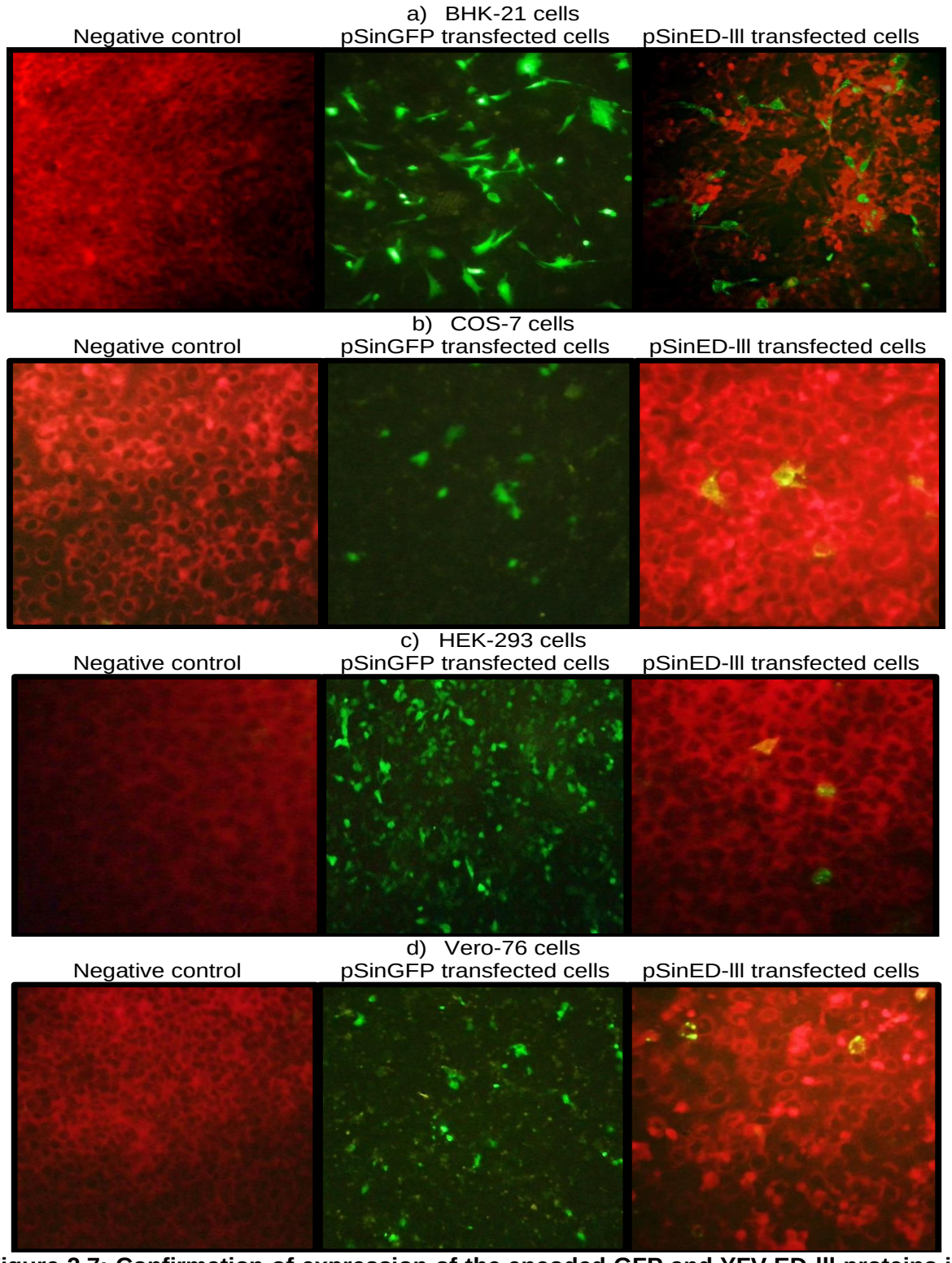

Figure 2.7: Confirmation of expression of the encoded GFP and YFV ED-III proteins in selected mammalian cell lines

Images for a) BHK-21 cells, b) COS-7 cells, c) HEK-293 cells and d) Vero-76 cells, including the negative controls (left) counterstained with Evans blue, cells expressing the GFP post-transfection with the pSinGFP replicon (middle) and cells expressing the YFV ED-III protein post-transfection with the pSinED-III replicon (right). Cells were visualised using an OPTIPHOT fluorescence microscope at 200X magnification.

BHK-21 and HEK-293 cells had higher transfection efficiencies of approximately 60% with the pSinGFP replicon, whereas COS-7 and Vero-76 cells had lower transfection efficiencies of approximately 10%. A similar trend was identified for the pSinED-lll replicon with the highest transfection efficiency, of approximately 30%, observed in BHK-21 cells. Transfection efficiency in HEK-293 and COS-7 cells was less than 1%. Subsequently, BHK-21 cells were utilised for the characterisation of the expressed histidine tagged protein.

2.3.5 Characterisation of the expressed YFV ED-lll protein in mammalian cells using anti-YFV ED-lll antibody

The recombinant YFV ED-lll protein was characterised in a mammalian cell line, BHK-21, using anti-YFV ED-lll antibody raised in a mouse. Mouse serum collected post-immunisation with the 17D YFV ED-lll protein shown to contain anti-YFV ED-lll antibody (Smouse, 2013) was used in an IFA to detect the expressed YFV ED-lll protein as illustrated in Figure 2.8.

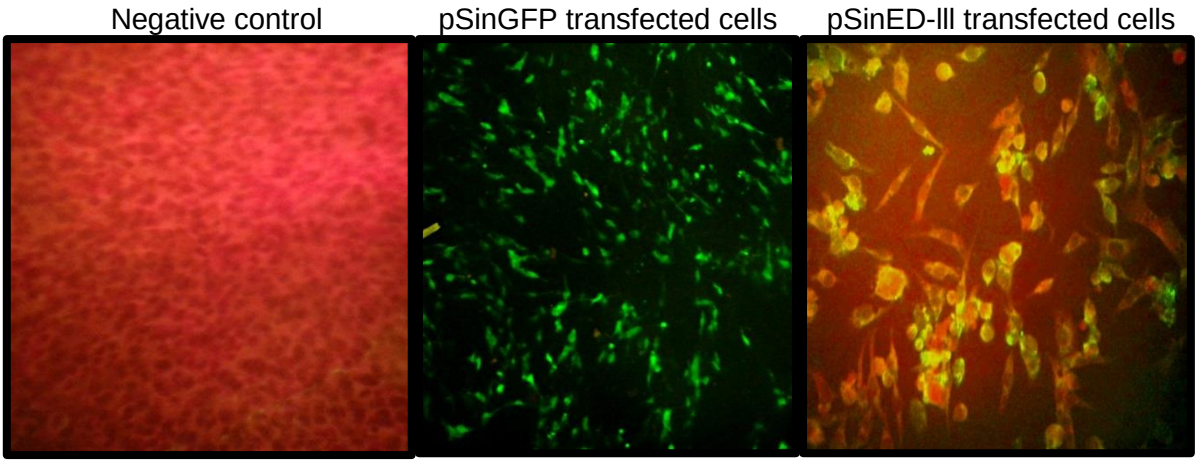

Figure 2.8: Characterisation of the expressed YFV ED-lll protein in the BHK-21 cell line using anti-YFV ED-lll antibody

Images for BHK-21 cells transfected using X-tremeGENE™ HP transfection reagent, including the negative controls (left) counterstained with Evans blue, cells transfected with the pSinGFP replicon expressing the GFP (middle) and cells transfected with the pSinED-lll replicon expressing the YFV ED-lll protein (right). Cells were visualised using an OPTIPHOT fluorescence microscope at 200X magnification.

The recombinant YFV ED-lll protein was expressed in BHK-21 cells after transfection with pSinED-lll replicon DNA. A higher transfection efficiency of approximately 70% was observed for the X-tremeGENE™ HP transfection reagent when compared to

Lipofectamine® 2000 as illustrated in Figure 2.8 compared to Figure 2.7a. Antibody directed against the YFV ED-III protein reacted with the expressed protein as indicated by specific fluorescence in the cytoplasmic region of transfected cells when compared to the lack of fluorescence in untransfected cells.

2.4 Discussion

DNA vaccination relies on the expression of a protein from a DNA construct, which mimics natural viral infection and induces a cell-mediated immune response shown to be essential for virus suppression and clearance during infection (Matloubian *et al.*, 1994). In addition, safety of DNA vaccination is superior due to the absence of replicating infectious virus making DNA vaccination suitable for use in immunocompromised individuals and infants. The addition of alphavirus NS genes to a DNA construct further enhances safety as replication only initially relies on the host cell encoded polymerase. Thereafter, RNA replication occurs under direction of the expressed viral RNA-dependent RNA polymerase and other NS proteins preventing the integration of DNA into the host cell genome as DNA is only present for the first round of replication. Utilisation of alphavirus NS proteins to facilitate replication of a DNA-launched replicon vaccine has been shown to enhance the level of protein expression (Ljungberg *et al.*, 2007) and the immunogenicity post-immunisation when compared to conventional DNA vaccines (Hariharan *et al.*, 1998; Ljungberg *et al.*, 2007; Dahiya *et al.*, 2012).

The YFV ED-III protein has been identified as a potential target for vaccination due to domain III containing all the major neutralising epitopes (Beasley & Barrett, 2002; Wu *et al.*, 2003; Sánchez *et al.*, 2005) and three immunodominant epitopes recognised by memory $CD8^+$ T-cells (de Melo *et al.*, 2013). Thus, the YFV ED-III protein has been identified as a target for both B- and T-cells. The ED-III protein of other viruses belonging to the genus *Flavivirus* has been shown to elicit protective immune responses in mice (Chen *et al.*, 2007; Chu *et al.*, 2007). The gene encoding the Asibi strain YFV ED-III protein was codon-optimised for expression in *Mus musculus* to facilitate high level expression of the encoded YFV ED-III protein in mouse muscle cells. Codon-optimisation has been shown to enhance the expression of an encoded viral protein, which has been correlated to a stronger immune response (André *et al.*, 1998; zur Megede *et al.*, 2000; Deml *et al.*, 2001; Cid-Arregui *et al.*, 2003; Gao *et al.*, 2003; zur Megede *et al.*, 2003; Ternette *et al.*, 2007; Carnero *et al.*, 2009). The 5' *Not*I and 3' *Xho*I restriction sites were utilised for directional cloning of the gene encoding the YFV ED-III protein. Subsequently, bidirectional nucleotide sequencing using primers flanking the site of insertion was used to confirm construct preparation and the YFV

ED-III coding sequence. Further confirmation of construct preparation and the functioning of replicon elements were achieved by confirmation of protein expression from pSinGFP and pSinED-III replicon DNA in mammalian cell culture.

Recombinant GFP was expressed in mammalian cells transfected with pSinGFP replicon DNA confirming construct preparation and the functioning of replicon elements. Similarly, expression of the YFV ED-III protein was confirmed using various mammalian cell lines in cell culture. Mammalian cells transfected with the replicon encoding the YFV ED-III protein, designated pSinED-III, were assayed for protein expression initially using antibody directed against the C-terminal histidine tag fused to the expressed protein. The recombinant histidine tag was detected in BHK-21, COS-7, HEK-293 and Vero-76 cells by indirect IFA using anti-His_6 mouse monoclonal antibody. Different transfection efficiencies were observed for the different cell lines evaluated, which may be explained by the transfectability or the ease of introduction of DNA into a cell. Additionally, certain methods of introduction may be more efficient or better suited to certain cell lines, which are reflected by higher rates of transfected cells. The expression of recombinant YFV ED-III antigen was further confirmed using YFV ED-III immune mouse serum. The immunogenicity of these constructs was subsequently evaluated using a mouse model.

CHAPTER 3: Immunogenicity of a DNA-launched Sindbis replicon encoding the yellow fever virus ED-lll protein in mice

3.1 Introduction

The YFV ED-lll protein contains epitopes recognised by B- and T-cells (Beasley & Barrett, 2002; Wu *et al.*, 2003; Sánchez *et al.*, 2005; de Melo *et al.*, 2013). Antibody directed to domain lll has also been shown to be an efficient blocker of flavivirus adsorption (Crill & Roehrig, 2001). In addition, the recombinant flavivirus ED-lll protein has been shown to elicit a cell-mediated immune response with a predominant Th1 phenotype characterised by the release of IFN-γ and lL-2, as well as a neutralising antibody response (Chu *et al.*, 2007; Etemad *et al.*, 2008; Verma *et al.*, 2009). Additionally, the immune response elicited by WNV and DEN ED-lll protein has been demonstrated to be protective in mice (Chen *et al.*, 2007; Chu *et al.*, 2007). As the YFV ED-lll protein contains epitopes recognised by B- and T-cells the use of this protein for immunisation may potentially induce both a cell-mediated and a humoral immune response, which have been considered to be important in YFV infection.

DNA vaccines were initially developed in an attempt to elicit a CTL response shown to be essential for the clearance of viral infections (Matloubian *et al.*, 1994). A DNA immunisation mechanistic study indicated that the intracellular and/or extracellular localisation and subsequent processing of an antigen determines the immune response induced (Whitton e*t al.*, 1999). Protein antigens are cleaved by endoproteases and exoproteases into peptides, which can associate with MHC class l or ll molecules for presentation to circulating T-cells. The peptide binding grooves of MHC class l and ll molecules differ structurally and peptide binding depends on the steric configuration. Therefore, MHC class l molecules bind peptides of 8 - 11 residues in length and MHC class ll molecules bind peptides of 10 - 34 residues in length (Chicz *et al.*, 1993). Peptides generated by cytoplasmic processing generally associate with MHC class l molecules (Oh *et al.*, 1997). After association with MHC class l or ll molecules, the MHC/peptide complexes are transported to the plasma membrane by different routes (Chicz *et al.*, 1993; Harding & Geuze, 1993; Wubbolts *et al.*, 1996). After fusion with the plasma membrane (Wubbolts *et al.*, 1996), MHC/peptide complexes are displayed to circulating T-cells, which become activated based on the affinity of the T-cell receptor for the displayed peptide (Ward & Qadri, 1997) and the bridging of two or more T-cell receptors (Cochran *et al.*, 2000). Peptides displayed on MHC class l molecules are recognised by $CD8^+$ T-cells, also known as CTL's, whereas peptides displayed on MHC class ll molecules are recognised by $CD4^+$ T-cells (Meuer *et al.*, 1982). However, a proportion of $CD4^+$ and $CD8^+$ T-cells can also recognise MHC class l (de Bueger

et al., 1992) and ll antigens (Spits e*t al.*, 1983), respectively. The activity of $CD4^+$ T-cells is important during an acute infection (Matloubian *et al.*, 1994), especially as $CD4^+$ T-cells are essential in generating and maintaining a virus-specific CTL or $CD8^+$ T-cell response (von Herrath *et al.*, 1996) and $CD4^+$ T-cells with a Th1 and Th2 phenotype have been shown to support clonal expansion and antibody production by B-cells (Smith *et al.*, 2000).

The development of $CD4^+$ Th subsets is mediated by cytokine production early in the immune response to an antigen and subsequently distinct patterns of cytokine release are associated with each type of Th subset. $CD4^+$ T-cells can differentiate into one of two Th phenotypes, designated Th1 and Th2, and functional heterogeneity may exist within each phenotype (Mosmann e*t al.*, 1986). The nature of the antigen and dose may play a role in triggering either a Th1 or Th2 phenotype. The development of a Th1 phenotype is primarily directed by IL-12 (Hsieh *et al.*, 1993) and is associated with the release of IL-2 and/or IFN-γ post-stimulation with an antigen (Mosmann *et al.*, 1986). A Th1 phenotype is generally associated with the induction of a cell-mediated immune response (Kurt-Jones e*t al.*, 1987) illustrated by the activation of macrophages and subsequent induction of IFN-γ and IL-2 release by antigen specific T-cells (Rossi-Bergmann *et al.*, 1993). A Th2 phenotype is directed by IL-4 (Hsieh *et al.*, 1992) and is associated with the release of IL-4 (Mosmann e*t al.*, 1986) and IL-10 (Hsieh *et al.*, 1993), amongst other cytokines, post-stimulation with an antigen. A Th2 phenotype is generally associated with the induction of an antibody response (Kurt-Jones e*t al.*, 1987) and B-cells have been shown to be more efficient in activating IL-4 production (Rossi-Bergmann *et al.*, 1993). The Th1 and Th2 phenotypes are reciprocally regulated by IFN-γ and IL-4, thus the production of IL-4 inhibits the development of a Th1 phenotype (Hsieh *et al.*, 1992). The development of a Th1 phenotype is suppressed by IL-10 due to the inhibition of IL-12 release by macrophages (Hsieh *et al.*, 1993). Both Th1 and Th2 phenotypes assist B-cells in antibody production. A Th2 phenotype strongly enhances antibody production, primarily IgE and IgG1 production, whereas a Th1 phenotype induces IgM and suppresses IgE production by B-cells. IFN-γ release by Th1 cells inhibits the enhancing activity on antibody production of Th2 cells (Mosmann e*t al.*, 1986) and partially inhibits the proliferative responses in Th2 cells induced by IL-4 (Fernanadez-Botran *et al.*, 1988). Fiorentino and colleagues demonstrated that a detectable antibody response is often absent during a cell-mediated immune response characterised by strong Th1 activity (Fiorentino *et al.*, 1989).

The aim of this chapter was to evaluate the immune response induced by the pSinED-lll replicon in mice. The specific cell-mediated and humoral immune responses elicited in response to immunisation were evaluated. Cytokine profiling was used to determine the

type of cell-mediated immune response and antibody against YFV was detected using ELISA and IFA to investigate humoral immune responses.

3.2 Methods and materials

3.2.1 Preparation of replicon DNA and recombinant protein for the immunisation of mice

Immune responses were determined for mice immunised with the replicon-based vaccine alone and for mice that were immunised with the replicon vaccine and boosted with a bacterially expressed recombinant YFV antigen. Similarly, mice were mock immunised with a replicon encoding GFP and selected groups were boosted with commercially purchased recombinant GFP.

Replicon DNA for the immunisation of mice was prepared using the EndoFree® Plasmid Maxi kit (Qiagen, Hilden, Germany) according to the manufacturer's instructions. Briefly, a starter culture was prepared by the inoculation of two 5 ml aliquots of pre-warmed 2X TY/kan broth with pSinGFP and pSinED-lll glycerol stock, respectively, and incubated at 37°C o/n with shaking at 200 rpm. Each culture was diluted 1:1 000 in a total volume of 100 ml 2X TY/kan and incubated at 37°C for approximately 16 hours with shaking at 200 rpm. The bacterial pellet was harvested by centrifugation at 6 000 x *g* for 15 minutes at 4°C. Each pellet was re-suspended in 10 ml P1 buffer and subsequently cells were lysed by the addition of P2 buffer and incubation at room temperature for 5 minutes. The addition of LyseBlue® to P1 buffer facilitated monitoring of cell lysis indicated by a colour change to blue. Thereafter, 10 ml pre-chilled P3 buffer was added to the cell lysate and filtered through separate QIAfilter cartridges, and the filtered lysate was incubated on ice for 30 minutes after the addition of 2,5 ml ER buffer. QIAGEN®-tips 500 were equilibrated, DNA was bound by the addition of the prepared filtered lysate, washed twice with 30 ml QC buffer and subsequently DNA was eluted in 15 ml QN buffer. DNA was precipitated with 10,5 ml isopropanol at room temperature and the DNA pellet harvested by centrifugation at 5 000 x *g* for 1 hour at 4°C. DNA was washed with 5 ml endotoxin-free 70% ethanol at room temperature and harvested by centrifugation at 5 000 x *g* for 1 hour at 4°C. After discarding the supernatant, each pellet was air-dried and re-dissolved in nuclease-free water. The DNA concentration of the pSinGFP and pSinED-lll replicon DNA was determined using a Nanodrop™ 2000.

Replicon DNA was confirmed by double restriction digestion using *Not*I and *Xho*I restriction endonucleases for excision of the gene encoding the GFP and YFV ED-lll protein from the

pSinGFP and pSinED-III replicon DNA, respectively. The double restriction digestion reaction mixture (Table 3.1) was incubated at 37°C for 2 hours.

Table 3.1: Composition of double restriction digestion reaction mixture for confirmation of replicon DNA for immunisation

Components:	pSinGFP reaction	pSinED-III reaction
	Volume (µl):	Volume (µl):
10X Buffer D	2,0	2,0
Replicon DNA	2,0	2,0
*Not*I (10 units/µl)	1,0	1,0
*Xho*I (10 units/µl)	1,0	1,0
Nuclease-free water	14,0	14,0
Total reaction volume	20,0	20,0

The DNA fragments were separated by agarose gel electrophoresis as described in section 2.1.1. After confirmation, replicon DNA was diluted in 0,9% sterile saline solution (refer to appendix F for preparation of saline solution) to a final concentration 2 µg/100 µl and 25 µg/100 µl replicon DNA for mouse experiments.

Commercially available recombinant purified GFP protein (Merck, California, USA) expressed in *E. coli* was used for mock immunising the control groups of mice receiving a mixed modal immunisation regime. The protein concentration was determined using the Quant-iT™ protein assay (Invitrogen™, Oregon, USA) according to the manufacturer's instructions. Briefly, Quant-iT™ working solution was prepared and three 200 µl aliquots of protein standards were prepared from stock standards by diluting each 1:20 in Quant-iT™ working solution. Protein samples were diluted at 1:200 in Quant-iT™ working solution, the Qubit™ fluorometer (Invitrogen™, Oregon, USA) was calibrated using the standard preparations and subsequently the protein concentrations were determined. The purified GFP protein was diluted in 0,9% sterile saline solution to 10 µg/100 µl.

Recombinant YFV ED-III protein was prepared as previously described (Smouse, 2013). Briefly, the 17D recombinant YFV ED-III protein was expressed in *E. coli* from a previously prepared pQE80L/ED-III construct containing the gene encoding the 17D YFV ED-III protein. The presence of the gene encoding the 17D YFV ED-III protein in pQE80L/ED-III stored as glycerol stocks at -80°C was confirmed by double restriction digestion of purified plasmid using *Bam*HI (Promega, Wisconsin, USA) and *Hind*III (Promega, Wisconsin, USA) restriction endonucleases. Plasmid was prepared from an o/n starter culture prepared by inoculation of

a 5 ml aliquot of LB/amp with 10 µl pQE80L/ED-lll glycerol stock and incubation at 37°C o/n with shaking at 200 rpm. Plasmid DNA was purified using the PureYield™ Plasmid Miniprep System according to the manufacturer's instructions and the presence of the gene encoding the 17D YFV ED-lll was confirmed by restriction digestion at 37°C for 2 hours as shown in Table 3.2.

Table 3.2: Composition of double restriction digestion reaction mixture for confirmation of pQE80L/ED-lll glycerol stock

Components:	pQE80L/ED-lll reaction
	Volume (µl):
10X Buffer E	2,0
pQE80L/ED-lll DNA (159,0 ng/µl)	2,0
*Bam*Hl (10 units/µl)	1,0
*Hind*lll (10 units/µl)	1,0
Nuclease-free water	14,0
Total reaction volume	20,0

DNA fragments were visualised by agarose gel electrophoresis as described in section 2.1.1. After confirmation of the presence of the gene encoding the 17D YFV ED-lll protein in pQE80L/ED-lll glycerol stock, protein expressed and purification was performed. Briefly, 25 ml LB/amp broth was inoculated with 250 µl pQE80L/ED-lll glycerol stock and incubated at 37°C o/n with shaking at 200 rpm. Each starter culture was diluted at 1:10 in 225 ml pre-warmed LB/amp broth and incubated at 37°C with shaking at 200 rpm until an optical density $(OD)_{600nm}$ of 1,5 to 1,6 was reached. Protein expression was induced by the addition of IPTG to a final concentration of 1 mM and cultures were incubated at 37°C for 4 hours with shaking at 200 rpm. Cells were harvested by centrifugation at 10 000 x *g* for 20 minutes at 4°C and the pellet was stored at -20°C until protein purification.

Bacterially expressed recombinant YFV ED-lll protein was purified from the pellets by immobilised metal ion chromatography (IMAC) utilising the affinity of the C-terminal histidine tag for a pre-charged nickel(ll) matrix. The lysis of the bacterial cells was facilitated by re-suspension of the thawed bacterial pellets in 20 ml Bugbuster® Protein Extraction Reagent (Novagen, California, USA) containing 20 µl Benzonase® Nuclease (Novagen, California, USA) and lyophilised lysozyme from chicken egg white (Sigma, Missouri, USA) to final concentration of 1 mg/ml. The cell suspension was incubated on ice for 30 minutes with gentle agitation and sonicated on ice ten times with 15 second bursts followed by 15 second resting intervals. After sonication, the cell suspension was clarified by centrifugation at 10

000 x *g* for 10 minutes at 4°C. The expressed protein has previously been shown to be in the insoluble phase (Smouse, 2013).

The recombinant YFV ED-lll protein was purified using a denaturing protein purification to facilitate the solubilisation of inclusion bodies containing the recombinant protein using Protino® Ni-TED 1000 columns (Macherey-Nagel, Düren, Germany) according to the manufacturer's instructions. Briefly, the pellets were washed by re-suspension in 2 ml lysis-equilibrium-wash (LEW) buffer followed by centrifugation at 10 000 x *g* for 30 minutes at 4°C. The supernatant was aspirated and the pellet was re-suspended in 2 ml denaturing solubilisation buffer containing 8 M urea (Promega, Wisconsin, USA) to facilitate the solubilisation of inclusion bodies. After incubation at room temperature for 1 hour with gentle agitation, the cell extract was obtained by centrifugation at 10 000 x *g* for 30 minutes at 20°C. After equilibration of a Protino® Ni-TED 1000 packed column with 2 ml denaturing solubilisation buffer, protein was bound to the pre-equilibrated column by the addition of the cell extract. The column was washed twice with 2 ml denaturing solubilisation buffer to reduce non-specific binding and subsequently protein was eluted in five 500 µl fractions using denaturing elution buffer containing 8 M urea and 0,25 M imidazole. The protein concentration of each fraction, designated eluate one to five, was determined using the Quant-iT™ protein assay according to the manufacturer's instructions.

Samples collected during protein purification were separated by sodium dodecyl sulphate polyacrylamide gel electrophoresis (SDS-PAGE) at 60V for 15 minutes followed by 140V for 75 minutes on a 12,5% resolving 4% stacking SDS-PAGE gel (Table 3.3).

Table 3.3: Composition of SDS-PAGE gel for electrophoretic analysis of protein purification product

Component:	12,5% Resolving gel	4% Stacking gel
	Volume (ml):	Volume (ml):
30%/8% Acryl/Bis-acrylamide (Sigma, Missouri, USA)	6,666	0,800
3 M Tris-HCl at a pH of 8,8 stock solution	2,130	-
0,5 M Tris-HCl at a pH of 6,8 stock solution	-	0,420
Deionised water	7,206	4,740
10% sodium dodecyl sulphate (SDS) (BDH, Poole, England)	0,400	0,060
Fresh 10% ammonium persulphate (APS) (Promega, Wisconsin, USA)	0,100	0,120
Tetramethylethylenediamine (TEMED) (Merck, Darmstadt, Germany)	0,020	0,012

The PageRuler™ prestained protein ladder (Thermo Scientific, Illinois, USA) with a range of 10 – 170 kDa was used for estimation of the size of the separated proteins. Samples were prepared for SDS-PAGE by the addition of Lane Marker Reducing Sample Buffer (Thermo Scientific, Illinois, USA) and incubation at 95°C for 5 minutes. Proteins were visualised by staining with 0,2% Coomassie Brilliant Blue (Fluka, Buchs, Germany) and the gel was destained using a destaining solution (refer to appendix F for preparation of stain and destain).

The eluate containing the highest purity and concentration YFV ED-lll protein was selected for characterisation and for immunisation of mice. The selected eluate was resolved by 12,5% resolving 4% stacking SDS-PAGE as described in section 3.2.1. Thereafter, a Western blot was performed to detect the C-terminal histidine tag fused to the YFV ED-lll protein using the Pierce® Fast Western Blotting kit (Thermo Scientific, Illinois, USA). Protein was transferred to a BioTrace™ polyvinylidene fluoride (PVDF) transfer membrane (PALL Corporation, Florida, Mexico) with a pore size of 0,2 µm after activation of the PVDF membrane in methanol for 5 minutes with gentle agitation, rinsing with deionised water for 2 minutes with gentle agitation and soaking in transfer buffer (refer to appendix F for buffer composition) for 3 minutes with gentle agitation. Prior to the transfer of protein, the SDS-PAGE gel was incubated in transfer buffer for 15 minutes with gentle agitation. Subsequently, proteins were transferred using a Trans-Blot® SD semi-dry electrophoretic transfer cell (Bio-rad, California, USA) at 20V for 1 hour. Post-transfer the PVDF membrane was washed twice with Tris-buffered saline (TBS) at a pH of 7,5 (refer to appendix F for buffer composition) for 10 minutes to remove any residual methanol and was incubated at 4°C o/n in mouse monoclonal anti-His_6 antibody diluted at 1:200 in antibody diluent. Unbound antibody was removed by washing the PVDF membrane three times using TBS containing 0,05% Tween® 20 for 10 minutes with gentle agitation. The PVDF membrane was incubated in optimised horseradish peroxidase reagent diluted at 1:10 in antibody diluent for 15 minutes with gentle agitation. The membrane was washed using TBS containing 0,05% Tween® 20 three times for 10 minutes with gentle agitation to remove any unbound antibody and reduce background, and a final wash for 10 minutes with gentle agitation using TBS. The SuperSignal® West Pico Substrate was prepared by a 1:1 dilution of SuperSignal® West Pico Luminol/Enhancer solution and SuperSignal® West Stable Peroxide solution. The PVDF membrane was exposed to SuperSignal® West Pico Substrate for 5 minutes with gentle agitation, covered in clear plastic wrap to prevent drying and bound antibody visualised by exposure of the membrane and CL-XPosure™ X-ray film (Thermo Scientific, Illinois, USA) to X-ray for 30 seconds. The image was developed for 3

minutes in developer solution (Axim, Gauteng, RSA) and fixed for 2 minutes in fixer solution (Axim, Gauteng, RSA). The film was rinsed with water to remove any residual fixer solution.

After characterisation of the expressed YFV ED-lll protein, refolding of the protein was facilitated by ultrafiltration. The selected eluate was diluted 1:3 in LEW buffer and filtered using a Millipore filter (Millipore Corporation, Massachusetts, USA) with a molecular weight cut-off of 10 kDa facilitating the removal of water and salts to approximately half the initial volume. The recombinant 17D YFV ED-lll protein, estimated to be 13,35 kDa in size, was retained during ultrafiltration. The protein concentration was determined using the Quant-iT™ protein assay according to the manufacturer's instructions. The refolded purified 17D YFV ED-lll protein was diluted in 0,9% sterile saline solution and filter sterilised using a 0,22µm filter (GVS, California, USA). The concentration of the purified 17D YFV ED-lll protein was confirmed and adjusted to 10 µg/100 µl in 0,9% filter sterilised saline solution.

3.2.2 Immunisation of mice

Eight groups containing five six week old NIH mice obtained from Animal Unit at the University of the Free State were inoculated by the IM route according to the immunisation regime (Table 3.4) approved by the University of the Free State's Animal Ethics Committee (ECUFS NR 24/2011). Mice were kept five in a cage of 27cm by 43cm at a height of 15cm with bedding, and food and water *ad libitum*. Inoculations were administered by Dr. Stephen Robinson (BVSc). Doses were administered in a volume of 100 µl to the tibialis anterior muscle. Mice were monitored daily throughout the study with additional monitoring after the administration of immunisations. Mice were anaesthetised using inhalant halothane, exsanguinated and sera were collected from the orbital sinus for the determination of antibody responses by trained personnel from the Animal Unit at the University of the Free State two weeks after administration of the final immunisations. Spleens were aseptically removed and splenocytes were isolated and stimulated *in vitro* to facilitate the characterisation of the cell-mediated immune response.

Four control groups were immunised with the pSinGFP replicon and/or purified GFP. Control groups 1 and 3 received three consecutive DNA immunisations with the pSinGFP replicon containing 2 µg and 25 µg replicon DNA, respectively. Whereas control groups 2 and 4 received two DNA immunisations followed by a booster with 10 µg purified GFP. The four experimental groups were immunised with the pSinED-lll replicon and/or purified YFV ED-lll protein. Groups 5 and 7 received three consecutive DNA immunisations with the pSinED-lll replicon containing 2 µg and 25 µg replicon DNA, respectively. Groups 6 and 8

received a mixed modal immunisation regime consisting of two DNA immunisations followed by a booster with 10 µg recombinant purified YFV ED-III protein.

Table 3.4: Immunisation regime, including the day of inoculation, the vaccine description and the dose administered

Group:	Day:	Vaccine description:	Dose (µg):
1	0	pSinGFP DNA	2
	14	pSinGFP DNA	2
	28	pSinGFP DNA	2
2	0	pSinGFP DNA	2
	14	pSinGFP DNA	2
	28	rGFP protein	10
3	0	pSinGFP DNA	25
	14	pSinGFP DNA	25
	28	pSinGFP DNA	25
4	0	pSinGFP DNA	25
	14	pSinGFP DNA	25
	28	rGFP protein	10
5	0	pSinED-III DNA	2
	14	pSinED-III DNA	2
	28	pSinED-III DNA	2
6	0	pSinED-III DNA	2
	14	pSinED-III DNA	2
	28	rED-III protein	10
7	0	pSinED-III DNA	25
	14	pSinED-III DNA	25
	28	pSinED-III DNA	25
8	0	pSinED-III DNA	25
	14	pSinED-III DNA	25
	28	rED-III protein	10

3.2.3 Determination of antibody responses against YFV by indirect ELISA and indirect IFA

Mouse sera were screened for antibody against YFV using a previously described and optimised in house indirect ELISA (Smouse, 2013). YFV cell lysate antigen was prepared from Vero-76 cells infected with 17D YFV at a multiplicity of infection (MOI) of 0,1. Post-infection cells were incubated at 37°C and monitored for cytopathic effect (CPE). Infection of cells by 17D YFV was determined by an IFA using human sera from a vaccinated individual. Briefly, an aliquot of infected cells was re-suspended in 10% FBS in PBS at a pH of 7,4, 10 µl applied to a microscope slide, dried and fixed in pre-chilled acetone for 20 minutes. Serum from an individual vaccinated against YFV, designated VBD19/09,

previously confirmed to contain antibody against YFV by ELISA, as well as neutralising antibody by a neutralisation test (Smouse, 2013) was diluted 1:10 in PBS, applied to each well and incubated at 37°C for 20 minutes in a humid container. Three 15 second washes were performed followed by a 15 second rinse with deionised water. Goat anti-human IgG FITC (Zymed Laboratories, Cardiff, UK) at a dilution of 1:40 in 0,1% Evans blue in PBS were reacted with the cells at 37°C for 30 minutes in a humid container. After washing, cells were visualised using an OPTIPHOT fluorescence microscope. Following confirmation of minimum 80% infectivity, infected cells were harvested by centrifugation at 12 500 x *g* for 20 minutes at 4°C. The pellet was re-suspended in borate buffered saline (BBS) at a pH of 9,0 (refer to appendix F for buffer composition) containing 1% Triton X-100 and sonicated on ice at 5 minute intervals. The supernatant was clarified and collected by centrifugation at 10 000 x *g* for 20 minutes at 4°C. The supernatant was collected for use as detection antigen and mock antigen was prepared using uninfected cells. The supernatant was stored at -80°C.

The ELISA was used for the detection of antibodies induced by the candidate vaccine. Unless otherwise specified, triplicate washes were performed for 10 seconds with 300 µl PBS at a pH of 7,4 containing 0,1% Tween® 20 per well, all incubations were performed at 37°C for 1 hour and all volumes were 100 µl. Sera from two vaccinated individuals were included as positive controls. Optimal dilutions were determined for the mock antigen and YFV cell lysate antigen previously based on protein content and checkerboard titration (Smouse, 2013). A 96-well Nunc-Immuno™ MicroWell™ PolySorp® plate (Nunc, Koeln, Germany) was coated with mock antigen at a dilution of 1:800 and YFV cell lysate antigen at a dilution of 1:500 dilution in PBS. The plate was incubated at 4°C o/n in a humid container to facilitate the binding of protein. After washing, each well was blocked with 200 µl 10% skim milk (Elite, Gauteng, RSA) in PBS to reduce non-specific binding. Control samples and mouse sera were diluted at 1:100 using 2% skim milk in PBS and diluted sera were added to the respective wells (Figure 3.1) and incubated at 37°C for 3 hours in a humid container.

After washing, control wells were incubated with goat anti-human IgG horseradish peroxidase (HRPO) conjugate (KPL, Maryland, USA) and wells reacted with mouse sera were incubated with goat anti-mouse IgG HRPO conjugate (KPL, Maryland, USA) diluted 1:2 000 using 2% skim milk in PBS. After washing, 2,2'-azino-bis(3-ethylbenzothiazoline-6-sulphonic acid (ABTS) was added to each well facilitating a colour change in positive reactors. After incubation at room temperature for 20 minutes in the dark, the OD_{405nm} was measured using a Sunrise™ absorbance reader (TECAN, Saltzburg, Austria). The net OD_{405nm} was calculated by subtracting the $OD_{405nm\ Mock\ antigen}$ from the $OD_{405nm\ YFV\ cell\ lysate\ antigen}$. The cut-off value was calculated using the OD_{405nm} values for negative mouse sera from five

mice vaccinated in an unrelated study with bacterially expressed Crimean-Congo haemorrhagic fever virus nucleoprotein. Two positive controls, designated VBD19/09 and VBD49/09, from individuals vaccinated against YFV previously confirmed to have an antibody response against YFV and a neutralising antibody response were included (Smouse, 2013).

Cut-off value = net OD_{405nm} + 2 standard deviations

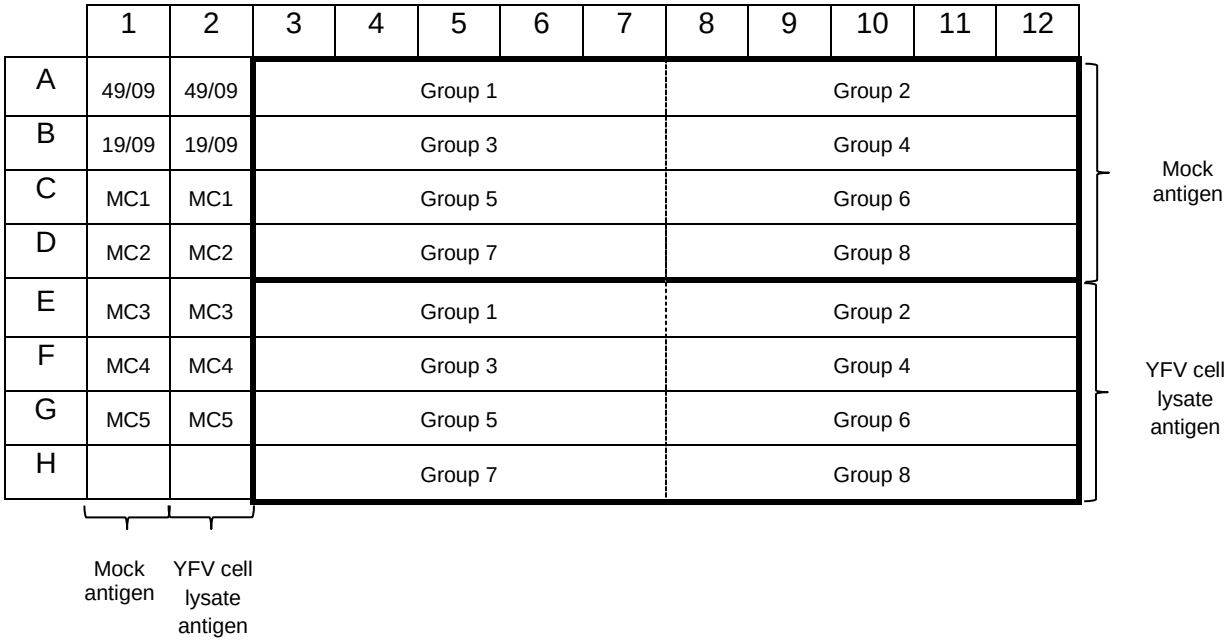

Figure 3.1: Layout of 96-well plate for the detection of anti-YFV antibodies in sera collected from mice

Positive controls (VBD49/09 and 19/09) were included to confirm reactivity of the detection antigen with anti-YFV antibody. Positive controls were obtained from individuals vaccinated against YFV previously shown to have an antibody response against YFV. A panel of negative mouse control sera, designated MC 1 to 5, were included to facilitate the determination of a cut-off value to differentiate positive from negative reactors.

To confirm the results obtained by indirect ELISA, sera were tested using a commercially available indirect IFA (Euroimmun, Lübeck, Germany). The IFA using YFV-infected cells was performed according to the manufacturer's instructions and modified to test mouse sera. Briefly, biochip slides containing 10 tests per slide, comprising of uninfected and YFV-infected cells, were incubated with mouse sera diluted 1:2 in sample buffer at room temperature for 30 minutes. Biochip slides were rinsed and subsequently washed with PBS containing 0,2% Tween® 20 for 5 minutes with gentle agitation. Thereafter, slides were reacted with goat anti-mouse IgG FITC diluted 1:20 in 0,1% Evans blue in PBS at room

temperature for 30 minutes. After washing, embedding medium was used to mount a cover glass and an OPTIPHOT fluorescence microscope was used for visualisation.

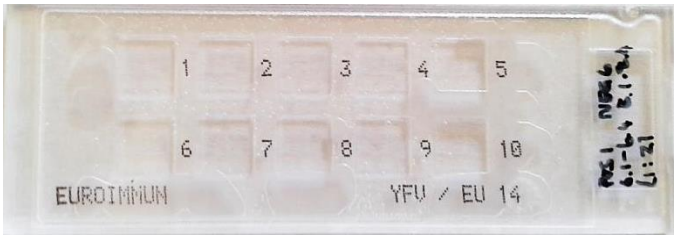

Figure 3.2: Illustration of an anti-YFV biochip slide for the detection of antibodies directed against YFV

Positive sera were diluted two-fold from 1:2 to determine the endpoint antibody titre. A two-fold serial dilution of control mouse serum (Smouse, 2013) in sample buffer was prepared starting at 1:10 and was diluted up to 1:160. The reciprocal of the highest dilution of mouse serum that reacted represented the antibody titre.

3.2.4 Determination of cytokine responses by the stimulation of cultured splenocytes

Spleens harvested from mice were processed for the isolation of splenocytes for culture. The spleen was aseptically removed, placed in a small petri dish in 10 ml cold PBS and cells were forced from the splenic capsule using mechanical disruption. Cell suspensions were incubated at room temperature for 10 minutes to remove large tissue debris, the supernatant was transferred to a clean tube and cells were harvested by centrifugation at 300 x *g* for 8 minutes at 4°C. After centrifugation, the supernatant was aspirated and the pellet was re-suspended in 7 ml cold PBS. Cells were harvested by centrifugation at 300 x *g* for 8 minutes at 4°C and re-suspended in RPMI 1640 (Lonza, Verviers, Belgium) supplemented with 10% FBS, 100 U/ml pen/strep, L-glu to a final concentration of 2 mM and NEAA's. Thereafter, the cell preparation was passed through a 70 µm Nylon cell strainer (BD Falcon™, New Jersey, USA) and incubated on ice until the completion of cell counting.

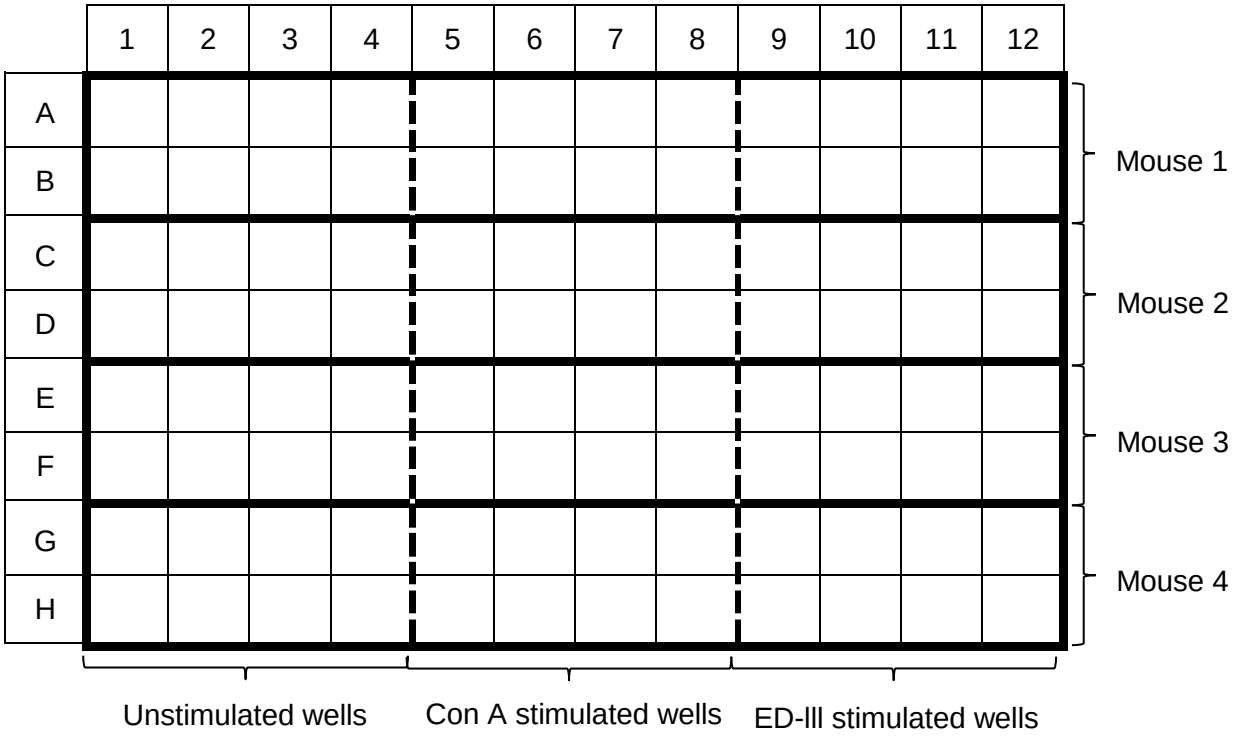

Figure 3.3: Layout of 96-well plates for stimulation of splenocytes

Splenocytes were counted using the trypan blue exclusion method using 0,4% trypan blue in PBS and seeded at 5 x 10^5 cells/well in a 96-well plate (NUNC, Roskilde, Denmark). Splenocytes were stimulated on the day of seeding with 0,25 µg concanavalin A (con A) (Sigma, California, USA) or 0,25 µg purified YFV ED-lll protein per well (Figure 3.3). Unstimulated cells were used as controls. Stimulation was performed in duplicate for each cytokine to be tested. The cell culture supernatant was harvested 3 days post-stimulation and stored at -20°C until testing.

Supernatant fluid from cell culture was used for cytokine profiling performed using commercially available ELISA MAX Mouse IFN-γ, Mouse IL-2, Mouse IL-4 and Mouse IL-10 Deluxe sets (BioLegend, California, USA) according to the manufacturer's instructions. Briefly, Nunc-Immuno™ MicroWell™ MaxiSorp® 96-well plates were coated with 100 µl capture antibody diluted 1:200 in working concentration coating buffer by incubation at 4°C o/n in a humid container. Each plate was washed four times for 60 seconds with 300 µl PBS at a pH of 7,4 containing 0,05% Tween® 20 per well. All subsequent washes were performed in an identical manner, unless otherwise stated, and residual wash buffer was removed after every wash. Each well was blocked with 200 µl diluent A diluted 1:5 using PBS at room temperature for 1 hour with shaking at 200 rpm.

Table 3.5: Concentration of cytokine standards prepared by two-fold serial dilution

Row	IFN-γ (pg/ml):	IL-2 (pg/ml):	IL-4 (pg/ml):	IL-10 (pg/ml):
A	1 000,00	125,00	125,00	2 000,00
B	500,00	62,50	62,50	1 000,00
C	250,00	31,25	31,25	500,00
D	125,00	15,63	15,63	250,00
E	62,50	7,81	7,81	125,00
F	31,25	3,91	3,91	62,50
G	15,63	1,95	1,95	31,25
H	0,00	0,00	0,00	0,00

A range of cytokine standards was prepared for each cytokine by two-fold serial dilution as illustrated in Table 3.5. On each plate, a 100 µl aliquot of each dilution was added per well in triplicate to construct a standard curve used to calculate the concentration of cytokine in each sample. A 100 µl aliquot of supernatant fluid from unstimulated, con A stimulated and YFV ED-lll stimulated cells was added in duplicate for each mouse (Figure 3.4). Plates were incubated at room temperature for 2 hours with shaking at 200 rpm.

	1	2	3	4	5	6	7	8	9	10	11	12
A				U	C	E	U	C	E	U	C	E
B				U	C	E	U	C	E	U	C	E
C				U	C	E	U	C	E	U	C	E
D				U	C	E	U	C	E	U	C	E
E				U	C	E	U	C	E	U	C	E
F				U	C	E	U	C	E	U	C	E
G				U	C	E	U	C	E	U	C	E
H				U	C	E	U	C	E	U	C	E

Standards

Figure 3.4: Layout of 96-well plates for the detection of cytokines by ELISA

The highlighted area containing six blocks each, includes the duplicate unstimulated (U), con A stimulated (C) and ED-lll stimulated (E) wells, representing the cell culture supernatant collected for each mouse.

After washing, a 100 µl aliquot of the detection antibody diluted 1:200 in diluent A was added to each well and plates were incubated at room temperature for 1 hour with shaking at 200 rpm. After washing, a 100 µl avidin-HRPO diluted 1:1 000 in diluent A was added to each well and plates were incubated at room temperature for 30 minutes with shaking at 200 rpm. Thereafter, each plate was washed five times for 60 seconds with 300 µl PBS containing 0,05% Tween® 20 per well to reduce background. Positive reactors were detected by the addition of 100 µl of 3,3',5,5'-tetramethylbenzidine (TMB) substrate solution per well and plates were incubated at room temperature for 20 minutes in the dark. The reaction was stopped by the addition of a 100 µl 2N sulphuric acid to each well and the OD_{450nm} was measured using a Sunrise™ absorbance reader. A standard curve was constructed for each plate using the mean absorbance values for each concentration of standard. The concentration of cytokine for each well was determined using the equation of the standard curve.

3.2.5 Comparison of cytokine release for different groups of mice

The student t-test was applied to determine whether the release of cytokine was significantly different in experimental groups when compared to control groups. The p-value or probability value was calculated using Excel® 2010 (Microsoft®, Washington, USA) software with two-tailed distribution and two-sample unequal variance parameters. To determine dose and/or regime-related induction of immune responses the t-test was applied to groups receiving different regimes at the same dose and groups receiving the same regime at different dosages. Dose or regime-related effects were based on the net release of cytokine for each mouse in the experimental group calculated by subtraction of the mean cytokine release for each corresponding control group from each mouse in the experimental group.

3.2.6 Detection of humoral anti-vector immunity elicited post-immunisation

Mouse sera were screened for antibodies against SINV using an indirect ELISA developed and optimised in an unrelated study (Hanekom, 2014). The detection of a humoral immune response against the encoded SINV NS proteins was performed as the SINV NS proteins facilitate the replication of the construct *in vivo* and antibody against it may reduce the efficacy of booster doses. SINV cell lysate antigen was prepared using Vero-76 cells infected at a MOI of 0,1 with the SINV EgAR339 strain. Cells were monitored daily for CPE and harvested after initial signs of CPE by centrifugation at 12 500 x *g* for 20 minutes at 4°C. Cells were lysed in BBS at a pH of 9,0 supplemented with 1% Triton X-100. Thereafter, cells were sonicated at 5 minute intervals on ice. The supernatant was obtained by centrifugation

at 10 000 x *g* for 20 minutes at 4°C. Mock antigen was prepared using uninfected cells. The supernatant was stored at -80°C.

Unless otherwise indicated, all incubations were performed in a humid container for 1 hour at 37°C, plates were washed three times for 10 seconds with 300 µl PBS at a pH of 7,4 containing 0,1% Tween® 20 per well and all volumes were 100 µl. Optimal dilutions of mock antigen and SINV cell lysate antigen was determined previously based on protein content and checkerboard titrations (Hanekom, 2014). A 96-well Nunc-Immuno™ MicroWell™ PolySorp® plate was coated with mock antigen at a dilution of 1:800 and SINV cell lysate antigen at a 1:1 000 dilution in PBS o/n at 4°C. After washing, wells were blocked with 200 µl 10% skim milk in PBS to reduce non-specific binding. After washing, mouse sera diluted 1:100 in 2% skim milk in PBS were added to the respective wells (Figure 3.5) and plates were incubated at 37°C for 3 hours in a humid container.

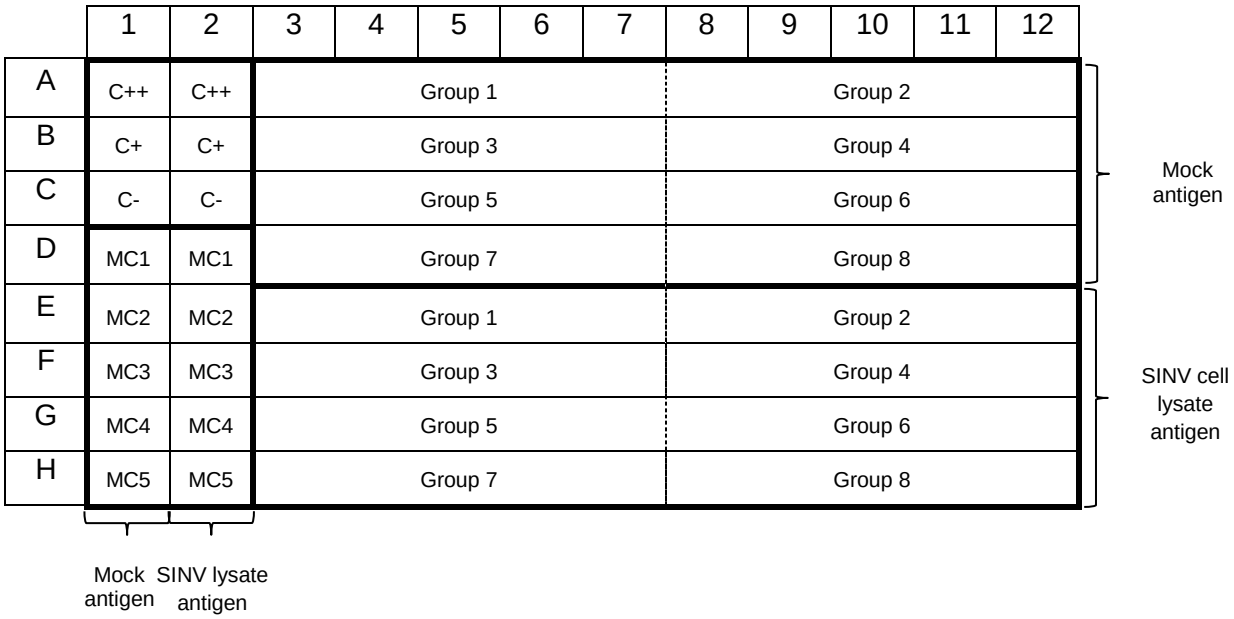

Figure 3.5: Layout of 96-well plate for the detection of anti-SINV antibodies by an ELISA

Positive and negative controls, included a high positive human control (C++) VBD27/08/05, a positive human control (C+) VBD58/08/17 and a negative human control (C-) VBD02/08/12. A panel of negative mouse control sera, designated MC1 to 5, were included to facilitate the determination of a cut-off value to differentiate positive from negative reactors.

Positive and negative controls were included to confirm reactivity of the SINV cell lysate antigen with anti-SINV antibody, which included human sera from SINV-infected and naïve individuals. The presence/absence of antibody in the positive and negative controls has been previously been confirmed by ELISA and the presence of neutralising antibody was determined by a neatralisation assay (Hanekom, 2014). A panel of negative mouse sera vaccinated in an unrelated study with the Crimean-Congo haemorrhagic fever virus nucleoprotein was used to determine a cut-off value. Control samples were diluted 1:100 in 2% skim milk in PBS.

After incubation and washing, goat anti-mouse IgG HRPO diluted 1:2 000 in 2% skim milk was added to each well. However, human control samples were incubated with goat anti-human IgG HRPO diluted at 1:2 000 in 2% skim milk. After incubation and washing, ABTS was added to each well, the plate was incubated at room temperature for 20 minutes in the dark and the OD_{405nm} was measured using a Sunrise™ absorbance reader. The net OD_{405nm} was calculated by subtracting the $OD_{405nm\ Mock\ antigen}$ from the $OD_{405nm\ SINV\ cell\ lysate\ antigen}$. The cut-off value was calculated using the OD_{405nm} values for the negative mouse sera from five mice.

$$Cut\text{-}off\ value = net\ OD_{405nm} + 3\ standard\ deviations$$

3.3 Results

3.3.1 Preparation of replicon DNA and recombinant protein for the immunisation of mice

Replicon DNA was purified using the EndoFree® Plasmid Maxi kit for efficient removal of endotoxin from the bacterial preparation yielding DNA suitable for immunisation. The presence of the genes encoding the GFP and the YFV ED-III protein in the purified pSinGFP and pSinED-III replicon DNA, respectively, was confirmed by restriction digestion analysis prior to the immunisation of mice. The presence of a band of approximately 1 108 bp and 696 bp in lanes 2 and 3 corresponds to the genes encoding the GFP and YFV ED-III protein, respectively, as illustrated in Figure 3.6.

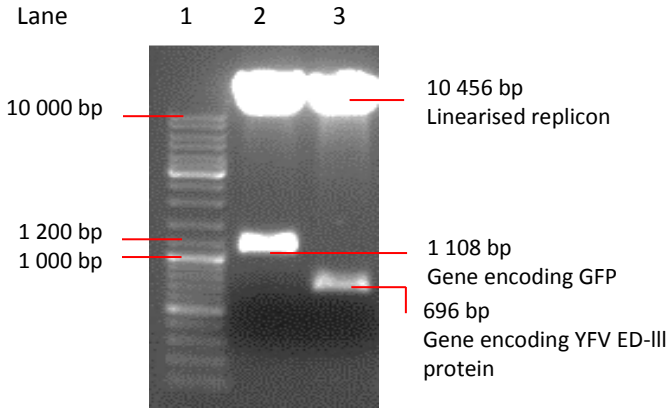

Figure 3.6: Agarose gel electrophoretic analysis to confirm the integrity of the purified pSinGFP and pSinED-III replicon DNA for the immunisation of mice

Lane 1 – O'GeneRuler™ molecular weight marker; Lane 2 – Purified pSinGFP replicon DNA double digested using *Not*I and *Xho*I; Lane 3 – Purified pSinED-III replicon DNA double digested using *Not*I and *Xho*I.

After preparation of replicon DNA for immunisation, recombinant YFV ED-III protein was expressed in a bacterial expression system. Prior to protein expression, DNA purified from an o/n culture prepared using pQE80L/ED-III glycerol stock was confirmed to contain the pQE80L/ED-III plasmid encoding the 17D YFV ED-III protein by double restriction digestion analysis using *Bam*HI and *Hind*III restriction endonucleases. The DNA fragment, approximately 300 bp in length, represents the gene encoding the 17D YFV ED-III protein, whereas the DNA fragment of approximately 4 751 bp represent the pQE80L plasmid. Thereafter, the pQE80L/ED-III glycerol stock was used for protein expression.

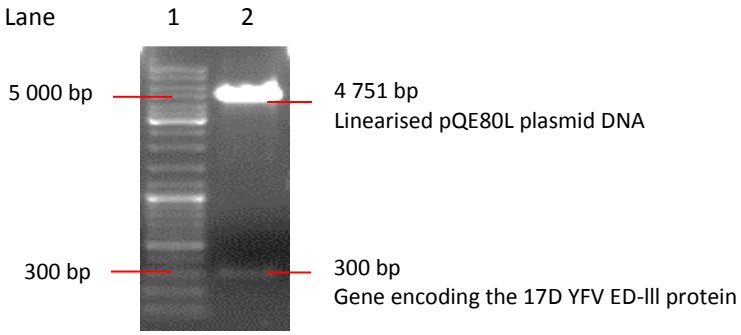

Figure 3.7: Agarose gel electrophoretic analysis for the confirmation of pQE80L/ED-III glycerol stock for protein expression

Lane 1 – O'GeneRuler™ molecular weight marker; Lane 2 – pQE80L/ED-III double digested using *Bam*HI and *Hind*III.

Expression of the 17D YFV ED-III protein from the pQE80L/ED-III plasmid was induced by the addition of IPTG to cultured bacteria. Subsequently, the 17D YFV ED-III protein was purified using pre-charged nickel(II) columns and the purified protein was collected in five 500 µl eluates. The protein concentration in each eluate was determined using the Quant-iT™ protein assay (Table 3.6).

Table 3.6: Protein concentration in each eluate after denaturing purification

Eluate:	Protein concentration (µg/ml):
1	1 354
2	2 160
3	960
4	706
5	598

Fractions collected during protein purification were separated by SDS-PAGE, including the washing, binding and elution flow-through as illustrated in Figure 3.8.

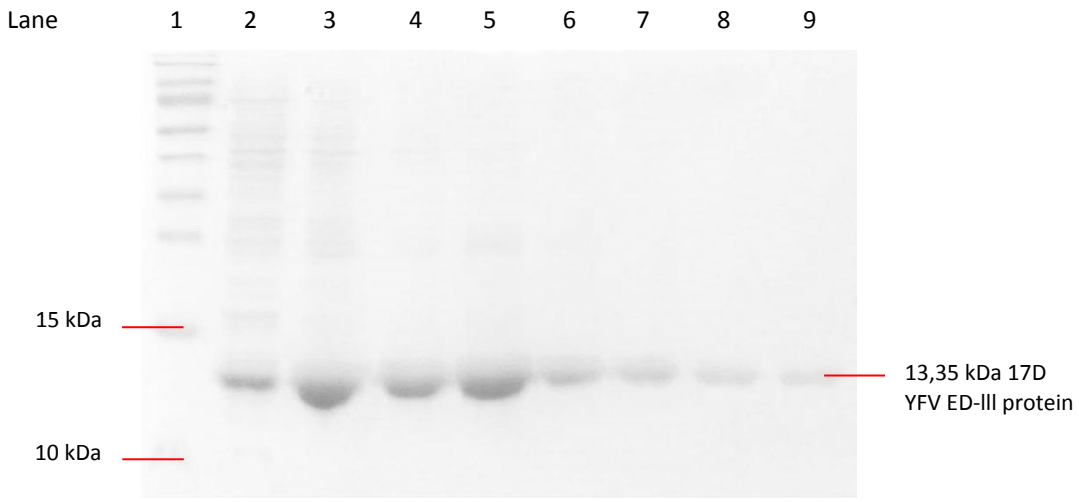

Figure 3.8: SDS-PAGE analysis of fractions collected during protein purification

Lane 1 – 3 µl PageRuler™ prestained protein ladder; Lane 2 – 5 µl Fraction collected during washing; Lane 3 – 5 µl Fraction collected during binding; Lane 4 – 5 µl Eluate 1; Lane 5 – 5 µl Eluate 2; Lane 6 – 5 µl Eluate 3; Lane 7 – 5 µl Eluate 4; Lane 8 – 5 µl Eluate 5; Lane 9 – 2 µl Positive control consisting of purified 17D YFV ED-III protein.

Eluate 2 contained purified 17D YFV ED-III protein, approximately 13,35kDa in size, at a high concentration and was selected for characterisation, refolding and immunisation. The 17D YFV ED-III protein was characterised in a Western blot using anti-His_6 mouse monoclonal antibody as illustrated in Figure 3.9. The 17D YFV ED-III protein was expressed fused to an N-terminal histidine tag, which was detected by anti-His_6 mouse monoclonal antibody.

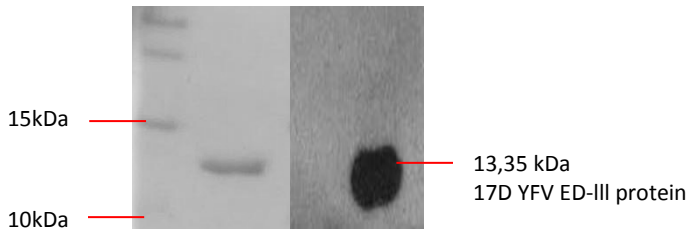

Figure 3.9: Characterisation of the expressed 17D YFV ED-III protein by Western blotting using anti-His_6 mouse monoclonal antibody

After characterisation of the expressed 17D YFV ED-III protein, the protein was ultra-filtered to remove urea facilitating protein refolding/renaturation. The integrity and purity of the GFP and 17D YFV ED-III proteins were confirmed by SDS-PAGE prior to immunisation as illustrated in Figure 3.10.

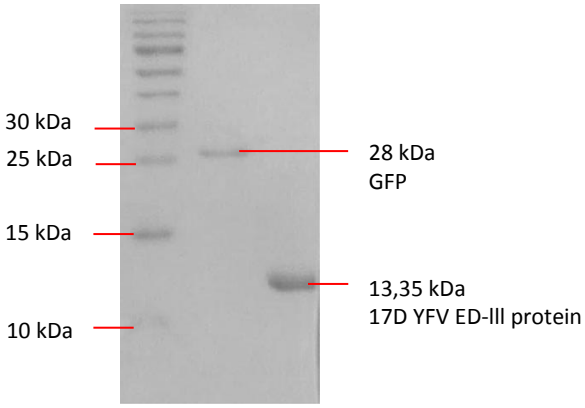

Figure 3.10: SDS-PAGE analysis for confirmation of integrity and purity of the GFP and 17D YFV ED-III proteins to be used for the immunisation of mice

Lane 1 – 3 µl PageRuler™ prestained protein ladder; Lane 2 – Recombinant GFP protein; Lane 3 – Recombinant 17D YFV ED-III protein.

The protein concentration of the commercial GFP and refolded 17D YFV ED-lll protein was determined using the Quant-iT™ protein assay kit (Table 3.7) to facilitate accurate dose administration during immunisation.

Table 3.7: Protein concentrations of proteins used for mouse immunisations

Protein:	Protein concentration (µg/ml):
GFP	630
17D YFV ED-lll	1 462

3.3.2 Determination of antibody responses to immunisation

An indirect in house ELISA was used to detect antibodies elicited by immunisation to YFV. YFV cell lysate antigen was prepared using YFV-infected cells and was used as a detection antigen.

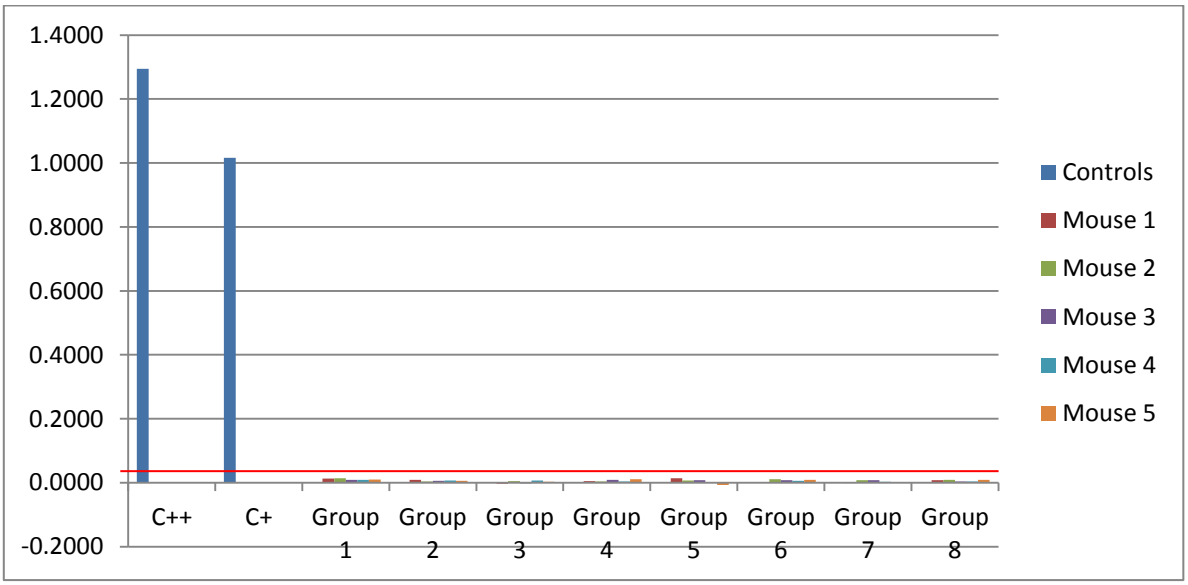

Figure 3.11: Graph anti-YFV antibody responses to immunisation as determined by an indirect ELISA using YFV cell lysate antigen as detection antigen

A high positive control (C++) VBD49/09 and a positive control (C+) VBD19/09 were included to confirm reactivity of anti-YFV antibody with the YFV cell lysate antigen used as detection antigen. Each bar represents the net OD_{405nm}.

Mouse sera did not contain antibody that reacted with the YFV cell lysate antigen as indicated by the net OD_{405nm} values below the calculated cut-off value of 0,04078 as

illustrated in Figure 3.11. The lack of reactivity may indicate the absence of anti-YFV antibody or an anti-YFV antibody titre below detectable level using the specified assay. Therefore, a commercial indirect IFA was utilised as a lower dilution of mouse sera may be applied facilitating the detection of low antibody titres. Only mice from the experimental groups receiving the pSinED-lll replicon and/or purified 17D YFV ED-lll protein were screened for anti-YFV antibody using the anti-YFV indirect IFA from Euroimmun as illustrated in Figure 3.12.

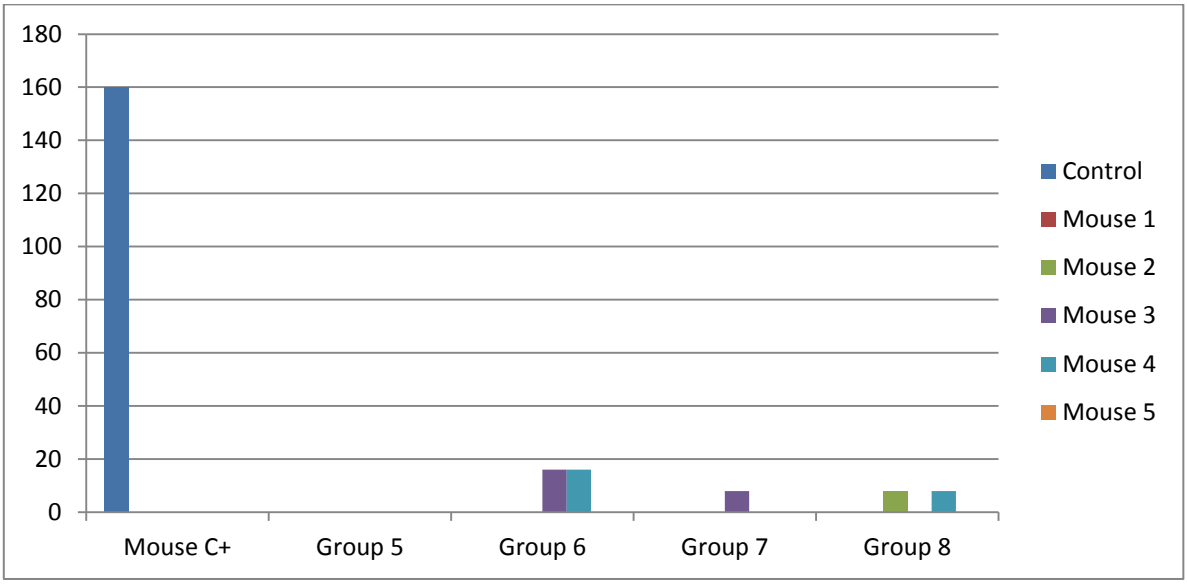

Group	5	6	7	8
Number of positive reactors	0/5	2/5	1/5	2/5

Figure 3.12: Graph anti-YFV antibody responses to immunisation as determined by an indirect IFA using YFV-infected and uninfected cells

Mouse serum obtained from a previous study confirmed to have anti-YFV ED-lll antibody was used as a positive control to confirm reactivity of anti-YFV ED-lll antibody with YFV-infected cells. The IFA results are reported as the reciprocal of the highest dilution of mouse sera at which anti-YFV antibody was detectable.

The antibody titre ranged from 8 to 16. Anti-YFV antibodies were detected in two mice receiving two immunisations containing 2 µg pSinED-lll replicon DNA followed by a 10 µg purified YFV ED-lll protein booster, one mouse receiving three consecutive DNA immunisations containing 25 µg pSinED-lll replicon and two mice receiving two immunisations containing 25 µg pSinED-lll replicon DNA followed by a 10 µg purified YFV ED-lll protein booster. The results indicate that the administration of a protein booster may

play a role in the induction of antibody responses due to the presence of intact protein in the extracellular environment.

3.3.3 Determination of cytokine responses to immunisation

The determination of cytokine release post-stimulation is important to facilitate the determination of the type of Th response induced by immunisation. Splenocytes will secrete cytokines upon re-stimulation with an antigen that have previously been encountered. Therefore, isolated splenocytes were stimulated *in vitro* with purified 17D YFV ED-lll protein to determine the type of cell-mediated immune response elicited. Secretion of IFN-γ, IL-2, IL-4 and IL-10 was determined using commercially available ELISA kits. Standard curves were constructed for each plate to facilitate the determination of the cytokine concentration in each well (refer to appendix E for standard curves).

IFN-γ is strongly associated with a Th1 response (Mosmann *et al.*, 1986), which is generally associated with the induction of a cell-mediated immune response (Kurt-Jones *et al.*, 1987). The IFN-γ response for each mouse is illustrated in Figure 3.13.

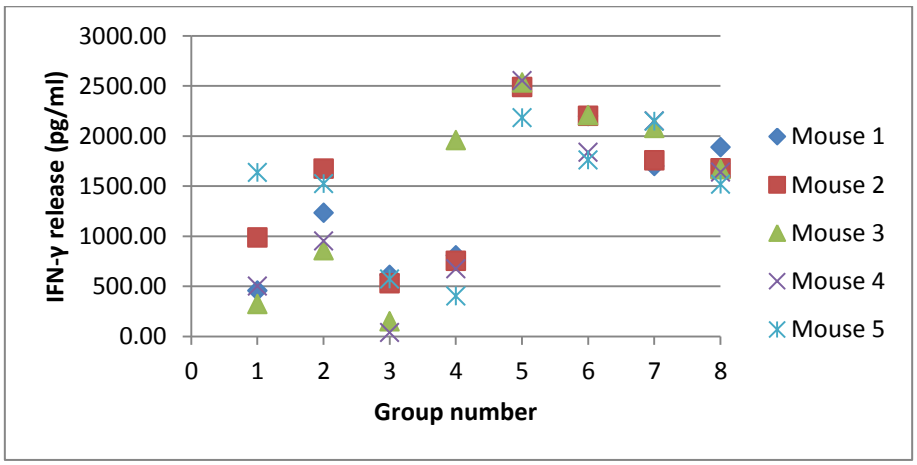

Figure 3.13: IFN-γ concentration post-stimulation of splenocytes with purified YFV ED-lll protein *in vitro*

The IFN-γ release differed significantly in the control groups, which included mice from groups 1 to 4. This may be due to bacterial impurities within the purified protein used for stimulation, especially as the control groups receiving a mixed model immunisation regime had higher IFN-γ release post-stimulation. This was reflected by the mean IFN-γ

concentration for each group of mice as illustrated in Figure 3.14. However, it is important to take into consideration that, similar to humans, immune responses vary between mice.

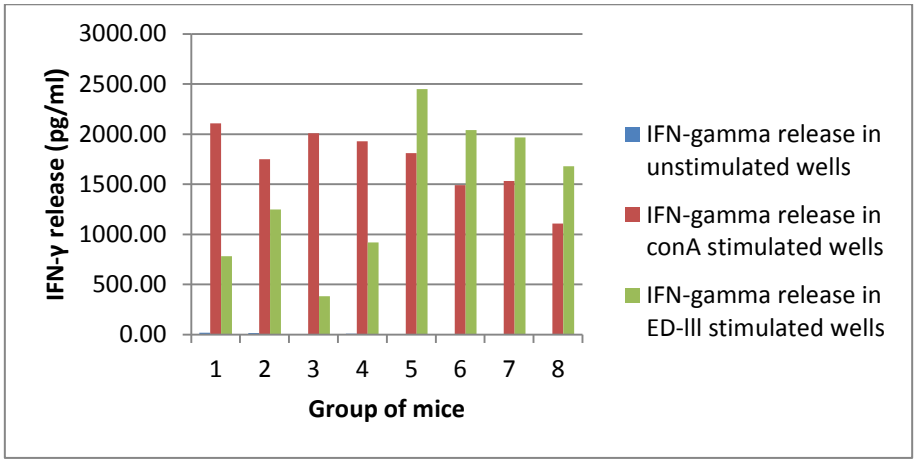

Figure 3.14: Mean IFN-γ concentration for each group of mice for the unstimulated, con A stimulated and YFV ED-lll stimulated splenocytes

The baseline IFN-γ release was determined using the cell culture supernatant harvested from unstimulated wells. The mean baseline IFN-γ release for control and experimental groups ranged from 2,68 - 16,90 pg/ml indicating the absence of infection in immunised mice. The isolated splenocytes were also stimulated with con A, a T-cell mitogen that induces murine T-cell proliferation (Stobo *et al.*, 1972). Stimulation of splenocytes with con A served as an indicator for T-cell proliferation and viability. The mean IFN-γ release for control and experimental groups stimulated with con A ranged from 1 105,90 – 2 107,60 pg/ml, confirming the viability of the splenocytes. Splenocytes were also stimulated with purified YFV ED-lll protein to simulate cytokine release after immunisation. IFN-γ release was noted in all groups of mice; however, control groups had significantly lower IFN-γ release as compared to the experimental groups. The induction of IFN-γ release post-stimulation in control groups may be attributed to bacterial impurities within the purified YFV ED-lll protein used for stimulation. Therefore, to determine the net IFN-γ release due to stimulation with the YFV ED-lll protein, the IFN-γ release in unstimulated and YFV ED-lll stimulated groups for each corresponding control group were deducted from the IFN-γ release for YFV ED-lll stimulated experimental groups. The net IFN-γ release, as illustrated in Figure 3.15, represents the IFN-γ release in response to the YFV ED-lll protein exclusively, thus facilitating a more accurate depiction of the IFN-gamma release post-stimulation.

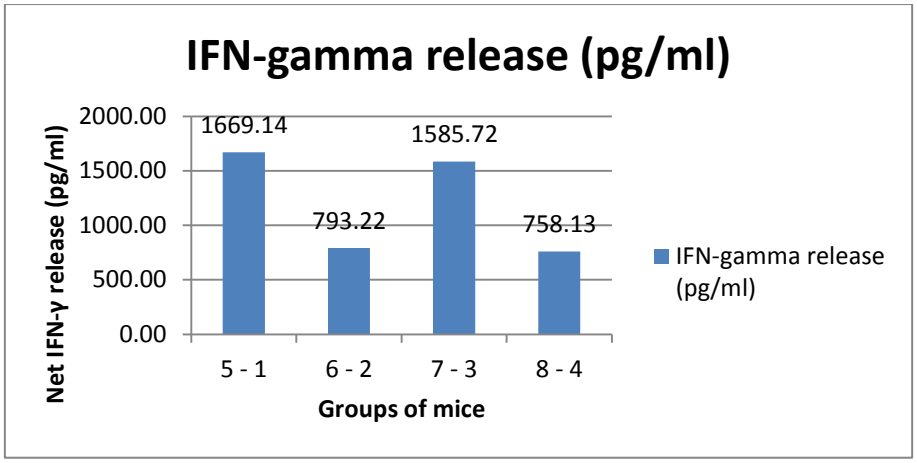

Figure 3.15: Net IFN-γ released post-stimulation with YFV ED-lll protein

Splenocytes released high levels of IFN-γ post-stimulation with the YFV ED-lll protein suggesting recognition of the YFV ED-lll protein. A similar response was observed irrespective of the dose administered as illustrated by the net IFN-γ release for groups 5 and 7, and groups 6 and 8, receiving 2 and 25 µg replicon DNA, respectively. However, a regime related response was observed for the groups of mice receiving three consecutive DNA immunisations as opposed to the mixed model immunisation regime, which included a protein booster. The IFN-γ release for groups receiving three consecutive DNA immunisations was approximately double the IFN-γ release observed in groups receiving a mixed modal immunisation regime. This suggests that the third DNA immunisation attributed to a stronger cell-mediated immune response as compared to groups receiving a protein booster. The inclusion of a protein booster was aimed at eliciting and/or enhancing the humoral immune response to immunisation.

The release of IL-2 post-stimulation was initially considered to be indicative of a cell-mediated immune response with a Th1 phenotype (Mosmann *et al.*, 1986); however, IL-2 has also been shown to play an essential role in the differentiation of $CD4^+$ T-cells into a Th2 phenotype (Cote-Sierra *et al.*, 2004). The release of IL-2 post-stimulation might therefore be associated with either a Th1 or Th2 phenotype and should be interpreted with the collective cytokine profile. The IL-2 release for each mouse is illustrated in Figure 3.16.

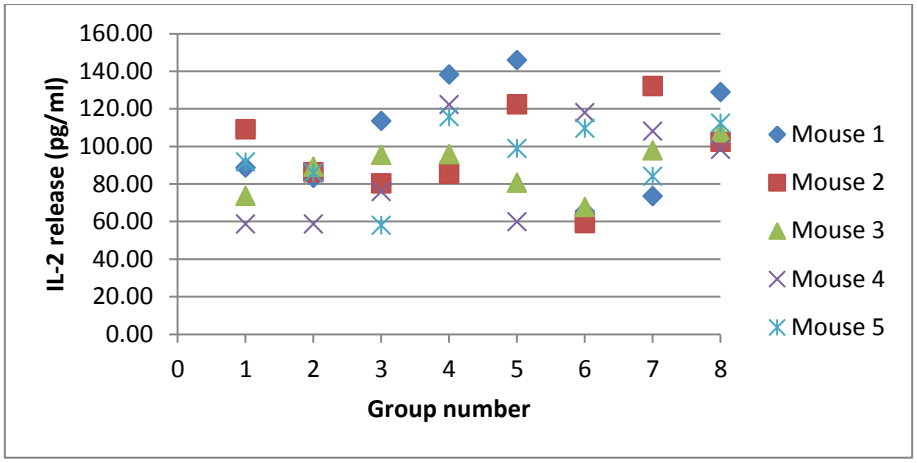

Figure 3.16: IL-2 concentration post-stimulation of splenocytes with purified YFV ED-III protein *in vitro*

IL-2 release varied within each group; however, little difference was noted between control and experimental groups. This was reflected by the mean IL-2 release for each group of mice illustrated in Figure 3.17.

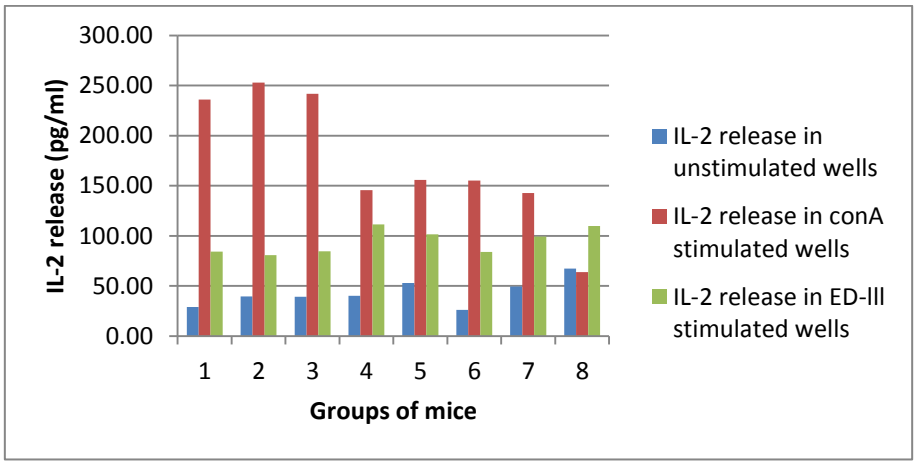

Figure 3.17: Mean IL-2 concentration for each group of mice for the unstimulated, con A stimulated and YFV ED-III stimulated splenocytes

The mean baseline IL-2 release ranged from 29,03 - 67,22 pg/ml, which indicated release of IL-2 in unstimulated splenocytes. The proliferation and subsequent release of IL-2 by splenocytes was confirmed by stimulation with con A. The mean IL-2 release post-stimulation with YFV ED-III ranged from 80,56 - 111,48 pg/ml indicating an increase in the

release of IL-2 post-stimulation in both control and experimental groups. Therefore, the release of IL-2 solely to recognition of the YFV ED-lll protein was determined by calculating the net IL-2 release as illustrated in Figure 3.18.

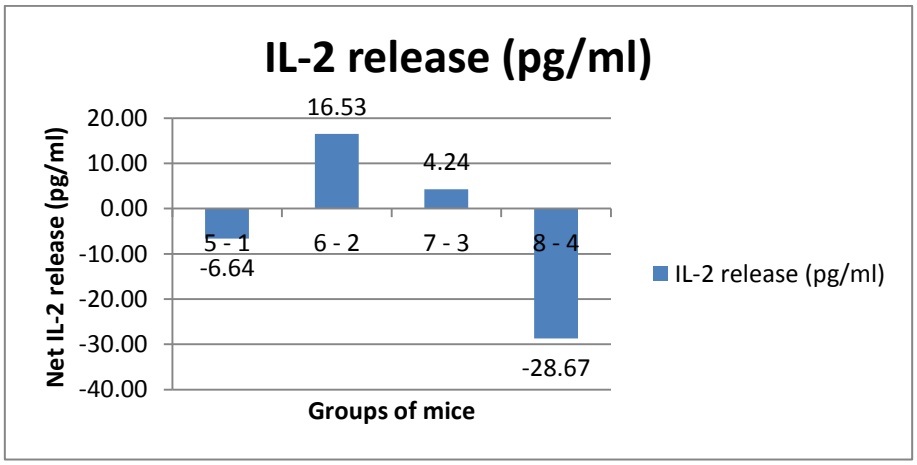

Figure 3.18: Net IL-2 released post-stimulation with YFV ED-lll protein

The net IL-2 release indicated low levels of release in response to the YFV ED-lll protein. Negative IL-2 values were obtained for groups 5 and 8, which indicated higher levels of IL-2 release in control groups as compared to the experimental groups. This phenomenon has previously been observed (Verma *et al.*, 2009), thus indicating the lack of IL-2 release post-stimulation in experimental groups.

The release of IL-4 and IL-10 post-stimulation was evaluated due to the direct and indirect association of IL-4 (Mosmann *et al.*, 1986) and IL-10, respectively, with the development of a Th2 response (Hsieh *et al.*, 1993). The IL-4 response for each mouse is illustrated in Figure 3.19.

A low level of IL-4 release was observed in control and experimental groups post-stimulation with the YFV ED-lll protein and little difference was noted in the release of IL-4 between the control and the experimental groups of mice.

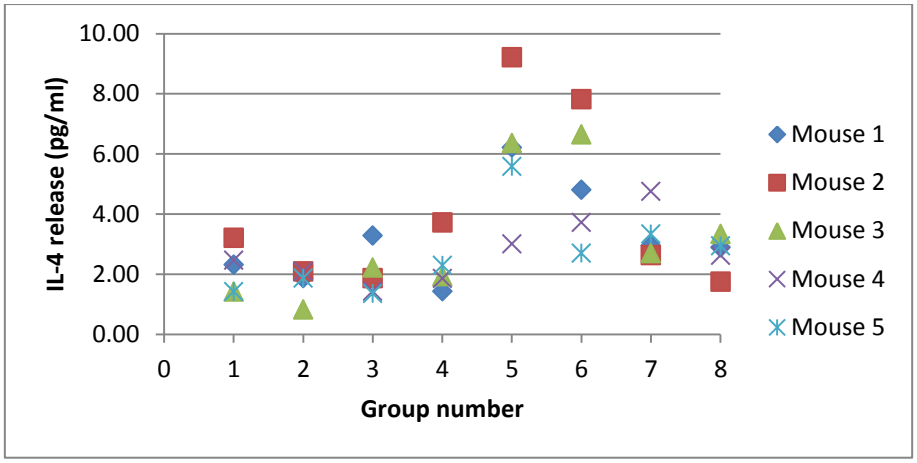

Figure 3.19: IL-4 concentration post-stimulation of splenocytes with purified YFV ED-III protein *in vitro*

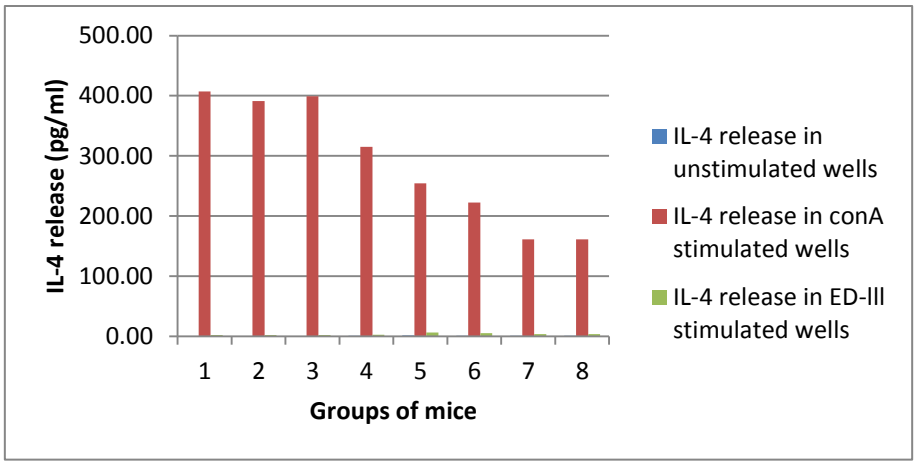

Figure 3.20: Mean IL-4 concentration for each group of mice for the unstimulated, con A stimulated and YFV ED-III stimulated splenocytes

In Figure 3.20, the IL-4 release for unstimulated, con A stimulated and YFV ED-III stimulated wells are illustrated. The mean baseline IL-4 release ranged from 0,40 - 1,42 pg/ml, whereas the mean IL-4 release for con A stimulated wells ranged from 78,48 - 406,97 pg/ml. The release of IL-4 post-stimulation with con A demonstrated the viability of the splenocytes. The mean IL-4 release post-stimulation with the YFV ED-III protein ranged from 1,75 - 6,07 pg/ml. The net IL-4 release for each experimental group is illustrated in Figure 3.21.

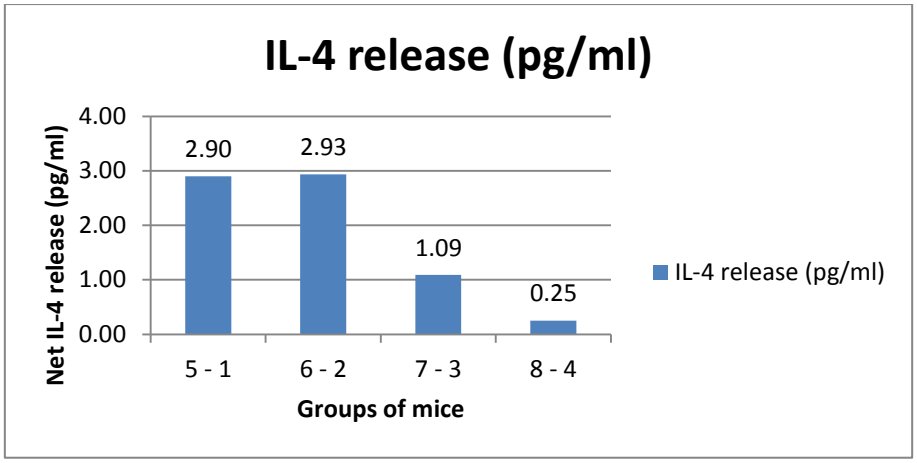

Figure 3.21: Net IL-4 released post-stimulation with YFV ED-III protein

Low level IL-4 release post-stimulation with purified YFV ED-III protein indicated the absence of an IL-4 directed Th2 immune response. As IFN-γ and IL-4 are reciprocally regulated to direct a Th1 or Th2 phenotype, respectively, a low level of IL-4 was expected as high level IFN-γ release was detected post-stimulation.

IL-10 antagonises the Th1 response by inhibiting the release of IL-12 from activated macrophages, which primarily directs the development of a Th1 response (Hsieh *et al.*, 1993). IL-10 has been shown to be a regulatory cytokine that plays a role in preventing the development of an overzealous immune response (Segal *et al.*, 1998). The IL-10 response for each mouse is illustrated in Figure 3.22.

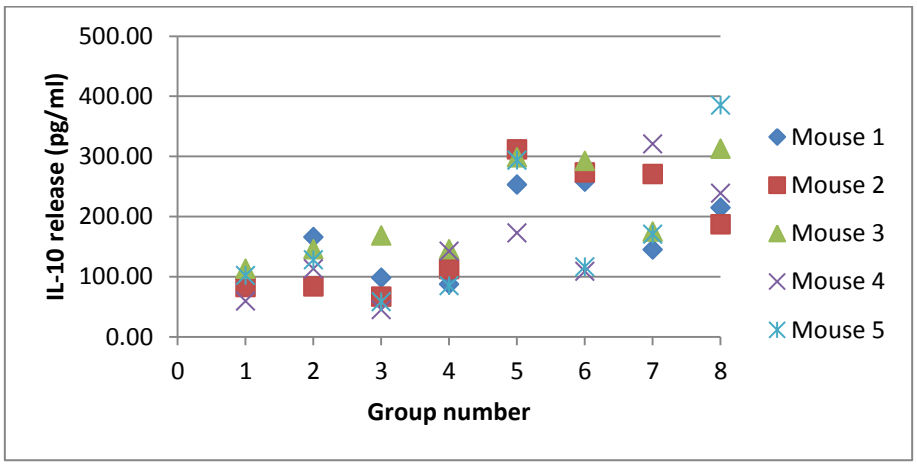

Figure 3.22: IL-10 concentration post-stimulation of splenocytes with purified YFV ED-III protein *in vitro*

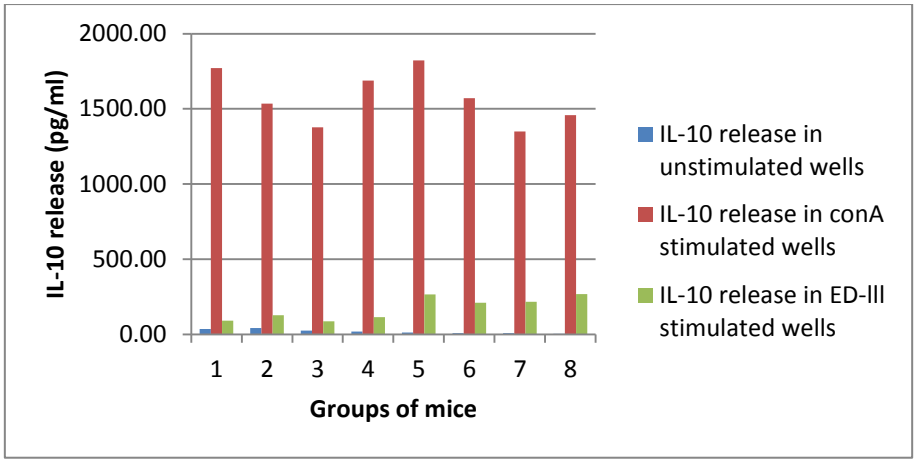

Figure 3.23: Mean IL-10 concentration for each group of mice for the unstimulated, con A stimulated and YFV ED-lll stimulated splenocytes

IL-10 release was higher in experimental groups as compared to control groups and varied significantly within experimental groups. The mean IL-10 release for unstimulated, con A stimulated and YFV ED-lll stimulated groups is illustrated in Figure 3.23.

The mean baseline IL-10 release ranged from 2,68 - 42,22 pg/ml, whereas the mean IL-10 release for con A stimulated wells ranged from 1 349,30 – 1 821,44 pg/ml. In splenocytes stimulated with the YFV ED-lll protein the mean IL-10 release ranged from 87,11 - 267,52 pg/ml. The net IL-10 release for each experimental group is illustrated in Figure 3.24.

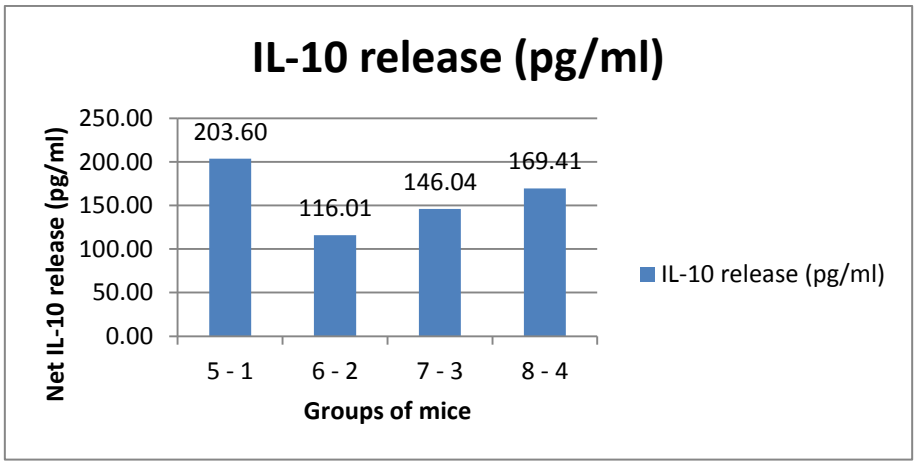

Figure 3.24: Net IL-10 released post-stimulation with YFV ED-lll protein

Post-stimulation with the YFV ED-lll protein, IL-10, associated with the development of a Th2 response, was released. IL-10 has been shown to regulate the inflammatory immune response to protect the host from an excessive immune response, which could otherwise result in immunopathology (Segal *et al.*, 1998). Another role for IL-10 has also been elucidated, which causes enhanced secretion of Th1 cytokines by $CD8^+$ T-cells; however, this role for IL-10 is only fulfilled when expressed in combination with IL-2 (Santin e*t al.*, 2000). Therefore, the absence of IL-2 release accompanied by IL-10 release suggests that the release of IL-10 did not contribute to the high levels of IFN-γ released, but may potentially play a regulatory role in preventing a disproportionate immune response.

3.3.4 Comparison of cytokine release for different groups of mice

The student t-test was performed to determine whether the release of each cytokine was significantly different between each corresponding control and experimental group as illustrated in Table 3.8.

Table 3.8: Comparison of control and experimental group for each cytokine evaluated

Cytokine:	Experimental group:	Control group:	p-value:	Statistically significant difference (p<0,05):
IFN-γ	Group 5	Group 1	0,001557	Yes
	Group 6	Group 2	0,004025	Yes
	Group 7	Group 3	0,000009	Yes
	Group 8	Group 4	0,046216	Yes
IL-2	Group 5	Group 1	0,359125	No
	Group 6	Group 2	0,814909	No
	Group 7	Group 3	0,323633	No
	Group 8	Group 4	0,881717	No
IL-4	Group 5	Group 1	0,013943	Yes
	Group 6	Group 2	0,020347	Yes
	Group 7	Group 3	0,045784	Yes
	Group 8	Group 4	0,362580	No
IL-10	Group 5	Group 1	0,001240	Yes
	Group 6	Group 2	0,110614	No
	Group 7	Group 3	0,015315	Yes
	Group 8	Group 4	0,010260	Yes

Significantly elevated levels of IFN-γ, IL-4 and IL-10 release were observed in experimental groups as compared to control groups; however, levels of IL-4 were only slightly elevated. To determine any dose and/or regime-related effects for the induction of each cytokine the student t-test was applied to groups with one variable remaining constant. To allow the

determination of a dose-related effect groups with an identical immunisation regime at different doses were compared. The dose and/or regime-related effects were evaluated for IFN-γ and IL-10 using the net IFN-γ and IL-10 release for each mouse within a group as illustrated in Table 3.9.

Table 3.9: Determination of dose and/or regime-related effects on the induction of IFN-γ and IL-10

Cytokine:	Experimental group:	Control group:	p-value:	Test for dose or regime-related effect:	Statistically significant difference (p<0,05):
IFN-γ	Group 5	Group 6	0,0002	Regime	Yes
	Group 7	Group 8	0,0003	Regime	Yes
	Group 5	Group 7	0,5008	Dose	No
	Group 6	Group 8	0,7840	Dose	No
IL-10	Group 5	Group 6	0,1007	Regime	No
	Group 7	Group 8	0,5593	Regime	No
	Group 5	Group 7	0,3295	Dose	No
	Group 6	Group 8	0,1899	Dose	No

A regime-related effect was noted in the induction of IFN-γ. Groups receiving three consecutive DNA immunisations had significantly higher levels of IFN-γ release as compared to groups receiving a mixed modal immunisation regime. Thus illustrating the significant boosting effect of the administration of a third dose of DNA on the cell-mediated immune response. However, no significant dose-related effects were noted for the release of IFN-γ and IL-10. The regime-related effect observed for IFN-γ was not observed for IL-10 release.

3.3.5 Detection of humoral anti-vector immunity elicited post-immunisation

The detection of antibodies against SINV is important as DNA vaccines generally require the administration of booster doses and anti-vector immunity could be detrimental to the immunogenicity of the vaccine. Mouse sera screened by ELISA did not contain anti-SINV antibody as illustrated in Figure 3.25.

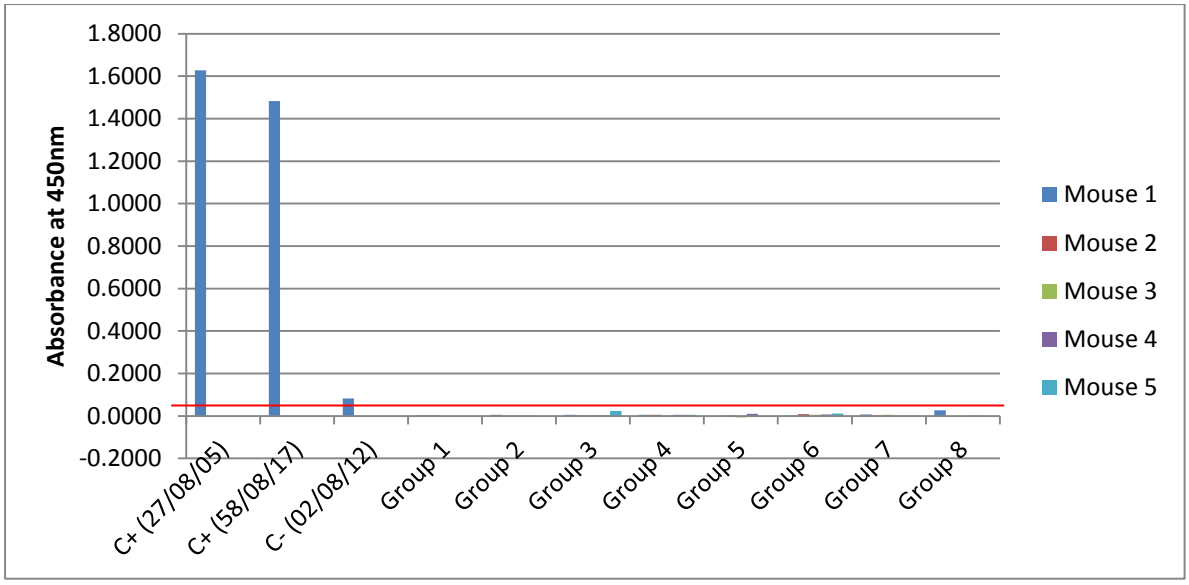

Figure 3.25: Graph anti-SINV antibody responses to immunisation as determined by an indirect ELISA using SINV cell lysate antigen

Positive and negative controls were included to confirm reactivity of anti-SINV antibody with SINV cell lysate antigen, including two positive controls (VBD27/08/05 and VBD58/08/17) and one negative control (VBD02/08/12). The net OD_{405nm} is represented by each bar.

Detection of anti-SINV antibody was confirmed by inclusion of positive and negative controls confirmed to be anti-SINV antibody positive and negative. Mouse sera did not contain anti-SINV antibody as indicated by the net OD_{405nm} values below the calculated cut-off value of 0,0397. The net OD_{405nm} obtained for the human negative control were slightly higher than the determined cut-off value; however, the cut-off value only applies to mouse sera as the cut-off was determined using a panel of negative mouse control sera. The net OD_{405nm} obtained for the human negative control was lower than a previously reported cut-off value using a panel of 18 negative human serum samples, which were determined to be 0,1548 (Hanekom, 2014). The results indicate that a humoral anti-vector immune response was not induced by immunisation.

3.4 Discussion

Evaluation of the type of immune response elicited by immunisation in an animal model is essential to determine the usefulness of a candidate vaccine at inducing a protective immune response. In the case of DNA vaccines, the vaccine construct can be altered to facilitate the induction of the desired immune response or enhance the immunogenicity of the construct by the addition of DNA elements. In this chapter, mice were immunised with

the pSinGFP (control) and pSinED-lll (experimental) DNA-launched replicon constructs and the immune response was determined.

Neutralising antibody has been shown to be the correlate of protection against YFV (Julander *et al.*, 2011); however, the contribution from the other arms of the immune response should not be undervalued, especially the role of the innate and cell-mediated immune responses (Gaucher *et al.*, 2008). YFV has been shown to activate both the cell-mediated and humoral arms of the immune response. The cell-mediated immune response has been shown to play a role early in infection during the viraemic phase and may therefore be important for controlling infection by preventing viral replication and dissemination due to the destruction of virally infected cells. The humoral immune response characterised by antibody with neutralising activity only develop later in infection (Reinhart *et al.*, 1998; Gaucher *et al.*, 2008). Therefore, the ideal vaccine against YFV should elicit both a cell-mediated and a humoral immune response. The humoral immune response elicited by the pSinED-lll replicon was evaluated by indirect ELISA and no detectable antibodies were demonstrated in sera diluted at 1:100. A commercially available IFA was used to confirm the results obtained by ELISA and 5/20 mice in the experimental groups receiving the DNA-launched pSinED-lll replicon had detectable, but low level antibody responses post-immunisation with an antibody titre ranging from 8 to 16. Due to the low antibody titres observed in mice antibody isotyping was not performed. Confirmation of the presence of neutralising antibody was not performed and is a limitation of the study. Neutralising antibody tests require biosafety facilities that were not available. Administration of the protein booster likely contributed to the development of an antibody response with 4/5 mice receiving a mixed modal regime having detectable antibody. However, one mouse with detectable antibody received a DNA only immunisation regime, therefore indicating the potential of the pSinED-lll replicon to elicit an antibody response; however, enhancement of the antibody response will be required.

A strong cell-mediated immune response was elicited by the pSinED-lll replicon post-immunisation as indicated by cytokine profiling using *in vitro* stimulated splenocytes. The ability of T-cells to proliferate and secrete cytokines post-stimulation was confirmed by stimulation with con A, a mitogen that activates all subsets of murine T-cells. Recombinant purified YFV ED-lll protein stimulated high levels of IFN-γ release, indicative of a predominantly Th1 phenotype associated with the killing of virally infected cells. A correlation was observed between the level of IFN-γ secreted and the regime administered. Mice receiving three consecutive DNA immunisations had significantly higher levels of IFN-γ release post-stimulation as compared to mice receiving two DNA immunisations followed by a protein booster. In comparison, increasing the dose of DNA replicon did not significantly

influence the levels of IFN-γ released, indicating that a low dose of pSinED-lll replicon DNA is sufficient to facilitate expression of the YFV ED-lll protein *in vivo* and subsequently induce a Th1 response characterised by the release of IFN-γ. Increased levels of IL-10, a regulatory cytokine, associated with a Th2 response were detected. Release of IL-10 has been shown to protect the host against a disproportionate pro-inflammatory response, which is mediated by high levels of Th1 cytokine release (Segal *et al.*, 1998). Expression of IL-10 is frequently delayed when compared to other pro-inflammatory cytokines (Trinchieri, 1997), therefore the effects of IL-10 on inhibiting the development of a Th1 phenotype are also delayed. The induction of IL-10 may have been in response to the high levels of IFN-γ released post-immunisation, hence would possibly have a role in regulating the immune response to protect the host *in situ*. A mechanistic study on DNA immunisation has shown that the immune response is dependent on the localisation of the expressed antigen and the processing pathway utilised for presentation to the immune response. In a study by Whitton and colleagues, a CTL response was elicited without a detectable antibody response, which was shown to be due to the intracellular degradation of the expressed without the release of any intact protein to the extracellular environment (Whitton *et al.*, 1999).

In theory, an immune response against the NS proteins encoded within the replicon should be absent or minimal due to the intracellular expression of the encoded SINV NS proteins. No antibody response to the SINV NS proteins was detected using ELISA. As the SINV NS proteins were encoded within the control, pSinGFP replicon DNA, as well as the experimental, pSinED-lll replicon DNA, antibody responses in both the control and experimental groups of mice were determined. This could be significant as it suggets there will be no interference from the humoral immune response with the administration of multiple boosters.

In this chapter, the DNA-launched pSinED-lll replicon encoding the YFV ED-lll protein was shown to elicit a predominantly Th1 response characterised by the release of IFN-γ post-stimulation with recombinant YFV ED-lll protein. The release of IL-10 may play a role in the prevention of an overzealous pro-inflammatory immune response. The potential of the pSinED-lll replicon to elicit a humoral immune response characterised by antibody production was illustrated; however, the antibody responses post-immunisation will need to be enhanced and neutralising antibody responses investigated.

CHAPTER 4: Discussion

YFV, a re-emerging mosquito-borne virus belonging to the family *Flaviviridae* and genus *Flavivirus* has been associated with disease in humans (Calisher *et al.*, 1989). Clinically YFV presents with mild disease, which in approximately 15% of patients can progress to a severe infection characterised by renal failure, jaundice and/or haemorrhage (ter Meulen *et al.*, 2004). YFV is a significant public health threat in yellow fever endemic areas (Stock *et al.*, 2013), which include the tropical regions of Africa and South America (WHO, 1953). Fatality rates ranging from 20 to over 50% have been reported (Monath, 1999; Vasconcelos *et al.*, 2001c) and the prevalence of YFV for the year 2013 in Africa was estimated to be 130 000 severe cases and 78 000 deaths (Garske *et al.*, 2014). The burden of disease is highest in Africa constituting approximately 90% of reported yellow fever cases (Mutebi & Barrett, 2002). In nature, YFV is maintained between non-human primates and certain mosquito species with humans contracting disease when disrupting this cycle. Humans are mostly dead-end hosts, because YFV virus is not efficiently transmitted from human to human by mosquitoes due to low level viraemia experienced in humans (Monath, 1999). Currently, the treatment of yellow fever consists of supportive care (Monath, 2005) and the administration of antibiotics to prevent the development of secondary bacterial infections. Several agents with antiviral activity against YFV have been identified; however, these agents have been shown to only be effective when administered prior to or soon after virus adsorption (Neyts *et al.*, 1996; Ono *et al.*, 2003).

Highly efficacious live attenuated vaccines are available against YFV (Theiler & Smith, 1937b). The success of the YFV vaccines has been attributed to the activation of both the cell-mediated and humoral arms of the immune system (Martins *et al.*, 2007) with neutralising antibodies being considered to confer protection against disease (Julander *et al.*, 2011). Due to the live attenuated nature of these vaccines, use in immunocompromised individuals has been contraindicated (WHO, 1998; Martin *et al.*, 2001b; Cetron *et al.*, 2002; Barwick & Yellow Fever Vaccine Safety Working Group, 2004; Staples *et al.*, 2010). Administration of these vaccines in patients with hypersensitivity to eggs and/or chicken has also been contraindicated due to the preparation of vaccine strain virus in whole chick embryo (Cetron *et al.*, 2002; Staples *et al.*, 2010). Adverse events have also been associated with the administration of the live attenuated vaccines against YFV, which include vaccine-associated neurotropic- and viscerotropic adverse events (CDC, 2002). Vaccine-associated viscerotropic adverse events with fatality rates exceeding 40% (Thomas *et al.*, 2013) results in multi-organ failure with disease resembling wild-type yellow fever infection (Martin *et al.*, 2001a; Vasconcelos *et al.*, 2001b). Therefore, the need for a safer alternative to complement the use of the available live attenuated vaccines is required to facilitate safe

immunisation and higher immunisation coverage. In this study, a DNA-launched Sindbis replicon encoding the YFV ED-III protein was prepared and the immunogenicity of the DNA-launched replicon was evaluated in a mouse model.

The DNA-launched pSinED-III replicon encoding the YFV ED-III protein was prepared using the DNA-launched pSinGFP replicon provided by Prof. Mark Heise. After excision of the gene encoding the GFP, a synthesised codon-optimised gene encoding the wild-type Asibi strain YFV ED-III protein was cloned into the linearised replicon and the presence of the gene for expression of the YFV ED-III protein was confirmed using nucleotide sequence analysis. Expression of recombinant YFV ED-III protein was confirmed by transfection of selected mammalian cell lines, including BHK-21, COS-7, HEK-293 and Vero-76. Expression in all cell lines with varying transfection efficiencies was confirmed by detection of the C-terminal histidine tag fused to the YFV ED-III protein using anti-His_6 mouse monoclonal antibody in an IFA. The BHK-21 cell line was selected for the characterisation of the expressed YFV ED-III protein due to the higher transfection efficiency observed as compared to the other selected mammalian cell lines. Subsequently, BHK-21 cells were transfected with pSinED-III replicon DNA and reacted with mouse sera previously shown to contain anti-YFV ED-III antibody. Positive fluorescence within the transfected cells confirmed expression of the YFV ED-III protein post-transfection and substantiated the use of the pSinED-III replicon for an immunisation study in mice.

Mice were immunised at two week intervals by the IM route using a DNA immunisation regime, as well as a mixed modal immunisation regime consisting of two DNA immunisations followed by a protein booster. Replicon DNA was administered at two different doses, 2 µg or 25 µg, to the respective groups of mice. Manthorpe and colleagues has previously shown that maximum gene expression was achieved seven to fourteen days post-immunisation with a DNA construct by the administration of 25 µg of DNA to the tibialis anterior muscle (Manthorpe *et al.*, 1993). DNA suitable for immunisation was obtained by purification using the EndoFree® Plasmid Maxi kit to facilitate efficient removal of endotoxin from the bacterial preparation. Two weeks after the administration of the final immunisations, spleens were harvested and sera were collected facilitating the determination of the type of immune response induced.

Both the cell-mediated and humoral immune response were investigated. Splenocytes were isolated and stimulated *in vitro* to facilitate cytokine profiling. Splenocytes were stimulated with con A, which served as a positive control, to illustrate the viability of the murine T-cells and the ability of the cells to proliferate and secrete cytokines. Splenocytes were also stimulated with purified recombinant 17D YFV ED-III protein to induce release of cytokines

associated with immunisation. Unstimulated splenocytes were used to determine the baseline cytokine release for each mouse. Cytokine profiling was performed post-stimulation using commercially available ELISA's specific for each cytokine. Cytokines associated with a Th1 and Th2 response were selected. IFN-γ and IL-2 are generally associated with a Th1 response, whereas IL-4 (Mosmann *et al.*, 1986) and IL-10 are associated with a Th2 response (Hsieh *et al.*, 1993). Levels of cytokine release differed significantly between control and experimental groups for IFN-γ, IL-4 and IL-10; however, levels of IL-4 were only slightly elevated when compared to control groups.

A predominantly Th1 phenotype within the $CD4^+$ T-cell population characterised by significantly elevated levels of IFN-γ release was elicited in response to immunisation, which have been associated with a cell-mediated immune response (Kurt-Jones e*t al.*, 1987). The level of IFN-γ release differed significantly between groups receiving three consecutive DNA immunisations and groups receiving a mixed modal immunisation regime. IFN-γ release was approximately doubled in groups 5 and 7 receiving three consecutive DNA immunisations as compared to groups 6 and 8 receiving two DNA immunisations followed by a protein booster. Thus illustrating the boosting effect of the administration of a third dose of replicon DNA on the cell-mediated immune response. However, no dose-related effects were noted between groups receiving an identical immunisation regime with 2 µg or 25 µg replicon DNA, respectively. Thus similar levels of IFN-γ induction was observed in groups 5 and 7 and groups 6 and 8 indicating that a low dose of replicon DNA is sufficient to induce a cell-mediated immune response post-immunisation. IFN-γ has been shown to modulate the abundance of $CD8^+$ T-cells by direct stimulation resulting in the enhancement of the $CD8^+$ T-cell response to infection (Whitmire *et al.*, 2005). The functional competence of memory $CD8^+$ T-cells is improved by IFN-γ secreting $CD4^+$ T-cells in the absence of IL-2 (Kumaraguru e*t al.*, 2005). IL-10 a regulatory cytokine associated with a Th2 response was significantly elevated post-stimulation. The release of IL-10 may have been in response to the highly elevated level of IFN-γ release, subsequently antagonising the Th1 response (Hsieh *et al.*, 1993) protecting the host from an excessive inflammatory immune response, which could potentially be detrimental to the host (Segal *et al.*, 1998). Further studies profiling cytokine release at various intervals after stimulation may help determine the role of IL-10 secretion. The levels of IL-10 release were more varied compared to the IFN-γ release and no regime- or dose-related effects were noted. Collectively, cytokine release indicated a predominantly Th1 phenotype within the $CD4^+$ T-cell population.

Antibody induction in response to immunisation was evaluated by indirect ELISA using whole cell lysate antigen and a commercial IFA using YFV-infected and uninfected cells. Sera diluted 1:100 from immunised and mock immunised mice tested by ELISA, showed no

detectable antibody response. Therefore, a commercial indirect IFA was employed to confirm results obtained by indirect ELISA and low antibody titres were detected in 5/20 mice. Low level antibody responses to YFV were detected in mice from groups 6, 7 and 8. Four of the five mice with anti-YFV antibody were immunised with a mixed modal immunisation regime, including a protein booster. Therefore, it is likely that the administration of a protein booster induced detectable antibody production post-immunisation. One mouse receiving only replicon DNA had a low titre antibody response illustrating the potential of the pSinED-lll replicon to induce an antibody response after IM administration; however, the antibody response post-immunisation requires optimisation. Future studies may investigate the incorporation of a secretion signal within the replicon construct to facilitate the transport of synthesised YFV ED-lll protein to the extracellular environment where circulating B-cells can encounter the protein and potentially lead to the induction of an enhanced antibody response. Co-administration with adjuvants to enhance the humoral immune response may also be explored.

The presence of antibody directed against SINV NS proteins encoded within the replicon, which could potentially impede the efficacy of immunisations administered subsequent to the primary immunisation, was investigated. Results revealed the absence of a detectable antibody response to SINV, thus indicating the absence of humoral anti-vector immunity. Future prospects may include the determination of the cell-mediated immune response against the encoded SINV NS proteins post-immunisation to establish the induction of cell-mediated anti-vector immunity.

A degree of variation in the antibody specificities has been observed in individuals vaccinated against YFV (Vratskikh *et al.*, 2013). In mice, antibody with potent neutralising activity has been shown to be directed against domain lll of the flavivirus E glycoprotein (Beasley & Barrett, 2002; Wu *et al.*, 2003; Sánchez *et al.*, 2005). However, in humans only a small proportion of IgG antibody is directed to domain lll in previously infected or vaccinated individuals with varying neutralising activity (Throsby *et al.*, 2006; Crill *et al.*, 2009; Wahala *et al.*, 2009; Vratskikh *et al.*, 2013). The proportion of antibody directed against flaviviral ED-lll has been shown to contribute to virus neutralisation (Throsby *et al.*, 2006; Crill *et al.*, 2009; Wahala *et al.*, 2009; de Alwis *et al.*, 2011), except for YFV, which in a recent study was found to not significantly contribute to the neutralisation of YFV (Vratskikh *et al.*, 2013). The discrepancy between mouse and human antibody specificities and neutralising capabilities may also be explained by a recent study that showed the majority of antibody post-infection with DEN in humans did not target the previously well-characterised epitopes identified on domain lll using mice (Wahala *et al.*, 2012). Therefore, the use of YFV ED-lll protein for immunisation may need to be re-evaluated. However, in a recent study the

anti-JEV ED-lll antibody was shown to block flavivirus entry and confer cross-protection (Fan *et al.*, 2013), which may indicate that the presence of sufficient levels of anti-ED-lll antibody could prevent virus entry irrespective of the neutralising activity of the antibody. Alternatively, the complete E protein could be used for immunisation. A DNA vaccine encoding the complete DEN-2 E protein has been shown to be fully protective against virus challenge in mice (Azevedo *et al.*, 2011). Although antibody directed against domain ll has been shown to dominate the immune response in humans to flavivirus infections, the neutralising activity of these antibodies are usually weak (Throsby *et al.*, 2006; Crill *et al.*, 2009; de Alwis *et al.*, 2011; Vratskikh *et al.*, 2013).

A limitation of the study was the inability to test for neutralising antibody responses due to biosafety considerations. However, the significance of neutalising antibody against YFV ED-lll in humans vaccinated with live attenuated vaccine needs to be further investigated and it is likely that a candidate vaccine should incorporate the gene encoding the complete E protein. Similarly, mouse challenge studies will also be required to determine whether the immune response elicited will protect a mouse against a lethal YFV challenge. This study has shown that the DNA-launched replicon vaccine has potential as a vaccine vector. In conclusion, the DNA-launched pSinED-lll replicon was shown to induce both a cell-mediated and a humoral immune response in mice; however, enhancement of the induced humoral immune response will be required.

References

Allison SL, Schalich J, Stiasny K, Mandl CW, Kunz C, Heinz FX. Oligomeric rearrangement of tick-borne encephalitis virus envelope proteins induced by an acidic pH. J Virol 1995; 69(2):695-700.

André S, Seed B, Eberle J, Schraut W, Bültmann A, Haas J. Increased immune response elicited by DNA vaccination with a synthetic gp120 sequence with optimized codon usage. J Virol 1998; 72(2):1497-503.

Augustin G. History of yellow fever. New Orleans: Searcy & Pfafl, Ltd., 1909.

Azevedo AS, Yamamura AM, Freire MS, Trindade GF, Bonaldo M, Galler R, Alves AM. DNA vaccines against dengue virus type 2 based on truncate envelope protein or its domain lll. PLoS One 2011; 6(7):e20528.

Barba-Spaeth G, Longman RS, Albert ML, Rice CM. Live attenuated yellow fever 17D infects human DCs and allows for presentation of endogenous and recombinant T cell epitopes. J Exp Med 2005; 202(9):1179-84.

Barwick ER, Yellow Fever Vaccine Safety Working Group. History of thymoma and yellow fever vaccination. Lancet 2004; 364(9438):936.

Bauer JH. The transmission of yellow fever by mosquitoes other than *Aedes aegypti*. Am J Trop Med 1928; 8(4):261-82.

Beasley DWC, Barrett ADT. Identification of neutralizing epitopes within structural domain lll of the West Nile virus envelope protein. J Virol 2002; 76(24):13097-100.

Belsher JL, Gay P, Brinton M, DellaValla J, Ridenour R, Lanciotti R, Perelygin A, Zaki S, Paddock C, Querec T, Zhu T, Pulendran B, Eidex RB, Hayes E. Fatal multiorgan failure due to yellow fever vaccine-associated viscerotropic disease. Vaccine 2007; 25(50):8480-5.

Boshart M, Weber F, Jahn G, Dorsch-Häsler K, Fleckenstein B, Schaffner W. A very strong enhancer is located upstream of an immediate early gene of human cytomegalovirus. Cell; 1985; 41(2):521-30.

Brandriss MW, Schlesinger JJ, Walsh EE. Immunogenicity of a purified fragment of 17D yellow fever envelope protein. J Infect Dis 1990; 161(6):1134-9.

Breugelmans JG, Lewis RF, Agbenu E, Veit O, Jackson D, Domingo C, Böthe M, Perea W, Niedrig M, Gessner BD, Yactavo S, yellow fever adverse events following immunization

group. Adverse events following yellow fever preventative vaccination campaigns in eight African countries from 2007 to 2010. Vaccine 2013; 31(14):1819-29.

Calarota S, Bratt G, Nordlund S, Hinkula J, Leandersson AC, Sandström E, Wahren B. Cellular cytotoxic response induced by DNA vaccination in HIV-1-infected patients. Lancet 1998; 351(9112):1320-5.

Calisher CH, Karabatsos N, Dalrymple JM, Shope RE, Porterfield JS, Westaway EG, Brandt WE. Antigenic relationships between flaviviruses as determined by cross-neutralization tests with polyclonal antisera. J Gen Virol 1989; 70(Pt 1):37-43.

Carnero E, Li W, Borderia AV, Moltedo B, Moran T, García-Sastre A. Optimization of human immunodeficiency virus gag expression by Newcastle disease virus vectors for the induction of potent immune responses. J Virol 2009; 83(2):584-97.

Centers for Disease Control and Prevention (CDC). Possible West Nile virus transmission to an infant through breast-feeding--Michigan, 2002. MMWR Morb Mortal Wkly Rep 2002; 51(39):877-8.

CDC. Transfusion-related transmission of yellow fever vaccine virus--California, 2009. MMWR Morb Mortal Wkly Rep 2010a; 59(2):34-7.

CDC. Transmission of yellow fever vaccine virus through breast-feeding - Brazil, 2009. MMWR Morb Mortal Wkly Rep 2010b; 59(5):130-2.

Cetron MS, Marfin AA, Julian KG, Gubler DJ, Sharp DJ, Barwick RS, Weld LH, Chen R, Clover RD, Deseda-Tous J, Marchessault V, Offit PA, Monath TP. Yellow fever vaccine. Recommendations of the Advisory Committee on Immunization Practices (ACIP), 2002. MMWR Recomm Rep 2002; 51(RR-17):1-11.

Chambers TJ, Weir RC, Grakoui A, McCourt DW, Bazan JF, Fletterick RJ, Rice CM. Evidence that the N-terminal domain of nonstructural protein NS3 from yellow fever virus is a serine protease responsible for site-specific cleavages in the viral polyprotein. Proc Natl Acad Sci U S A 1990; 87(22):8898-902.

Chan RC, Penney DJ, Little D, Carter IW, Roberts JA, Rawlinson WD. Hepatitis and death following vaccination with 17D-204 yellow fever vaccine. Lancet 2001; 358(9276):121-2.

Chang GJ, Cropp BC, Kinney RM, Trent DW, Gubler DJ. Nucleotide sequence variation of the envelope protein gene identifies two distinct genotypes of yellow fever virus. J Virol 1995; 69(9):5773-80.

Chen S, Yu M, Jiang T, Deng Y, Qin C, Qin E. Induction of tetravalent protective immunity against four dengue serotypes by the tandem domain lll of the envelope protein. DNA Cell Biol 2007; 26(6):361-7.

Chen Y, Maguire T, Hileman RE, Fromm JR, Esko JD, Linhardt RJ, Marks RM. Dengue virus infectivity depends on envelope protein binding to target cell heparin sulfate. Nat Med 1997; 3(8):866-71.

Chicz RM, Urban RG, Gorga JC, Vignali DA, Lane WS, Strominger JL. Specificity and promiscuity among naturally processed peptides bound to HLA-DR alleles. J Exp Med 1993; 178(1):27-47.

Chu JH, Chiang CC, Ng ML. Immunization of flavivirus West Nile recombinant envelope domain lll protein induced specific immune response and protection against West Nile virus infection. J Immunol 2007; 178(5):2699-705.

Chu JJH, Ng ML. Infectious entry of West Nile virus occurs through a clathrin-mediated endocytic pathway. J Virol 2004; 78(19):10543-55.

Chu PW, Westaway EG. Molecular and ultrastructural analysis of heavy membrane fractions associated with the replication of Kunjin virus RNA. Arch Virol 1992; 125(1-4):177-91.

Cid-Arregui A, Juárez V, zur Hausen H. A synthetic E7 gene of human papillomavirus type 16 that yields enhanced expression of the protein in mammalian cells and is useful for DNA immunization studies. J Virol 2003; 77(8):4928-37.

Clarke DH. Antigenic analysis of certain group B arthropodborne viruses by antibody adsorption. J Exp Med 1960; 111:21-32.

Cleaves GR. Identification of dengue type 2 virus-specific high molecular weight proteins in virus-infected BHK cells. J Gen Virol 1985; 66(Pt 12):2767-71.

Cochran JR, Cameron TO, Stern LJ. The relationship of MHC-peptide binding and T cell activation probed using chemically defined MHC class ll oligomers. Immunity 2000; 12(3):241-50.

Cote-Sierra J, Foucras G, Guo L, Chiodetti L, Young HA, Hu-Li J, Zhu J, Paul WE. Interleukin 2 plays a central role in Th2 differentiation. Proc Natl Acad Sci U S A 2004; 101(11):3880-5.

Crill WD, Hughes HR, Delorey MJ, Chang GJ. Humoral immune responses of dengue fever patients using epitope-specific serotype-2 virus-like particle antigens. PLoS One 2009; 4(4):e4991.

Crill WD, Roehrig JT. Monoclonal antibodies that bind to domain lll of dengue virus E glycoprotein are the most efficient blockers of virus adsorption to Vero cells. J Virol 2001; 75(16):7769-73.

Dahiya SS, Saini M, Kumar P, Gupta PK. Immunogenicity of a DNA-launched replicon-based canine parvovirus DNA vaccine expressing VP2 antigen in dogs. Res Vet Sci 2012; 93(2):1089-97.

Davis NC, Shannon RC. Studies on yellow fever in South America: V. Transmission experiments with certain species of *Culex* and *Aedes*. J Exp Med 1929; 50(6):803-8.

de Alwis R, Beltramello M, Messer WB, Sukupolvi-Petty S, Wahala WMPB, Kraus A, Olivarez NP, Pham Q, Brain J, Tsai W, Wang W, Halstead S, Kliks S, Diamond MS, Baric R, Lanzavecchia A, Sallusto F, de Silva AM. In-depth analysis of the antibody response of individuals exposed to primary dengue virus infection. PLoS Negl Trop Dis 2011; 5(6):e1188.

De Bueger M, Bakker A, Goulmy E. Existence of mature human CD4+ T cells with genuine class l restriction. Eur J Immunol 1992; 22(3):875-8.

de Melo AB, Nascimento EJM, Braga-Neto U, Dhalia R, Silva AM, Oelke M, Schneck JP, Sidney J, Sette A, Montenegro SM, Marques ET. T-cell memory responses elicited by yellow fever vaccine are targeted to overlapping epitopes containing multiple HLA-l and –ll binding motifs. PLoS Negl Trop Dis 2013; 7(1):e1938.

Deml L, Bojak A, Steck S, Graf M, Wild J, Schirmbeck R, Wolf H, Wagner R. Multiple effects of codon usage optimization on expression and immunogenicity of DNA candidate vaccines encoding the human immunodeficiency virus type 1 gag protein. J Virol 2001; 75(22):10991-11001.

Deubel V, Digoutte JP, Monath TP, Girard M. Genetic heterogeneity of yellow fever virus strains from Africa and the Americas. J Gen Virol 1986; 67(Pt 1):209-13.

Deubel V, Huerre M, Cathomas G, Drouet MT, Wuscher N, Le Guenno B, Widmer AF. Molecular detection and characterization of yellow fever virus in blood and liver specimens of a non-vaccinated fatal human case. J Med Virol 1997; 53(2):212-7.

Doblas A, Domingo C, Bae HG, Bohórquez CL, de Ory F, Niedrig M, Mora D, Carrasco FJ, Tenorio A. Yellow fever vaccine-associated viscerotropic disease and death in Spain. J Clin Virol 2006; 36(2):156-8.

Dupuis M, Denis-Mize K, Woo C, Goldbeck C, Selby MJ, Chen M, Otten GR, Ulmer JB, Donnelly JJ, Ott G, McDonald DM. Distribution of DNA vaccines determines their immunogenicity after intramuscular injection in mice. J Immunol 2000; 165(5):2850-8.

Edgil D, Diamond MS, Holden KL, Paranjape SM, Harris E. Translation efficiency determines differences in cellular infection among dengue virus type 2 strains. Virology 2003; 317(2):275-90.

Engel AR, Vasconcelos PF, McArthur MA, Barrett AD. Characterization of a viscerotropic yellow fever vaccine variant from a patient in Brazil. Vaccine 2006; 24(15):2803-9.

Etemad B, Batra G, Raut R, Dahiya S, Khanam S, Swaminathan S, Khanna N. An envelope domain lll-based chimeric antigen produced in *Pichia pastoris* elicits neutralizing antibodies against all four dengue virus serotypes. Am J Trop Med Hyg 2008; 79(3):353-63.

Fan J, Liu Y, Xie X, Zhang B, Yuan Z. Inhibition of Japanese encephalitis virus infection by flavivirus recombinant E protein domain lll. Virol Sin 2013; 28(3):152-60.

Fenner F. The classification and nomenclature of viruses. Summary of results of meetings of the International Committee on Taxonomy of Viruses in Madrid, September 1975. J Gen Virol 1976; 31(3):463-70.

Fernandez-Botran R, Sanders VM, Mosmann TR, Vitetta ES. Lymphokine-mediated regulation of the proliferative response of clones of T helper 1 and T helper 2 cells. J Exp Med 1988; 168(2):543-58.

Finlay CJ. New aspects of yellow fever etiology arising from experimental findings of the last three years. Public Health Pap Rep 1903; 29:68-70.

Fiorentino DF, Bond MW, Mosmann TR. Two types of mouse T helper cell. IV. Th2 clones secrete a factor that inhibits cytokine production by Th1 clones. J Exp Med 1989; 170(6):2081-95.

Frolov I, Hardy R, Rice CM. *Cis*-acting RNA elements at the 5' end of Sindbis virus genome RNA regulate minus- and plus-strand RNA synthesis. RNA 2001; 7(11):1638-51.

Fynan EF, Webster RG, Fuller DH, Haynes JR, Santoro JC, Robinson HL. DNA vaccines: protective immunizations by parental, mucosal and gene-gun inoculations. Proc Natl Acad Sci U S A 1993; 90(24):11478-82.

Kuhn S, Twele-Montecinos L, MacDonald J, Webster P, Law B. Case report: probable transmission of vaccine strain of yellow fever virus to an infant via breast milk. CMAJ 2011; 183(4):E243-5.

Galler R, Pugachev KV, Santos CLS, Ocran SW, Jabor AV, Rodrigues SG, Marchevsky RS, Freire MS, Almeida LF, Cruz AC, Yamamura AM, Rocco IM, da Rosa ES, Souza LT, Vasconcelos PF, Guirakhoo F, Monath TP. Phenotypic and molecular analyses of yellow fever 17DD vaccine viruses associated with serious adverse events in Brazil. Virology 2001; 290(2):309-19.

Gao F, Li Y, Decker JM, Peyerl FW, Bibollet-Ruche F, Rodenburg CM, Chen Y, Shaw DR, Allen S, Musonda R, Shaw GM, Zajac AJ, Letvin N, Hahn BH. Codon usage optimization of HIV type 1 subtype C *gag, pol*, *env*, and *nef* genes: *in vitro* expression and immune responses in DNA-vaccinated mice. AIDS Res Hum Retroviruses 2003; 19(9):817-23.

Garske T, Van Kerkhove MD, Yactayo S, Ronveaux O, Lewis RF, Staples JE, Perea W, Ferguson NM, Yellow Fever Expert Committee. Yellow fever in Africa: estimating the burden of disease and impact of mass vaccination from outbreak and serological data. PLoS Med 2014; 11(5):e1001638.

Gasteiger E, Gattiker A, Hoogland C, Ivanyi I, Appel RD, Bairock A. ExPASy: The proteomics server for in-depth protein knowledge and analysis. Nucleic Acids Res 2003; 31(13):3784-8.

Gaucher D, Therrien R, Kettaf N, Angermann BR, Boucher G, Filali-Mouhim A, Moser JM, Mehta RS, Drake DR, Castro E, Akondy R, Rinfret A, Yassine-Diab B, Said EA, Chouikh Y, Cameron MJ, Clum R, Kelvin D, Somogyi R, Greller LD, Balderas RS, Wilkinson P, Pantaleo G, Tartaglia J, Haddad EK, Sékaly RP. Yellow fever vaccine induces integrated multilineage and polyfunctional immune responses. J Exp Med 2008; 205(13):3119-31.

Gerasimon G, Lowry K. Rare case of fatal yellow fever vaccine-associated viscerotropic disease. South Med J 2005; 98(6):653-6.

Germain M, Francy DB, Monath TP, Ferrara L, Bryan J, Salaun JJ, Heme G, Renaudet J, Adam C, Digoutte JP. Yellow fever in the Gambia, 1978-1979: entomological aspects and epidemiological correlations. Am J Trop Med Hyg, 1980; 29(5):929-40.

Gollins SW, Porterfield JS. Flavivirus infection enhancement in macrophages: an electron microscopic study of viral cellular entry. J Gen Virol 1985; 66(Pt 9):1969-82.

Gollins SW, Porterfield JS. Flavivirus infection enhancement in macrophages: radioactive and biological studies on the effect of antibody on viral fate. J Gen Virol 1984; 65(Pt 8):1261-72.

Gollins SW, Porterfield JS. pH-dependent fusion between the flavivirus West Nile and liposomal model membranes. J Gen Virol 1986a; 67(Pt 1):157-66.

Gollins SW, Porterfield JS. The uncoating and infectivity of the flavivirus West Nile on interaction with cells: effects of pH and ammonium chloride. J Gen Virol 1986b; 67(Pt 9):1941-50.

Gorbalenya AE, Donchenko AP, Koonin EV, Blinov VM. N-terminal domains of putative helicases of flavi- and pestiviruses may be serine proteases. Nucleic Acids Res 1989; 17(10):3889-97.

Gorgas WC. The method of transmission of yellow fever from man to man. Public Health Pap Rep 1902; 28:238-46.

Grantham R, Gautier C, Gouy M, Mercier R, Pavé A. Codon catalog usage and the genome hypothesis. Nucleic Acids Res 1980; 8(1):r49-62.

Grote A, Hiller K, Scheer M, Münch R, Nörtemann B, Hempel DC, Jahn D. JCat: novel tool to adapt codon usage of a target to its potential expression host. Nucleic Acids Res 2005; 33(Web Server issue):W526-31.

Hacker UT, Jelinek T, Erhardt S, Eigler A, Hartmann G, Nothdurft HD, Endres S. In vivo synthesis of tumor necrosis factor-alpha in healthy humans after live yellow fever vaccination. J Infect Dis 1998; 177(3):774-8.

Haddow AJ, Smithburn KC, Dick GWA, Kitchen SF, Lumsden WHR. Implication of the mosquito *Aedes (Stegomyia) africanus* Theobald in the forest cycle of yellow fever in Uganda. Ann Trop Med Parasitol 1948; 42(2):218-23.

Hahn CS, Dalrymple JM, Strauss JH, Rice CM. Comparison of the virulent Asibi strain of yellow fever virus with the 17D vaccine strain derived from it. Proc Natl Acad Sci U S A 1987; 84(7):2019-23.

Hanekom HA. Development of detection assays for Sindbis virus and investigating *in vitro* infection of mammalian cells (MMedSc Virology, University of the Free State). 2014. Retrieved from ETD-db (etd-04112014-154931).

Harding CV, Geuze HJ. Immunogenic peptides bind to class ll MHC molecules in an early lysosomal compartement. J Immunol 1993; 151(8):3988-98.

Hardy RW, Rice CM. Requirements at the 3' end of the Sindbis virus genome for efficient synthesis of minus-strand RNA. J Virol 2005; 79(8):4630-9.

Hariharan MJ, Driver DA, Townsend K, Brumm D, Polo JM, Belli BA, Catton DJ, Hsu D, Mittelstaedt D, McCormack JE, Karovodin L, Dubensky TW, Chang SM, Banks TA. DNA immunization against herpes simplex virus: enhanced efficacy using a Sindbis virus-based vector. J Virol 1998; 72(2):950-8.

Hartikka J, Sawdey M, Cornefert-Jensen F, Margalith M, Barnhart K, Nolasco M, Vahlsing HL, Meek J, Marquet M, Hobart P, Norman J, Manthorpe M. An improved plasmid DNA expression vector for direct injection into sketetal muscle. Hum Gene Ther 1996; 7(10):1205-17.

Holbrook MR, Li L, Suderman MT, Wang H, Barrett ADT. The French neurotropic vaccine strain of yellow fever virus accumulates mutations slowly during passage in cell culture. Virus Res 2000; 69(1):31-9.

Hsieh CS, Heimberger AB, Gold JS, O'Garra A, Murphy KM. Differential regulation of T helper phenotype development by interleukins 4 and 10 in an alpha beta T-cell-receptor transgenic system. Proc Natl Acad Sci U S A 1992; 89(13):6065-9.

Hsieh CS, Macatonia SE, Tripp CS, Wolf SF, O'Garra A, Murphy KM. Development of TH1 CD4+ T cells through IL-12 produced by Listeria-induced macrophages. Science 1993; 260(5107):547-9.

Hügle T, Fehrmann F, Bieck E, Kohara M, Kräusslich HG, Rice CM, Blum HE, Moradpour D. The hepatitis C virus nonstructural protein 4B is an integral endoplasmic reticulum membrane protein. Virology 2001; 284(1):70-81.

Ishak R, Tovey DG, Howard CR. Morphogenesis of yellow fever virus 17D in infected cell cultures. J Gen Virol 1988; 69(Pt 2):325-35.

Jones CT, Patkar CG, Kuhn RJ. Construction and applications of yellow fever virus replicons. Virology 2005; 331(2):247-59.

Jones EM, Wilson DC. Clinical features of yellow fever cases at Vom Christian Hospital during the 1969 epidemic on the Jos Plateau, Nigeria. Bull World Health Organ 1972; 46(5):653-7.

Julander JG, Trent DW, Monath TP. Immune correlates of protection against yellow fever determined by passive immunization and challenge in the hamster model. Vaccine 2011; 29(35):6008-16.

Kapoor M, Zhang L, Ramachandra M, Kusukawa J, Ebner KE, Padmanabhan R. Association between NS3 and NS5 proteins of dengue virus type 2 in the putative RNA replicase is linked to differential phosphorylation of NS5. J Biol Chem 1995; 270(32):19100-6.

Khromykh AA, Sedlak PL, Westaway EG. *cis*- and *trans*- acting elements in flavivirus RNA replication. J Virol 2000; 74(7):3253-63.

Khromykh AA, Varnavski AN, Sedlak PL, Westaway EG. Coupling between replication and packaging of flavivirus RNA: evidence derived from the use of DNA-based full-length cDNA clones of Kunjin virus. J Virol 2001; 75(10):4633-40.

Koedood M, Fichtel A, Meier P, Mitchell PJ. Human cytomegalovirus (HCMV) immediate-early enhancer/promoter specificity during embryogenesis defines target tissues of congenital HCMV infection. J Virol 1995; 69(4):2194-207.

Koonin EV. Computer-assisted identification of a putative methyltransferase domain in NS5 protein of flaviviruses and lambda 2 protein of reovirus. J Gen Virol 1993; 74(Pt 4):733-40.

Koschinski A, Wengler G, Wengler G, Repp H. The membrane proteins of flaviviruses form ion-permeable pores in the target membrane after fusion: identification of the pores and analysis of their possible role in virus infection. J Gen Virol 2003; 84(Pt 7):1711-21.

Kumaraguru U, Banerjee K, Rouse BT. *In vivo* rescue of defective memory CD8+ T cells by cognate helper T cells. J Leukoc Biol 2005; 78(4):879-87.

Kümmerer BM, Rice CM. Mutations in the yellow fever virus nonstructural protein NS2A selectively block production of infectious particles. J Virol 2002; 76(10):4773-84.

Kurt-Jones EA, Hamberg S, Ohara J, Paul WE, Abbas AK. Heterogeneity of helper/inducer T lymphocytes. l. Lymphokine production and lymphokine responsiveness. J Exp Med 1987; 166(6):1774-87.

Langley KE, Villarejo MR, Fowler AV, Zamenhof PJ, Zabin I. Molecular basis of beta-galactosidase alpha-complementation. Proc Natl Acad Sci USA 1975; 72(4):1254-7.

Larkin MA, Blackshields G, Brown NP, Chenna R, McGettigan PA, McWilliam H, Valentin F, Wallace IM, Wilm A, Lopez R, Thompson JD, Gibson TJ, Higgins DG. Clustal W and Clustal X version 2.0. Bioinformatics 2007; 23(21):2947-8.

Lee E, Lobigs M. E protein domain lll determinants of yellow fever virus 17D vaccine strain enhance binding to glycosaminoglycans, impede virus spread, and attenuate virulence. J Virol 2008; 82(12):6024-33.

Lepineic L, Dalgarno L, Huong VT, Monath TP, Digoutte JP, Deubel V. Geographic distribution and evolution of yellow fever viruses based on direct sequencing of genomic cDNA fragments. J Gen Virol 1994; 75(Pt 2):417-23.

Lindenbach BD, Rice CM. *trans*-Complementation of yellow fever virus NS1 reveals a role in early RNA replication. J Virol 1997; 71(12):9608-17.

Ljungberg K, Whitmore AC, Fluet ME, Moran TP, Shabman RS, Collier ML, Kraus AA, Thompson JM, Montefiori DC, Beard C, Johnston RE. Increased immunogenicity of a DNA-launched Venezuelen equine encephalitis virus-based replicon DNA vaccine. J Virol 2007; 81(24):13412-23.

MacGregor RR, Boyer JD, Ugen KE, Lacy KE, Gluckman SJ, Bagarazzi ML, Chattergoon MA, Baine Y, Higgins TJ, Ciccarelli RB, Coney LR, Ginsberg RS, Weiner DB. First human trial of a DNA-based vaccine for treatment of human immunodeficiency virus type 1 infection: safety and host response. J Infect Dis 1998; 178(1):92-100.

Mackenzie JM, Jones MK, Young PR. Immunolocalization of the dengue virus nonstructural glycoprotein NS1 suggests a role in viral RNA replication. Virology 1996; 220(1):232-40.

Mackenzie JM, Westaway EG. Assembly and maturation of the flavivirus Kunjin virus appear to occur in the rough endoplasmic recticulum and along the secretory pathway, respectively. J Virol 2001; 75(22):10787-99.

Mandl CW, Guirakhoo F, Holzmann H, Heinz FX, Kunz C. Antigenic structure of the flavivirus envelope protein E at the molecular level, using tick-borne encephalitis virus as a model. J Virol 1989; 63(2):564-71.

Mandl CW, Holzmann H, Meixner T, Rauscher S, Stadler PF, Allison SL, Heinz FX. Spontaneous and engineered deletions in the 3' noncoding region of tick-borne encephalitis virus: construction of highly attenuated mutants of a flavivirus. J Virol 1998; 72(3):2132-40.

Manthorpe M, Cornefert-Jensen F, Hartikka J, Felgner J, Rundell A, Margalith M, Dwarki V. Gene therapy by intramuscular injection of plasmid DNA: studies on firefly luciferase gene expression in mice. Hum Gene Ther 1993; 4(4):419-31.

Martinez X, Brandt C, Saddallah F, Tougne C, Barrios C, Wild F, Dougan G, Lambert PH, Siegrist CA. DNA immunization circumvents deficient induction of T helper type 1 and cytotoxic T lymphocyte responses in neonates and during early life. Proc Natl Acad Sci U S A 1997; 94(16):8726-31.

Martin M, Tsai TF, Cropp B, Chang GJ, Holmes DA, Tseng J, Shieh W, Zaki SR, Al-Sanouri I, Cutrona AF, Ray G, Weld LH, Cetron MS. Fever and multisystem organ failure associated with 17D-204 yellow fever vaccination: a report of four cases. Lancet 2001a; 358(9276):98-104.

Martin M, Weld LH, Tsai TF, Mootrey GT, Chen RT, Niu M, Cetron MS, GeoSentinel Yellow Fever Working Group. Advanced age a risk factor for illness temporally associated with yellow fever vaccination. Emerg Infect Dis 2001b; 7(6):945-51.

Martins MA, Silva ML, Marciano AP, Peruhype-Magalhães V, Eloi-Santos SM, Ribeiro JG, Correa-Oliveira R, Homma A, Kroon EG, Teixeira-Carvalho A, Marins-Filho OA. Activation/modulation of adaptive immunity emerges simultaneously after 17DD yellow fever first-time vaccination: is this the key to prevent severe adverse reactions following immunization? Clin Exp Immunol 2007; 148(1):90-100.

Matloubian M, Concepcion RJ, Ahmed R. CD4+ T cells are required to sustain CD8+ cytotoxic T-cell responses during chronic viral infection. J Virol 1994; 68(12):8056-63.

Meuer SC, Schlossman SF, Reinherz EL. Clonal analysis of human cytotoxic T lymphocytes: T4+ and T8+ effector T cells recognize products of different major histocompatibility complex regions. Proc Natl Acad Sci U S A 1982; 79(14):4395-9.

Monath TP. Facing up to re-emergence of urban yellow fever. Lancet 1999; 353(9164):1541.

Monath TP. Yellow fever. Medicine 2005; 33(7):21-3.

Monath TP, Barrett AD. Pathogenesis and pathophysiology of yellow fever. Adv Virus Res 2003; 60:343-95.

Monath TP, Fowler E, Johnson CT, Balser J, Morin MJ, Sisti M, Trent DW. An inactivated cell-culture vaccine against yellow fever. N Engl J Med 2011; 364(14):1326-33.

Monath TP, Lee CK, Julander JG, Brown A, Beasley DW, Watts DM, Hayman E, Guertin P, Makowiecki J, Crowell J, Levesque P, Bowick GC, Morin M, Fowler E, Trent DW. Inactivated yellow fever 17D vaccine: development and nonclinical safety, immunogenicity and protective activity. Vaccine 2010; 28(22):3827-40.

Montgomery DL, Shiver JW, Leander KR, Perry HC, Friedman A, Martinez D, Ulmer JB, Donnelly JJ, Liu MA. Heterologous and homologous protection against influenza A by DNA vaccination: optimization of DNA vectors. DNA Cell Biol 1993; 12(9):777-83.

Mosmann TR, Cherwinski H, Bond MW, Giedlin MA, Coffman RL. Two type of murine helper T cell clone. I. Definition according to profiles of lymphokine activities and secreted proteins. J Immunol 1986; 136(7):2348-57.

Mutebi JP, Barrett AD. The epidemiology of yellow fever in Africa. Microbes Infect 2002; 4(14):1459-68.

Mutebi JP, Wang H, Li L, Bryant JE, Barrett ADT. Phylogenetic and evolutionary relationships among yellow fever virus isolates in Africa. J Virol 2001; 75(15):6999-7008.

Muylaert IR, Chambers TJ, Galler R, Rice CM. Mutagenesis of the N-linked glycosylation sites of the yellow fever virus NS1 protein: effects on virus replication and mouse neurovirulence. Virology 1996; 222(1):159-68.

Nagata T, Uchijima M, Yoshida A, Kawashima M, Koide Y. Codon optimization effect on translational efficiency of DNA vaccine in mammalian cells: analysis of plasmid DNA encoding a CTL epitope derived from microorganisms. Biochem Biophys Res Commun 1999; 261(2):445-51.

Narum DL, Kumar S, Rogers WO, Fuhrmann SR, Liang H, Oakley M, Taye A, Sim BK, Hoffman SL. Codon optimization of gene fragments encoding *Plasmodium falciparum* merzoite proteins enhances DNA vaccine protein expression and immunogenicity in mice. Infect Immun 2001; 69(12):7250-3.

Neyts J, Meerbach A, McKenna P, De Clercq E. Use of the yellow fever virus vaccine strain 17D for the study of strategies for the treatment of yellow fever virus infections. Antiviral Res 1996; 30(2-3):125-32.

Ng ML, Pederson JS, Toh BH, Westaway EG. Immunofluorescent sites in vero cells infected with the flavivirus Kunjin. Arch Virol 1983; 78(3-4):177-90.

Niedrig M, Kürsteiner O, Herzog C, Sonnenberg K. Evaluation of an indirect immunofluorescence assay for detection of immunoglobulin M (IgM) and IgG antibodies against yellow fever virus. Clin Vaccine Immunol 2008; 15(2):177-81.

Nunes MR, Palacios G, Cardoso JF, Martins LC, Sousa EC Jr, de Lima CP, Medeiros DB, Savji N, Desai A, Rodrigues SG, Carvalho VL, Lipkin WI, Vasconcelos PF. Genomic and phylogenetic characterization of Brazilian yellow fever virus strains. J Virol 2012; 86(24):13263-71.

Oh YK, Harding CV, Swanson JA. The efficiency of antigen delivery from macrophage phagosomes into cytoplasm for MHC class l-restricted antigen presentation. Vaccine 1997; 15(5):511-8.

Ono L, Wollinger W, Rocco IM, Coimbra TL, Gorin PA, Sierakowski MR. *In vitro* and *in vivo* antiviral properties of sulfated galactomannans against yellow fever virus (BeH111 strain) and dengue 1 virus (Hawaii strain). Antiviral Res 2003; 60(3):201-8.

Perelygin AA, Scherbik SV, Zhulin IB, Stockman BM, Li Y, Brinton MA. Positional cloning of the murine flavivirus resisitance gene. Proc Nat Acad Sci U S A 2002; 99(14):9322-7.

Philip CB. The experimental transmission of yellow fever by mosquitoes. Science 1930; 71(1850):614-5.

Poland JD, Calisher CH, Monath TP, Downs WG, Murphy K. Persistence of neutralizing antibody 30-35 years after immunization with 17D yellow fever vaccine. Bull World Health Organ 1981; 59(6):895-900.

Prince AM, Whalen R, Brotman B. Successful nucleic acid based immunization of newborn chimpanzees against hepatitis B virus. Vaccine 1997; 15(8):916-9.

Pujhari S, Baig TT, Hansra S, Zakhartchouk AN. Development of a DNA-launched replicon as a vaccine for porcine reproductive syndrome virus. Virus Res 2013; 173(2):321-6.

Pulendran B, Miller J, Querec TD, Akondy R, Moseley N, Laur O, Glidewell J, Monson N, Zhu T, Staprans S, Lee D, Brinton MA, Perelygin AA, Vellozzi C, Brachman P, Lalor S, Teuwen D, Eidex RB, Cetron M, Priddy F, del Rio C, Altman J, Ahmed R. Case of yellow fever vaccine-associated viscerotropic disease with prolonged vireamia, robust adaptive immune responses, and polymorphisms in CCR5 and RANTES genes. J Infect Dis 2008; 198(4):500-7.

Pushko P, Parker M, Ludwig GV, Davis NL, Johnston RE, Smith JF. Replicon-helper systems from attenuated Venezuelen equine encephalitis virus: expression of heterologous genes *in vitro* and immunization against heterologous pathogens *in vivo*. Virology 1997; 239(2):389-401.

Reed W, Carroll J, Agramonte A, Lazear JW. The etiology of yellow fever-a preliminary note. Public Health Pap Rep 1900; 26:37-53.

Reed W, Carroll J. The etiology of yellow fever: a supplemental note. American Medicine 1902; 3:301-5.

Reed W, Carroll J, Agramonte A. The etiology of yellow fever: an additional note. JAMA 1901; 36:431-40.

Reinhart B, Jaspert R, Niedrig M, Kostner C, L'age-Stehr J. Development of viremia and humoral and cellular parameters of immune activation after vaccination with yellow fever virus strain 17D: a model of human flavivirus infection. J Med Virol 1998; 56(2):159-67.

Rey FA, Heinz FX, Mandl C, Kunz C, Harrison SC. The envelope glycoprotein from tick-borne encephalitis virus at 2 A resolution. Nature 1995; 375(6529):291-8.

Rice CM, Lenches EM, Eddy SR, Shin SJ, Sheets RL, Strauss JH. Nucleotide sequence of yellow fever virus: implications for flavivirus gene expression and evolution. Science 1985; 229(4715):726-33.

Rombel IT, Sykes KF, Rayner S, Johnston SA. ORF-FINDER: a vector for high-throughput gene identification. Gene 2002; 282(1-2):33-41.

Rossi-Bergmann B, Müller I, Godinho EB. TH1 and TH2 T-cell subsets are differentially activated by macrophages and B cells in murine leishmaniasis. Infect Immun 1993; 61(5):2266-9.

Sanarelli G. A lecture on yellow fever. With a description of the *Bacillus icteroides*: delivered before the University of Montevideo on June 10th, 1897. Br Med J 1897; 2(1905):7-11.

Sánchez MD, Pierson TC, McAllister D, Hanna SL, Puffer BA, Valentine LE, Murtadha MM, Hoxie JA, Doms RW. Characterization of neutralizing antibodies to West Nile virus. Virology 2005; 336(1):70-82.

Santin AD, Hermonat PL, Ravaggi A, Bellone S, Pecorelli S, Roman JJ, Parham GP, Cannon MJ. Interleukin-10 increases Th1 cytokine production and cytotoxic potential in human papillomavirus-specific CD8+ cytotoxic T lymphocytes. J Virol 2000; 74(10):4729-37.

Sawyer WA, Lloyd W. The use of mice in tests of immunity against yellow fever. J Exp Med 1931; 54(4):533-55.

Saxena S, Dahiya SS, Sonwane AA, Patel CL, Saini M, Rai A, Gupta PK. A Sindbis virus replicon-based DNA vaccine encoding the rabies virus glycoprotein elicits immune responses and complete protection in mice from lethal challenge. Vaccine 2008; 26(51):6592-601.

Schlesinger JJ, Brandriss MW, Cropp CB, Monath TP. Protection against yellow fever in monkeys by immunization with yellow fever virus nonstructural protein NS1. J Virol 1986; 60(3):1153-5.

Schlesinger JJ, Brandriss MW. Growth of 17D yellow fever virus in a macrophage-like cell line, U937: role of Fc and viral receptors in antibody-mediated infection. J Immunol 1981; 127(2):659-65.

Schlesinger JJ, Walsh EE, Brandriss MW. Analysis of 17D yellow fever virus envelope protein epitopes using monoclonal antibodies. J Gen Virol 1984; 65(Pt 10):1637-44.

Schlesinger WR (ed). The Togaviruses: biology, structure, replication. Chapter 8: Togavirus morphology and morphogenesis. New York: Academic Press, 1980.

Segal BM, Dwyer BK, Shevach EM. An interleukin (IL)-10/IL-12 immunoregulatory circuit controls susceptibility to autoimmune disease. J Exp Med 1998; 187(4):537-46.

Seligman SJ, Cohen JE, Itan Y, Casanova JL, Pezzullo JC. Defining risk groups to yellow fever vaccine-associated viscerotropic disease in the absence of denominator data. Am J Trop Med Hyg 2014; 90(2):267-71.

Shannon RC, Whitman L, Franca M. Yellow fever virus in jungle mosquitoes. Science 1938; 88(2274):110-1.

Sharp PM, Li WH. The codon adaptation index – a measure of directional synonymous codon usage bias, and its potential applications. Nucleic Acids Res 1987; 15(3):1281-95.

Sievers F, Wilm A, Dineen D, Gibson TJ, Karplus K, Li W, Lopez R, McWilliam H, Remmert M, Söding J, Thompson JD, Higgins DG. Fast, scalable generation of high-quality protein multiple sequence alignments using Clustal Omega. Mol Syst Biol 2011; 7:539.

Smetana HF. The histopathology of experimental yellow fever. Virchows Arch Pathol Anat Physiol Klin Med 1962; 335:411-27.

Smith KM, Pottage L, Thomas ER, Leishman AJ, Doig TN, Xu D, Liew FY, Garside P. Th1 and Th2 CD4+ T cells provide help for B cell clonal expansion and antibody synthesis in a similar manner *in vivo*. J Immunol 2000; 165(6):3136-44.

Smouse SL. Identification of antigenic regions and linear B cell epitopes on yellow fever virus (MMedSc Virology, University of the Free State). 2013. Retrieved from ETD-db (etd-09162013-125200).

Soper FL. Jungle yellow fever in South America. The British Medical Journal 1936; 1(3922):481.

Spits H, Ijssel H, Thompson A, de Vries JE. Human T4+ and T8+ cytotoxic T lymphocyte clones directed at products of different class ll major histocompatibility complex loci. J Immunol 1983; 131(2):678-83.

Stadler K, Allison SL, Schalich J, Heinz FX. Proteolytic activation of tick-borne encephalitis virus by furin. J Virol 1997; 71(11):8475-81.

Staples JE, Gershman M, Fischer M, CDC. Yellow fever vaccine: recommendations of the Advisory Committee on Immunization Practices (ACIP). MMWR Recomm Rep 2010; 59(RR-7): 1-27.

Stiasny K, Allison SL, Mandl CW, Heinz FX. Role of metastability and acidic pH in membrane fusion by tick-borne encephalitis virus. J Virol 2001; 75(16):7392-8.

Stiasny K, Allison SL, Marchler-Bauer A, Kunz C, Heinz FX. Structural requirements for low-pH-induced rearrangements in the envelope glycoprotein of tick-borne encephalitis virus. J Virol 1996; 70(11):8142-7.

Stobo JD, Rosenthal AS, Paul WE. Functional heterogeneity of murine lymphoid cells. l. Responsiveness to and surface binding of concanavalin A and phytohemagglutinin. J Immunol 1972; 108(1):1-17.

Stock NK, Laraway H, Faye O, Diallo M, Niedrig M, Sall AA. Biological and phylogenetic characteristics of yellow fever virus lineages from West Africa. J Virol 2013; 87(5):2895-907.

Stokes A, Bauer JH, Hudson NP. Experimental transmission of yellow fever virus to laboratory animals. Excerpts from The American Journal of Tropical Medicine 1928;8:103. Int J Infect Dis 1997; 2(1):54-9.

Strober W. Trypan blue exclusion test of cell viability. Curr Protoc Immunol 2001; Appendix B:Appendix B.

Sun SQ, Liu XT, Guo HC, Yin SH, Shang YJ, Feng X, Liu ZX, Xie QG. Protective immune responses in guinea pigs and swine induced by a suicidal DNA vaccine of the capsid gene of swine vesicular disease virus. J Gen Virol 2007; 88(Pt 3):842-8.

Tan BH, Fu J, Sugrue RJ, Yap EH, Chan YC, Tan YH. Recombinant dengue type 1 virus NS5 protein expressed in *Escherichia coli* exhibits RNA-dependent RNA polymerase activity. Virology 1996; 216(2):317-25.

Tanji Y, Hijikata M, Satoh S, Kaneko T, Shimotohno K. Hepatitis C virus-encoded nonstructural protein NS4A has versatile functions in viral protein processing. J Virol 1995; 69(3):1575-81.

ter Meulen J, Sakho M, Koulemou K, Magassouba N, Bah A, Preiser W, Daffis S, Klewitz C, Bae HG, Niedrig M, Zeller H, Heinzel-Gutenbrunner M, Koivogui L, Kaufmann A. Activation of the cytokine network and unfavorable outcome in patients with yellow fever. J Infect Dis 2004; 190(10):1821-7.

Ternette N, Tippler B, Überla K, Grunwald T. Immunogenicity and efficacy of codon optimized DNA vaccines encoding the F-protein of respiratory syncytial virus. Vaccine 2007; 25(41):7271-9.

Theiler M, Smith HH. The effect of prolonged cultivation *in vitro* upon the pathogenicity of yellow fever virus. J Exp Med 1937a; 65(6):767-86.

Theiler M, Smith HH. The use of yellow fever virus modified by *in vitro* cultivation for human immunization. J Exp Med 1937b; 65(6):787-800.

Theiler M. Susceptibility of white mice to the virus of yellow fever. Science 1930; 71(1840):367.

Thomas RE, Spragins W, Lorenzetti DL. How many published cases of serious adverse events after yellow fever vaccination meet Brighton Collaboration diagnostic criteria? Vaccine 2013; 31(52):6201-9.

Throsby M, Geuijen C, Goudsmit J, Bakker AQ, Korimbocus J, Kramer RA, Clijsters-van der Horst M, de Jong M, Jongeneelen M, Thijsse S, Smit R, Visser TJ, Bijl N, Marissen WE, Loeb M, Kelvin DJ, Preiser W, ter Meulen J, de Kruif J. Isolation and characterization of human monoclonal antibodies from individuals infected with West Nile virus. J Virol 2006; 80(14):6982-92.

Torshin IY. Three-dimensional models of human 2'-5' oligoadenylate synthetases: a new computational method for reconstructing an enzyme assembly. Med Sci Monit 2005; 11(7):BR235-47.

Trinchieri G. Cytokines acting on or secreted by macrophages during intracellular infection (IL-10, IL-12, IFN-gamma). Curr Opin Immunol 1997; 9(1):17-23.

Ulmer JB, Donnelly JJ, Parker SE, Rhodes GH, Feigner PL, Dwarki VJ, Gromkowski SH, Deck RR, DeWitt CM, Friedman A, Hawe LA, Leander KR, Martinez D, Perry HC, Shiver JW, Montgomery DL, Liu MA. Heterologous protection against influenza by injection of DNA encoding a viral protein. Science 1993; 259(5102):1745-9.

Unknown. Yellow fever epidemiology and control. Br Med J 1944; 2(4367):377-8.

Vasconcelos PFC, Bryant JE, Travassos da Rosa APA, Tesh RB, Rodrigues SG, Barrett ADT. Genetic divergence and dispersal of yellow fever virus, Brazil. Emerg Infect Dis 2004; 10(9):1578-84.

Vasconcelos PFC, Costa ZG, Travassos da Rosa ES, Luna E, Rodrigues SG, Barros VL, Dias JP, Monteiro HA, Oliva OF, Vasconcelos HB, Oliveira RC, Sousa MR, Barbosa Da Silva J, Cruz AC, Martins EC, Travassos Da Rose JF. Epidemic of jungle yellow fever in Brazil, 2000: implications of climatic alterations in disease spread. J Med Virol 2001a; 65(3):598-604.

Vasconcelos PFC, Luna EJ, Galler R, Silva LJ, Coimbra TL, Barros VL, Monath TP, Rodigues SG, Laval C, Costa ZG, Vilela MF, Santos CL, Papaiordanou PM, Alves VA, Andrade LD, Sato HK, Rosa ES, Froguas GB, Lacava E, Almeida LM, Cruz AC, Rocco IM, Santos RT, Oliva OF, Brazilian Yellow Fever Vaccine Evaluation Group. Serious adverse events associated with yellow fever 17DD vaccine in Brazil: a report of two cases. Lancet 2001b; 358(9276):91-7.

Vasconcelos PFC, Rosa AP, Rodrigues SG, Rosa ES, Monteiro HA, Cruz AC, Barros VL, Souza MR, Rosa JF. Yellow fever in Pará State, Amazon Region of Brazil, 1998-1999: entomologic and epidemiologic findings. Emerg Infect Dis 2001c; 7(3 Suppl):565-9.

Vázquez S, Valdés O, Pupo M, Delgado I, Álvarez M, Pelegrino JL, Guzmán MG. MAC-ELISA and ELISA inhibition methods for detection of antibodies after yellow fever vaccination. J Virol Methods 2003; 110(2):179-84.

Verma SK, Kumar S, Gupta N, Vedi S, Bhattacharya SM, Lakshmana Rao PV. Bacterially expressed recombinant envelope protein domain lll of Japanese encephalitis virus (rJEV-Dlll) elicits Th1 type of immune response in BALB/c mice. Vaccine 2009; 27(49):6905-9.

von Herrath MG, Yokoyama M, Dockter J, Oldstone MB, Whitton JL. CD4-deficient mice have reduced levels of memory cytotoxic T lymphocytes after immunization and show diminished resistance to subsequent virus challenge. J Virol 1996; 70(2):1072-9.

Vratskikh O, Stiasny K, Zlatkovic J, Tsouchnikas G, Jarmer J, Karrer U, Roggendorf M, Roggendorf H, Allwinn R, Heinz FX. Dissection of antibody specificities induced by yellow fever vaccination. PLoS Pathog 2013; 9(6):e1003458.

Wang E, Weaver SC, Shope RE, Tesh RB, Watts DM, Barrett ADT. Genetic variation in yellow fever virus: duplication in the 3' noncoding region of strains from Africa. Virology 1996; 225(2):274-81.

Wang H, Jennings AD, Ryman KD, Late CM, Wang E, Ni H, Minor PD, Barrett AD. Genetic variation among strains of wild-type yellow fever virus from Senegal. J Gen Virol 1997; 78(Pt 6):1349-52.

Wang R, Doolan DL, Le TP, Hedstrom RC, Coonan KM, Charoenvit Y, Jones TR, Hobart P, Margalith M, Ng J, Weiss WR, Sedegah M, de Taisne C, Norman JA, Hoffmann SL. Induction of antigen-specific cytotoxic T lymphocytes in humans by a malaria DNA vaccine. Science 1998; 282(5388):476-80.

Ward ES, Qadri A. Biophysical and structural studies of TCRs and ligands: implications for T cell signaling. Curr Opin Immunol 1997; 9(1):97-106.

Wengler G, Wengler G. Cell-associated West Nile flavivirus is covered with E + pre-M protein heterodimes which are destroyed and reorganized by proteolytic cleavage during virus release. J Virol 1989; 63(6):2521-6.

Whitmire JK, Tan JT, Whitton JL. Interferon-gamma acts directly on CD8+ T cells to increase their abundance during virus infection. J Exp Med 2005; 201(7):1053-9.

Whittembury A, Ramirez G, Hernández H, Ropero AM, Waterman S, Ticona M, Brinton M, Uchuya J, Gershman M, Toledo W, Staples E, Campos C, Martínez M, Chang GJ, Cabezas C, Lanciotti R, Zaki S, Montgomery JM, Monath T, Hayes E. Viscerotropic disease following yellow fever vaccination in Peru. Vaccine 2009; 27(43):5974-81.

Wahala WMPB, Huang C, Butrapet S, White LJ, de Silva AM. Recombinant dengue type 2 viruses with altered E protein domain lll epitopes are efficiently neutralized by human immune sera. J Virol 2012; 86(7):4019-23.

Wahala WMPB, Kraus AA, Haymore LB, Accavitti-Loper MA, de Silva AM. Dengue virus neutralization by human immune sera: role of envelope protein domain lll-reactive antibody. Virology 2009; 392(1):103-13.

Whitton JL, Rodriguez F, Zhang J, Hassett DE. DNA immunization: mechanistic studies. Vaccine 1999: 17(13-14):1612-9.

Wolff JA, Malone RW, Williams P, Chong W, Acsadi G, Jani A, Felgner PL. Direct gene transfer into mouse muscle *in vivo*. Science 1990; 247(4949 Pt 1):1465-8.

World Health Organization (WHO) Committee on International Quarantine. Delineation of yellow fever endemic zones – Africa and America. Geneva: WHO, 1953.

WHO. District guidelines for yellow fever surveillance. Geneva: WHO, 1998.

WHO Division of Epidemiological Surveillance and Health Situation and Trend Assessment. Global health situation and projections estimates. Geneva: WHO, 1992.

WHO. Prevention and control of yellow fever in Africa. Geneva: WHO, 1986.

WHO. Yellow fever in Africa. WHO Chronicle. 1967; 21(9):393-6.

WHO Scientific Group. Arthropod-borne and rodent-borne viral diseases. Geneva: WHO, 1985.

Wubbolts R, Fernandez-Borja M, Oomen L, Verwoerd D, Janssen H, Calafat J, Tulp A, Dusseljee S, Neefjes J. Direct vesicular transport of MHC class ll molecules from lysosomal structures to the cell surface. J Cell Biol 1996; 135(3):611-22.

Wu KP, Wu CW, Tsao YP, Kuo TW, Lou YC, Lin CW, Wu SC, Cheng JW. Structural basis of a flavivirus recognized by its neutralizing antibody: solution structure of the domain lll of the Japanese encephalitis virus envelope protein. J Biol Chem 2003; 278(46):46007-13.

Xiong C, Levis R, Shen P, Schlesinger S, Rice CM, Huang HV. Sindbis virus: an efficient, broad host range vector for gene expression in animal cells. Science 1989; 243(4895):1188-91.

Yenofsky RL, Fine M, Pellow JW. A mutant neomycin phosphotransferase ll gene reduces the resistance of transformants to antibiotic selection pressure. Proc Natl Acad Sci U S A 1990; 87(9):3435-9.

zur Megede J, Chen MC, Doe B, Schaefer M, Greer CG, Selby M, Otten GR, Barnett SW. Increased expression and immunogenicity of sequence-modified human immunodeficiency virus type 1 *gag* gene. J Virol 2000; 74(6):2628-35.

zur Megede J, Otten GR, Doe B, Liu H, Leung L, Ulmer JB, Donnelly JJ, Barnett SW. Expression and immunogenicity of sequence-modified human immunodeficiency virus type 1 subtype B *pol* and *gagpol* DNA vaccines. J Virol 2003; 77(11):6197-207.

Appendix A: Codon-optimisation of wild-type YFV ED-lll gene

Alignment of the gene encoding wild-type YFV ED-lll protein and the codon-optimised YFV ED-lll gene using Clustal W2

```
Wild-type       AAGGGGACATCCTACAAAATGTGCACTGACAAAATGTCTTTTGTCAAGAACCCAACTGAC 60
CodonOptimised  AAGGGCACCAGCTACAAGATGTGCACCGACAAGATGAGCTTCGTGAAGAACCCCACCGAC 60
                ***** **   ****** ******** ***** ***   ** ** ******** ** ***

Wild-type       ACTGGCCATGGCACTGTTGTGATGCAGGTGAAAGTGCCAAAAGGAGCCCCCTGCAAGATT 120
CodonOptimised  ACCGGCCACGGCACCGTGGTGATGCAGGTGAAGGTGCCCAAGGGCGCCCCCTGCAAGATC 120
                ** ***** ***** ** ************** ***** ** ** **************

Wild-type       CCAGTGATAGTAGCTGATGATCTTACAGCGGCAATCAATAAAGGCATTTTGGTTACAGTT 180
CodonOptimised  CCCGTGATCGTGGCCGACGACCTGACCGCCGCCATCAACAAGGGCATCCTGGTGACCGTG 180
                ** ***** ** ** ** ** ** ** ** ** ***** ** *****  **** ** **

Wild-type       AACCCCATCGCCTCAACCAATGATGATGAAGTGCTGATTGAGGTGAACCCACCTTTTGGA 240
CodonOptimised  AACCCCATCGCCAGCACCAACGACGACGAGGTGCTGATCGAGGTGAACCCCCCCTTCGGC 240
                ************   ***** ** ** ** ******** ********** ** ** **

Wild-type       GACAGCTACATTATCGTTGGGACAGGAGATTCACGTCTCACTTACCAGTGGCACAAAGAG 300
CodonOptimised  GACAGCTACATCATCGTGGGCACCGGCGACAGCAGGCTGACCTACCAGTGGCACAAGGAG 300
                *********** ***** ** ** ** **     * ** ** ************** ***
```

Alignment of amino acid sequence of the wild-type YFV ED-lll protein and the codon-optimised YFV ED-lll using Clustal W2

```
Wildtype            MKGTSYKMCTDKMSFVKNPTDTGHGTVVMQVKVPKGAPCKIPVIVADDLTAAINKGILVT 60
CodonOptimised      MKGTSYKMCTDKMSFVKNPTDTGHGTVVMQVKVPKGAPCKIPVIVADDLTAAINKGILVT 60
                    ************************************************************

Wildtype            VNPIASTNDDEVLIEVNPPFGDSYIIVGTGDSRLTYQWHKE 101
CodonOptimised      VNPIASTNDDEVLIEVNPPFGDSYIIVGTGDSRLTYQWHKE 101
                    *****************************************
```

Codon usage by mice for the wild-type Asibi strain YFV ED-lll

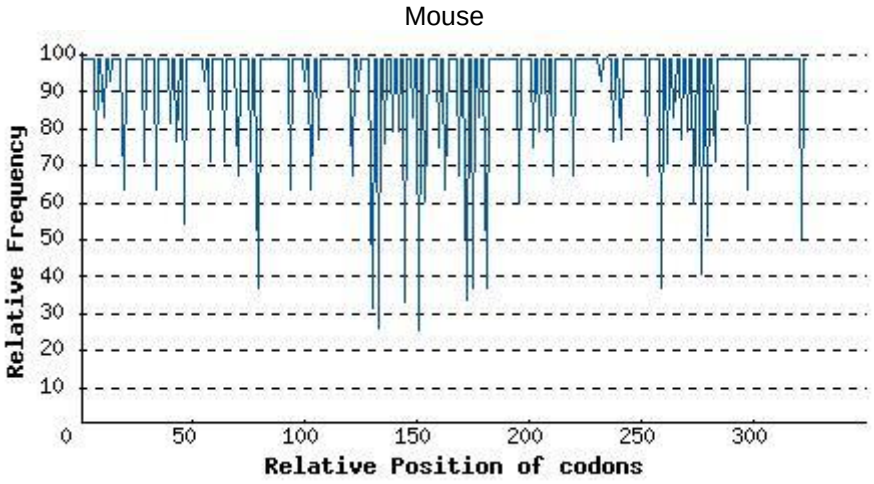

CAI : 0.78

Codon usage by mice for mouse codon-optimised wild-type Asibi strain YFV ED-III

Mouse

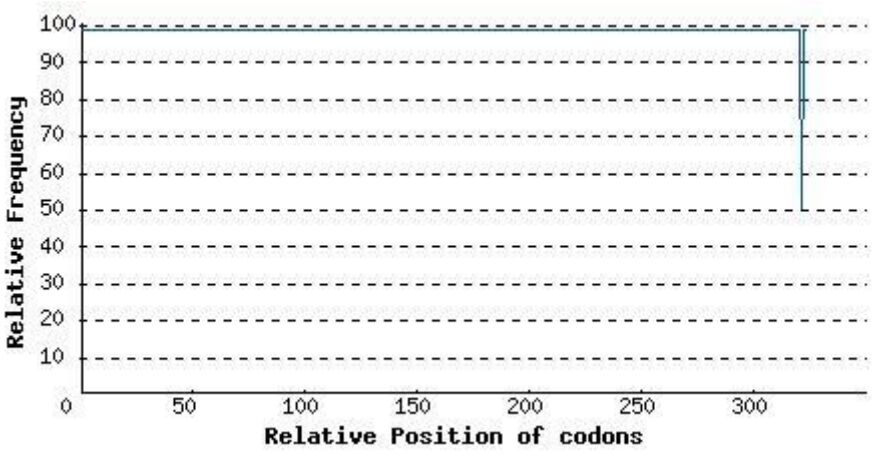

CAI : 0.99

Codon usage by humans for mouse codon-optimised wild-type Asibi strain YFV ED-III

Human

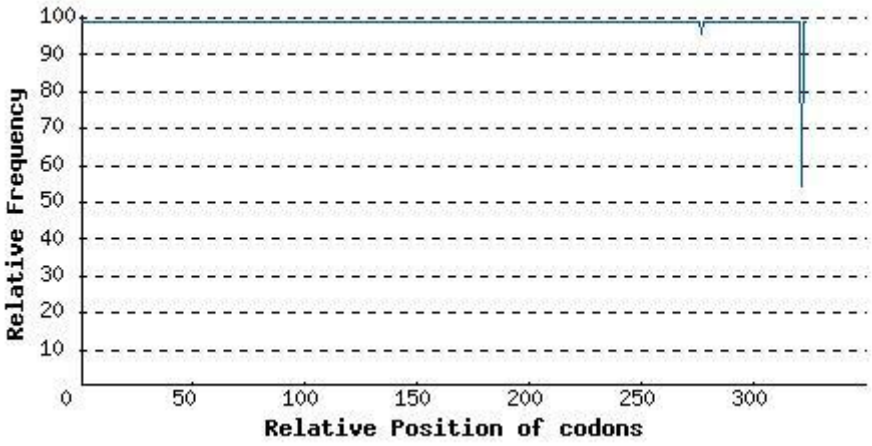

CAI : 0.99

Appendix B: Vector maps for plasmids

Vector map for pUC57/ED-lll

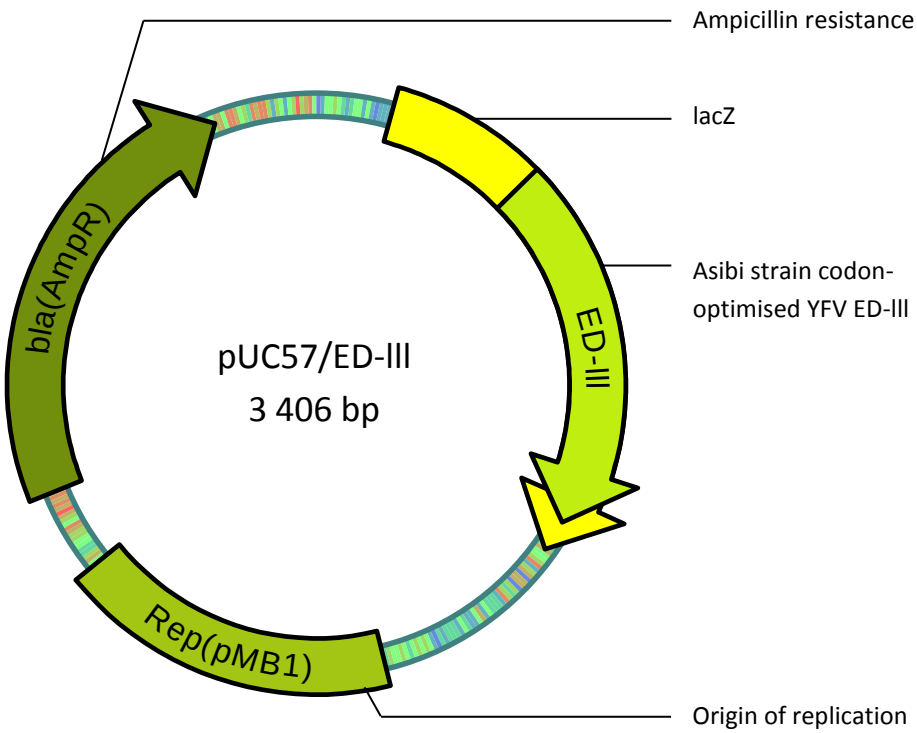

Vector map for pSinGFP

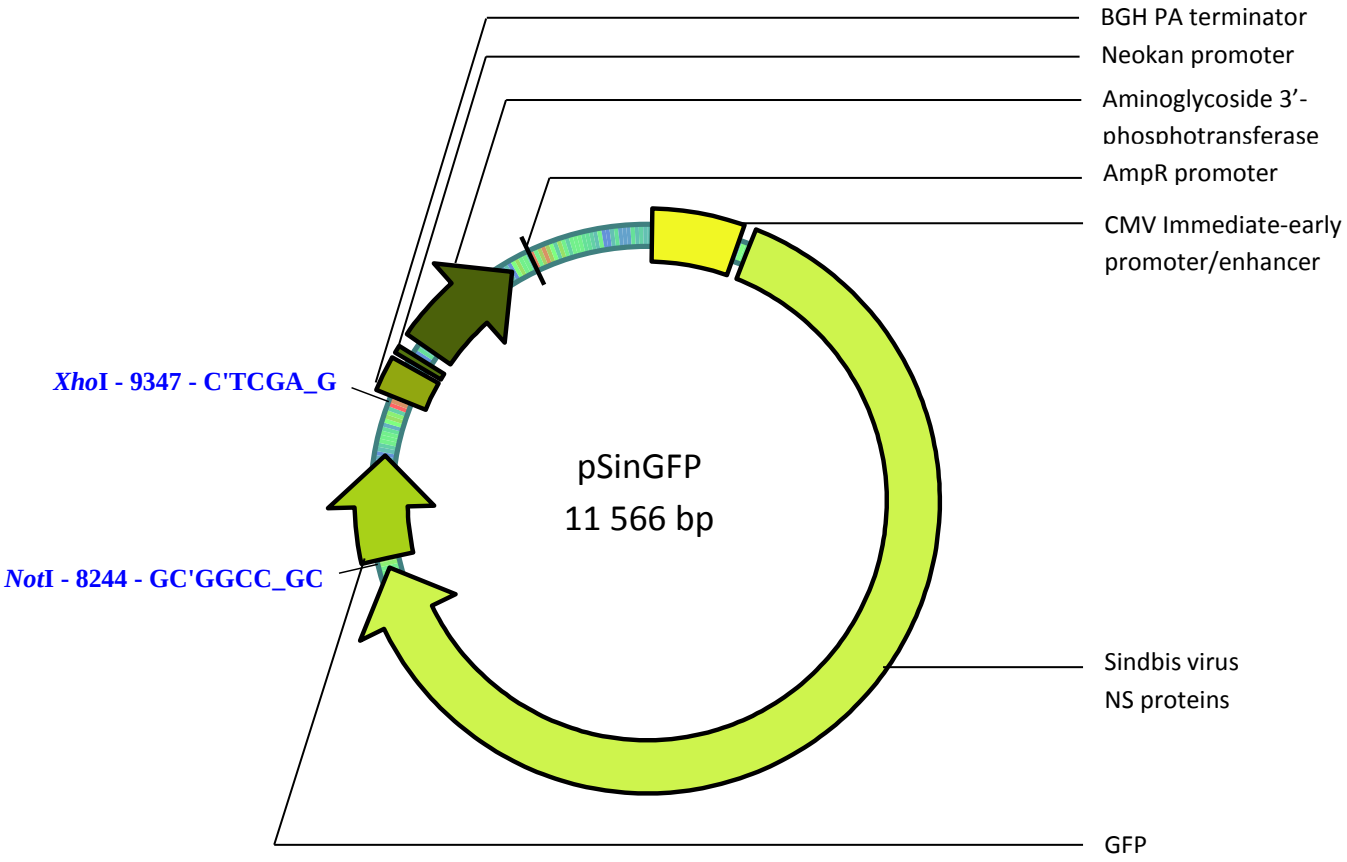

***AmpR (Ampicillin-resistance promoter)**

Vector map for pSinED-lll

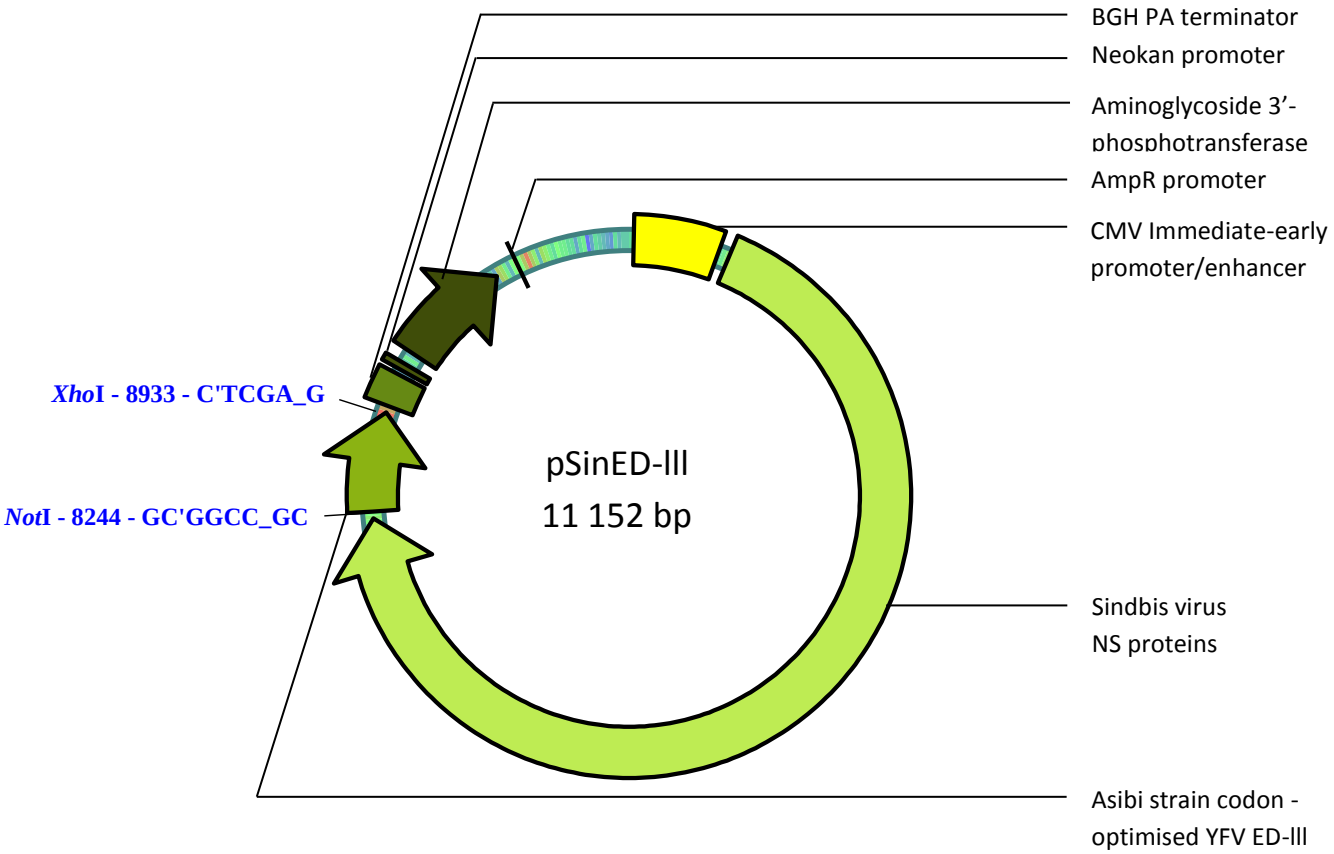

***AmpR** (Ampicillin-resistance promoter)

Appendix C: Sequencing results for the pSinED-lll replicon

Nucleotide and amino acid sequence data for pSinED-lll

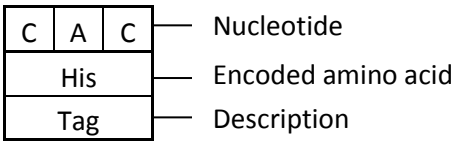

A	T	G	A	A	G	G	G	C	A	C	C	A	G	C	T	A	C	A	A	G	A	T	G
Met			Lys			Gly			Thr			Ser			Tyr			Lys			Met		
Asibi strain codon-optimised ED-lll																							

T	G	C	A	C	C	G	A	C	A	A	G	A	T	G	A	G	C	T	T	C	G	T	G
Cys			Thr			Asp			Lys			Met			Ser			Phe			Val		
Asibi strain codon-optimised ED-lll																							

A	A	G	A	A	C	C	C	C	A	C	C	G	A	C	A	C	C	G	G	C	C	A	C
Lys			Asn			Pro			Thr			Asp			Thr			Gly			His		
Asibi strain codon-optimised ED-lll																							

G	G	C	A	C	C	G	T	G	G	T	G	A	T	G	C	A	G	G	T	G	A	A	G
Gly			Thr			Val			Val			Met			Gln			Val			Lys		
Asibi strain codon-optimised ED-lll																							

G	T	G	C	C	C	A	A	G	G	G	C	G	C	C	C	C	C	T	G	C	A	A	G
Val			Pro			Lys			Gly			Ala			Pro			Cys			Lys		
Asibi strain codon-optimised ED-lll																							

A	T	C	C	C	C	G	T	G	A	T	C	G	T	G	G	C	C	G	A	C	G	A	C
Ile			Pro			Val			Ile			Val			Ala			Asp			Asp		
Asibi strain codon-optimised ED-lll																							

C	T	G	A	C	C	G	C	C	G	C	C	A	T	C	A	A	C	A	A	G	G	G	C
Leu			Thr			Ala			Ala			Ile			Asn			Lys			Gly		
Asibi strain codon-optimised ED-lll																							

A	T	C	C	T	G	G	T	G	A	C	C	G	T	G	A	A	C	C	C	C	A	T	C
Ile			Leu			Val			Thr			Val			Asn			Pro			Ile		
Asibi strain codon-optimised ED-lll																							

G	C	C	A	G	C	A	C	C	A	A	C	G	A	C	G	A	C	G	A	G	G	T	G
Ala			Ser			Thr			Asn			Asp			Asp			Glu			Val		
Asibi strain codon-optimised ED-lll																							

C	T	G	A	T	C	G	A	G	G	T	G	A	A	C	C	C	C	C	C	C	T	T	C
Leu			Met			Glu			Val			Asn			Pro			Pro			Phe		
Asibi strain codon-optimised ED-lll																							

G	G	C	G	A	C	A	G	C	T	A	C	A	T	C	A	T	C	G	T	G	G	G	C
Gly			Asp			Ser			Tyr			Ile			Ile			Val			Gly		
Asibi strain codon-optimised ED-lll																							

A	C	C	G	G	C	G	A	C	A	G	C	A	G	G	C	T	G	A	C	C	T	A	C
Thr			Gly			Asp			Ser			Arg			Leu			Thr			Tyr		
Asibi strain codon-optimised ED-lll																							

C	A	G	T	G	G	C	A	C	A	A	G	G	A	G	C	A	C	C	A	C	C	A	C
Gln			Trp			His			Lys			Glu			His			His			His		
Asibi strain codon-optimised ED-lll															Hexahistidine tag								

C	A	C	C	A	C	C	A	C	T	A	A	A	G	C	G	G	C	A	T	C	G	A	T
His			His			His			Stop			3’ UTR & polyA tail of SinV											
Histidine tag																							

A	C	T	A	G	T	A	C	G	C	C	C	C	A	A	T	G	A	C	C	C	G	A	C
3’ UTR & polyA tail of SinV																							

C	A	G	C	A	A	A	A	C	T	C	G	A	T	G	T	A	C	T	T	C	C	G	A
3’ UTR & polyA tail of SinV																							

G	G	A	A	C	T	G	A	T	G	T	G	C	A	T	A	A	T	G	C	A	T	C	A
3’ UTR & polyA tail of SinV																							

G	G	C	T	G	G	T	A	T	A	T	T	A	G	A	T	C	C	C	C	G	C	T	T
3’ UTR & polyA tail of SinV																							

A	C	C	G	C	G	G	G	C	A	A	T	A	T	A	G	C	A	A	C	A	C	C	A
3’ UTR & polyA tail of SinV																							

A	A	A	C	T	C	G	A	C	G	T	A	T	T	T	C	C	G	A	G	G	A	G	G
3’ UTR & polyA tail of SinV																							

C	G	C	A	G	T	G	C	A	T	A	A	T	G	C	T	G	C	G	C	A	G	T	G
3’ UTR & polyA tail of SinV																							

T	T	G	C	C	A	A	A	T	A	A	T	C	A	C	T	A	T	A	T	T	A	A	C
3’ UTR & polyA tail of SinV																							

C	A	T	T	T	A	T	T	C	A	G	C	G	G	A	C	G	C	C	A	A	A	A	C
3’ UTR & polyA tail of SinV																							

T	C	A	A	T	G	T	A	T	T	T	C	T	G	A	G	G	A	A	G	C	A	T	G
3’ UTR & polyA tail of SinV																							

G	T	G	C	A	T	A	A	T	G	C	C	A	T	G	C	A	G	C	G	T	C	T	G
3’ UTR & polyA tail of SinV																							

C	A	T	A	A	C	T	T	T	T	T	A	T	T	A	T	T	T	C	T	T	T	T	A
3’ UTR & polyA tail of SinV																							

T	T	A	A	T	C	A	A	C	A	A	A	A	T	T	T	T	G	T	T	T	T	T	A
3’ UTR & polyA tail of SinV																							

A	C	A	T	T	T	C	A	A	A	A	A	A	A	A	A	A	A	A	A	A	A	A	A
3’ UTR & polyA tail of SinV																							

A	A	G	G	G	G	A	T	C	T	C	G	A	G	C
3’ UTR & polyA tail of SinV								*Xho*l restriction site						

Aligned nucleotide sequence of the synthesised gene encoding the YFV ED-lll protein and the sequence data obtained for the pSinED-lll replicon

```
YFVED-lll       ATGAAGGGCACCAGCTACAAGATGTGCACCGACAAGATGAGCTTCGTGAAGAACCCCACC
pSinED-lll      ATGAAGGGCACCAGCTACAAGATGTGCACCGACAAGATGAGCTTCGTGAAGAACCCCACC
                ************************************************************

YFVED-lll       GACACCGGCCACGGCACCGTGGTGATGCAGGTGAAGGTGCCCAAGGGCGCCCCCTGCAAG
pSinED-lll      GACACCGGCCACGGCACCGTGGTGATGCAGGTGAAGGTGCCCAAGGGCGCCCCCTGCAAG
                ************************************************************

YFVED-lll       ATCCCCGTGATCGTGGCCGACGACCTGACCGCCGCCATCAACAAGGGCATCCTGGTGACC
pSinED-lll      ATCCCCGTGATCGTGGCCGACGACCTGACCGCCGCCATCAACAAGGGCATCCTGGTGACC
                ************************************************************

YFVED-lll       GTGAACCCCATCGCCAGCACCAACGACGACGAGGTGCTGATCGAGGTGAACCCCCCCTTC
pSinED-lll      GTGAACCCCATCGCCAGCACCAACGACGACGAGGTGCTGATCGAGGTGAACCCCCCCTTC
                ************************************************************

YFVED-lll       GGCGACAGCTACATCATCGTGGGCACCGGCGACAGCAGGCTGACCTACCAGTGGCACAAG
pSinED-lll      GGCGACAGCTACATCATCGTGGGCACCGGCGACAGCAGGCTGACCTACCAGTGGCACAAG
                ************************************************************

YFVED-lll       GAGCACCACCACCACCACCACTAA
pSinED-lll      GAGCACCACCACCACCACCACTAA
                ************************
```

Aligned amino acid sequence of the synthesised gene encoding the YFV ED-lll protein and the translated sequence data obtained for the pSinED-lll replicon

```
YFVED-lll       MKGTSYKMCTDKMSFVKNPTDTGHGTVVMQVKVPKGAPCKIPVIVADDLTAAINKGILVT
pSinED-lll      MKGTSYKMCTDKMSFVKNPTDTGHGTVVMQVKVPKGAPCKIPVIVADDLTAAINKGILVT
                ************************************************************

YFVED-lll       VNPIASTNDDEVLIEVNPPFGDSYIIVGTGDSRLTYQWHKEHHHHHH
pSinED-lll      VNPIASTNDDEVLIEVNPPFGDSYIIVGTGDSRLTYQWHKEHHHHHH
                ************************************************
```

Appendix D: Raw data obtained for ELISA's

Indirect ELISA for the detection of anti-YFV antibodies

<>	1	2	3	4	5	6	7	8	9	10	11	12
A	0.2930	1.5870	0.0400	0.0450	0.0450	0.0410	0.0380	0.0450	0.0320	0.0430	0.0370	0.0660
B	0.4880	1.5040	0.0500	0.0390	0.0510	0.0450	0.0430	0.0420	0.0400	0.0360	0.0390	0.0580
C	0.1020	0.1280	0.0470	0.0380	0.0400	0.0470	0.0500	0.0370	0.0370	0.0410	0.0390	0.0390
D	0.0820	0.1140	0.0460	0.0440	0.0540	0.0400	0.0410	0.0420	0.0400	0.0420	0.0430	0.0460
E	0.0760	0.0940	0.0530	0.0590	0.0540	0.0500	0.0480	0.0540	0.0360	0.0490	0.0440	0.0720
F	0.0910	0.1260	0.0470	0.0440	0.0490	0.0520	0.0460	0.0470	0.0440	0.0450	0.0430	0.0690
G	0.0960	0.1240	0.0610	0.0450	0.0480	0.0480	0.0430	0.0390	0.0480	0.0490	0.0450	0.0480
H			0.0450	0.0520	0.0620	0.0430	0.0410	0.0500	0.0490	0.0460	0.0470	0.0550

Sandwich ELISA's for detection of IFN-γ release

Plate 1:

<>	1	2	3	4	5	6	7	8	9	10	11	12
A	1.0020	1.0680	1.0240	0.0230	2.0150	0.4480	0.0260	2.1290	1.9690	0.0240	1.9710	0.6060
B	0.4810	0.4100	0.4270	0.0240	1.6120	0.4960	0.0220	1.5110	1.3410	0.0220	1.6790	1.3290
C	0.2300	0.2570	0.2040	0.0200	1.5250	0.5400	0.0190	1.2880	1.6500	0.0230	1.7430	2.0800
D	0.1430	0.1480	0.1450	0.0220	2.7160	1.4650	0.0260	1.4070	0.8440	0.0400	2.0460	0.9660
E	0.0910	0.0840	0.0700	0.0260	1.6180	3.4840	0.0200	1.5360	1.5670	0.0210	1.6840	1.9830
F	0.0570	0.0580	0.0660	0.0260	1.5540	0.3370	0.0200	1.9690	1.8090	0.0250	1.7590	0.6790
G	0.0430	0.0490	0.0540	0.0520	2.9880	0.3790	0.0880	1.9960	3.4250	0.0270	1.6250	0.7310
H	0.0260	0.0240	0.0230	0.0770	3.5570	0.6540	0.0260	0.0200	0.8760	0.0190	1.9750	0.3620

Plate 2:

<>	1	2	3	4	5	6	7	8	9	10	11	12
A	1.3570	1.4420	1.4200	0.0220	3.1880	0.3260	0.0250	2.7950	1.0010	0.0190	2.9210	3.3950
B	0.6850	0.6990	0.7200	0.0190	0.8180	0.1330	0.0320	2.6980	1.1460	0.0320	2.8080	3.6140
C	0.3630	0.3750	0.4050	0.0190	3.0320	0.0190	0.0170	2.2950	2.7190	0.0280	2.0260	3.5280
D	0.2070	0.2180	0.2170	0.0190	3.0630	0.1250	0.0220	2.1520	2.7980	0.0170	2.3330	3.4780
E	0.1160	0.1260	0.1210	0.0170	3.1080	1.4330	0.0180	2.3550	1.1350	0.0170	2.8100	3.5340
F	0.0890	0.0810	0.0780	0.0190	3.2810	0.2020	0.0200	2.8170	0.7850	0.0180	2.5710	3.5980
G	0.0500	0.0480	0.0450	0.0550	3.2360	1.3280	0.0440	2.8660	0.5660	0.0170	2.7790	3.5540
H	0.0190	0.0160	0.0170	0.0230	3.2880	0.9740	0.0200	2.6850	0.5950	0.0190	3.2390	3.6250

Plate 3:

<>	1	2	3	4	5	6	7	8	9	10	11	12
A	1.6460	1.7030	1.6270	0.0210	2.3180	3.4740	0.0180	2.6610	2.8340	0.0200	2.5430	3.3960
B	0.8600	0.8330	0.8380	0.0220	2.3210	3.5400	0.0170	2.5210	3.0770	0.0200	2.6690	3.2860
C	0.4140	0.3900	0.4130	0.0170	2.5210	3.4830	0.0170	2.0040	1.0500	0.0260	2.3120	3.4340
D	0.2130	0.2250	0.2290	0.0200	2.2290	3.5800	0.0200	1.7560	1.7800	0.0230	2.7420	3.4740
E	0.1230	0.1120	0.1210	0.0200	2.2390	3.5330	0.0190	2.3420	2.3190	0.0180	1.9690	3.4110
F	0.0720	0.0680	0.0690	0.0200	2.2950	3.5410	0.0220	2.7250	3.1510	0.0190	2.5230	3.4890
G	0.0440	0.0400	0.0440	0.0270	2.8700	3.5450	0.0210	2.4410	3.1750	0.0340	2.1070	3.2050
H	0.0160	0.0170	0.0180	0.0410	2.8720	3.5500	0.0200	2.3900	2.4740	0.0180	2.1530	2.8610

Plate 4:

<>	1	2	3	4	5	6
A	1.9810	2.0960	2.0850	0.0220	1.9960	3.3740
B	1.0400	1.0880	1.1340	0.0200	2.3400	1.3990
C	0.5730	0.5640	0.6260	0.0250	2.5110	3.3760
D	0.4170	0.3060	0.3050	0.0250	2.7210	3.3310
E	0.1590	0.1610	0.1570	0.0200	2.0130	3.2950
F	0.0800	0.0920	0.0720	0.0190	1.9510	0.0260
G	0.0530	0.0550	0.0530	0.0170	1.8960	3.0510
H	0.0250	0.0210	0.0180	0.0190	1.6950	1.1960

Sandwich ELISA's for detection of IL-2 release

Plate 1:

<>	1	2	3	4	5	6	7	8	9	10	11	12
A	1.1720	1.2190	1.2360	0.4320	2.3470	0.9260	0.2760	2.0340	1.0340	0.2930	2.3460	0.6370
B	0.6510	0.6900	0.6690	0.2240	2.6130	0.8490	0.2720	2.5290	0.7990	0.4100	2.5860	0.5600
C	0.3360	0.3630	0.3830	0.4820	2.1820	1.0830	0.4660	2.4760	0.7060	0.4020	2.2850	0.7690
D	0.1860	0.1810	0.1880	0.1330	2.5510	1.0830	0.2490	2.8290	0.9640	0.5470	2.2780	0.9520
E	0.1040	0.1060	0.1020	0.6730	1.7030	0.8710	0.3470	2.3160	0.9730	1.0570	2.1430	0.6820
F	0.0640	0.0660	0.0630	0.2620	2.0190	0.6150	0.6050	2.1920	0.7540	0.4230	2.3830	1.5700
G	0.0460	0.0480	0.0450	0.1310	2.4890	1.0090	0.3390	2.8810	0.7920	0.4990	2.3460	0.7550
H	0.0240	0.0260	0.0250	0.2660	2.5610	0.1880	0.4910	2.4620	0.9910	1.0400	2.4170	0.8580

Plate 2:

<>	1	2	3	4	5	6	7	8	9	10	11	12
A	1.0770	1.1870	1.1250	0.1300	1.8290	1.1350	0.3450	1.1800	0.8100	0.5150	1.5510	1.0700
B	0.6580	0.6260	0.6530	0.1400	2.0010	0.6450	0.4090	0.7530	0.7910	0.6180	1.0240	1.6090
C	0.3340	0.3520	0.3410	0.3340	2.2330	0.6570	0.4330	0.7010	0.4770	0.7920	0.6620	0.9970
D	0.1890	0.1830	0.1870	0.0630	2.2740	0.7760	0.4020	1.3660	1.3110	0.6340	0.7070	1.2640
E	0.1080	0.1030	0.1020	0.2520	2.5040	0.7290	0.2420	0.6300	1.0380	0.2780	1.0750	0.8010
F	0.0740	0.0630	0.0630	0.1460	2.4450	0.3830	0.2800	0.5380	1.2200	0.7650	1.3930	0.7170
G	0.0430	0.0420	0.0480	0.4770	2.3800	1.3240	0.4650	1.7570	1.2810	0.3970	1.9710	0.6440
H	0.0240	0.0230	0.0290	0.2650	2.2600	1.2190	0.6720	1.8060	0.8610	0.1730	1.9620	0.5020

Plate 3:

<>	1	2	3	4	5	6	7	8	9	10	11	12
A	1.0050	0.9410	0.9980	0.4170	1.6810	1.0140	0.2110	1.7460	1.0950	0.8130	1.5400	0.7540
B	0.5450	0.5330	0.5380	0.3760	1.7170	0.5640	0.0970	1.9340	0.7820	0.2620	1.3380	0.8110
C	0.2720	0.2940	0.2860	0.3450	1.5160	0.6600	0.1650	1.2970	0.8490	0.6390	0.7330	0.9160
D	0.1470	0.1250	0.1540	0.2280	1.3180	0.3950	0.2950	1.2600	0.8970	0.6700	0.8220	0.8080
E	0.0870	0.0600	0.0440	0.1620	0.6870	0.4430	0.3970	1.1700	0.5430	0.0820	1.1080	0.7000
F	0.0530	0.0210	0.0370	0.2690	0.6680	0.5170	0.3490	1.8550	0.6410	0.1530	1.3560	0.6480
G	0.0400	0.0190	0.0270	0.2830	0.5880	0.5950	0.3370	0.6570	0.9060	0.2530	0.6800	0.7730
H	0.0220	0.0200	0.0200	0.1770	1.2960	0.4970	0.3400	0.7400	1.1920	0.3320	0.7470	1.2730

Plate 4:

<>	1	2	3	4	5	6
A	0.8930	1.0060	1.0170	0.8850	0.8440	0.7710
B	0.4380	0.5760	0.5590	0.4130	0.5370	0.8620
C	0.2270	0.3030	0.2960	0.6480	0.3130	0.7880
D	0.1300	0.1540	0.1620	0.4990	0.3070	0.9190
E	0.0620	0.0800	0.0860	0.5000	0.3430	0.7260
F	0.0370	0.0490	0.0500	0.6590	1.0720	0.8440
G	0.0330	0.0350	0.0350	0.6750	0.1540	0.8530
H	0.0180	0.0210	0.0200	0.6000	0.2300	0.9290

Sandwich ELISA's for detection of IL-4 release

Plate 1:

<>	1	2	3	4	5	6	7	8	9	10	11	12
A	0.7600	0.8280	0.9920	0.0310	3.0660	0.0480	0.0290	2.6820	0.0230	0.0250	2.6070	0.0450
B	0.4190	0.4260	0.4850	0.0340	2.9540	0.0340	0.0260	2.7990	0.0470	0.0320	2.6460	0.0340
C	0.2820	0.2320	0.2560	0.0260	2.5540	0.0510	0.0260	2.8660	0.0450	0.0300	2.4410	0.0320
D	0.1670	0.1430	0.1340	0.0280	2.6220	0.0430	0.0260	2.8260	0.0310	0.0260	2.3640	0.0440
E	0.0800	0.0670	0.0790	0.0260	2.3760	0.0320	0.0250	2.8100	0.0430	0.0410	2.4200	0.0380
F	0.0630	0.0500	0.0510	0.0320	2.4720	0.0380	0.0280	2.7700	0.0360	0.0310	2.5710	0.0570
G	0.0390	0.0340	0.0340	0.0270	3.0080	0.0430	0.0320	2.0160	0.0380	0.0270	2.6990	0.0370
H	0.0220	0.0230	0.0230	0.0240	2.9890	0.0410	2.1220	2.5700	0.0240	0.0390	2.5180	0.0390

Plate 2:

<>	1	2	3	4	5	6	7	8	9	10	11	12
A	0.8060	0.8280	0.9860	0.0260	2.6890	0.0350	0.0250	2.0290	0.0500	0.0340	1.9090	0.0560
B	0.4550	0.4860	0.6060	0.0270	2.5850	0.0390	0.0280	1.9630	0.0450	0.0370	1.9360	0.0740
C	0.2470	0.2500	0.3370	0.0220	2.6800	0.0290	0.0260	2.3060	0.0340	0.0350	1.7560	0.0710
D	0.1360	0.1140	0.1590	0.0230	2.5540	0.0340	0.0270	2.3180	0.0360	0.0380	1.6360	0.1010
E	0.0770	0.0740	0.0820	0.0220	2.8670	0.0310	0.0340	1.7950	0.0390	0.0250	1.5720	0.0810
F	0.0540	0.0570	0.0500	0.0210	2.9240	0.0310	0.0260	2.2100	0.0300	0.0260	1.4800	0.0510
G	0.0360	0.0300	0.0290	0.0260	2.6680	0.0340	0.0230	2.7980	0.0380	0.0220	2.2200	0.0460
H	0.0230	0.0230	0.0270	0.0230	2.9150	0.0290	0.0210	2.6790	0.0370	0.0260	2.2250	0.0390

Plate 3:

<>	1	2	3	4	5	6	7	8	9	10	11	12
A	0.9520	0.9390	1.0340	0.0500	1.7860	0.0870	0.0370	1.9500	0.0650	0.0380	1.4410	0.0530
B	0.6430	0.6920	0.6970	0.0410	1.8610	0.0590	0.0340	1.7870	0.0520	0.0420	1.2400	0.0480
C	0.3450	0.5060	0.4940	0.0400	1.9980	0.0600	0.0350	1.7660	0.0540	0.0460	0.7470	0.0620
D	0.2060	0.2100	0.2960	0.0350	1.9120	0.0740	0.0280	1.4530	0.0470	0.0460	0.7750	0.0710
E	0.1140	0.0930	0.1520	0.0310	1.7960	0.0920	0.0290	1.8070	0.0440	0.0310	1.4840	0.0600
F	0.0720	0.0590	0.0760	0.0380	1.9600	0.0890	0.0300	2.0090	0.0610	0.0350	1.5250	0.0510
G	0.0500	0.0410	0.0370	0.0390	1.5120	0.0870	0.0350	0.9100	0.0500	0.0380	0.9540	0.0460
H	0.0320	0.0280	0.0290	0.0450	1.5110	0.0710	0.0300	0.9130	0.0500	0.0430	1.0590	0.0580

Plate 4:

<>	1	2	3	4	5	6
A	0.6560	0.8410	0.8830	0.0320	0.7840	0.0370
B	0.5130	0.6180	0.6500	0.0310	0.7100	0.0370
C	0.3440	0.4190	0.4730	0.0360	0.2250	0.0410
D	0.2300	0.2530	0.2700	0.0320	0.4390	0.0530
E	0.0800	0.1150	0.1580	0.0270	0.4850	0.0480
F	0.0520	0.0420	0.0780	0.0250	0.2960	0.0370
G	0.0410	0.0350	0.0430	0.0280	0.2950	0.0550
H	0.0290	0.0310	0.0290	0.0320	0.3400	0.0340

Sandwich ELISA's for detection of IL-10 release

Plate 1:

<>	1	2	3	4	5	6	7	8	9	10	11	12
A	1.7160	1.8330	1.8320	0.0650	1.8610	0.1080	0.0740	1.5650	0.1230	0.0670	1.3580	0.1350
B	0.9930	0.9530	0.9580	0.0610	1.6390	0.1280	0.0620	1.2610	0.1230	0.0650	1.2190	0.1310
C	0.4630	0.4730	0.4760	0.0660	1.8440	0.1120	0.0620	1.5120	0.2030	0.0640	1.2350	0.1460
D	0.2420	0.1980	0.2380	0.0640	1.7810	0.0990	0.0600	1.5540	0.1580	0.0690	1.3250	0.1470
E	0.1260	0.1360	0.1300	0.0620	1.5390	0.1290	0.0610	1.4980	0.0720	0.0650	1.2260	0.1420
F	0.0880	0.0830	0.0910	0.0600	1.5290	0.1370	0.0700	1.4990	0.1410	0.0720	0.9960	0.0970
G	0.0710	0.0480	0.0600	0.0590	1.7060	0.0940	0.1150	1.4490	0.1640	0.0590	1.2670	0.1030
H	0.0480	0.0450	0.0480	0.0650	1.5210	0.0750	0.0610	1.4720	0.1610	0.0580	0.9300	0.0800

Plate 2:

<>	1	2	3	4	5	6	7	8	9	10	11	12
A	1.9320	1.8410	1.7950	0.0630	1.5360	0.2250	0.0680	1.7470	0.1460	0.0610	1.6810	0.2950
B	1.0950	1.0270	1.0110	0.0660	1.5040	0.1700	0.0660	1.6200	0.1480	0.0580	1.6140	0.2520
C	0.5260	0.5650	0.5890	0.0590	1.0400	0.0890	0.0630	1.6830	0.1770	0.0600	1.7400	0.3060
D	0.2530	0.2310	0.2860	0.0580	1.2840	0.0830	0.0610	1.7770	0.1770	0.0560	1.8330	0.3470
E	0.1380	0.1320	0.1190	0.0610	1.6450	0.0980	0.0620	1.4660	0.1900	0.0600	1.7150	0.3040
F	0.0970	0.0890	0.0920	0.0610	1.3350	0.0980	0.0600	1.5930	0.1580	0.0610	1.5390	0.3250
G	0.0650	0.0620	0.0600	0.0670	1.1100	0.1270	0.0570	1.7430	0.1090	0.0520	1.6850	0.1870
H	0.0430	0.0410	0.0470	0.0630	1.3350	0.1220	0.0630	1.5860	0.1350	0.0520	1.8770	0.2150

Plate 3:

<>	1	2	3	4	5	6	7	8	9	10	11	12
A	1.9830	2.0800	1.9730	0.0720	1.7700	0.2980	0.0730	1.5860	0.1700	0.0770	1.1720	0.2300
B	1.1990	1.0710	1.1410	0.0710	**0.5270**	0.4110	0.0710	1.4010	0.1690	0.0680	1.4800	0.2410
C	0.5350	0.6140	0.5730	0.0670	1.6710	0.3540	0.0690	1.4790	0.1330	0.0750	1.4760	0.3980
D	0.3390	0.3370	0.3350	0.0670	1.4690	0.2830	0.0650	1.6560	0.2210	0.0760	1.4390	0.3650
E	0.1750	0.1800	0.1700	0.0680	1.8130	0.3640	0.0620	1.2770	0.1930	0.0600	1.4110	0.2380
F	0.1160	0.1220	0.1170	0.0700	1.7740	0.3040	0.0630	1.4070	0.2190	0.0620	1.4160	0.2250
G	0.0870	0.0880	0.0840	0.0720	1.6660	0.3860	0.0710	1.5100	0.3450	0.0650	1.3110	0.2960
H	0.0580	0.0620	0.0620	0.0740	1.8100	0.3210	0.0720	1.5150	0.3180	0.0650	1.4850	0.2550

Plate 4:

<>	1	2	3	4	5	6
A	1.4650	1.6280	1.5860	0.0630	1.3690	0.2240
B	0.9120	0.9200	0.9460	0.0690	1.4440	0.2070
C	0.4760	0.5320	0.5660	0.0650	1.3950	0.3010
D	0.2960	0.3100	0.3270	0.0710	1.3090	0.3310
E	0.1770	0.1890	0.1730	0.0670	1.1070	0.2490
F	0.1120	0.1340	0.1340	0.0680	1.2040	0.2650
G	0.0850	0.0920	0.0840	0.0720	1.1100	0.4030
H	0.0590	0.0580	0.0630	0.0680	0.3250	0.3450

Indirect ELISA for the detection of anti-SINV antibodies

<>	1	2	3	4	5	6	7	8	9	10	11	12
A	0.1550	1.7830	0.0390	0.0460	0.0460	0.0450	0.0400	0.0490	0.0360	0.0430	0.0400	0.0530
B	0.2460	1.7290	0.0360	0.0350	0.0400	0.0430	0.0410	0.0400	0.0420	0.0360	0.0350	0.0570
C	0.1980	0.2810	0.0430	0.0330	0.0450	0.0380	0.0410	0.0350	0.0350	0.0380	0.0370	0.0360
D	0.0830	0.1020	0.0340	0.0370	0.0440	0.0370	0.0370	0.0220	0.0460	0.0440	0.0450	0.0470
E	0.0570	0.0710	0.0430	0.0500	0.0450	0.0420	0.0370	0.0540	0.0370	0.0440	0.0410	0.0530
F	0.0700	0.0840	0.0420	0.0380	0.0440	0.0460	0.0650	0.0450	0.0470	0.0380	0.0410	0.0630
G	0.0870	0.0990	0.0420	0.0360	0.0390	0.0480	0.0360	0.0380	0.0440	0.0430	0.0440	0.0470
H	0.0870	0.1170	0.0410	0.0410	0.0500	0.0380	0.0400	0.0490	0.0460	0.0440	0.0460	0.0460

Appendix E: Standard curves for ELISA to facilitate determination of the cytokine concentration

Standard curves for the determination of the IFN-γ concentration

Plate 1:

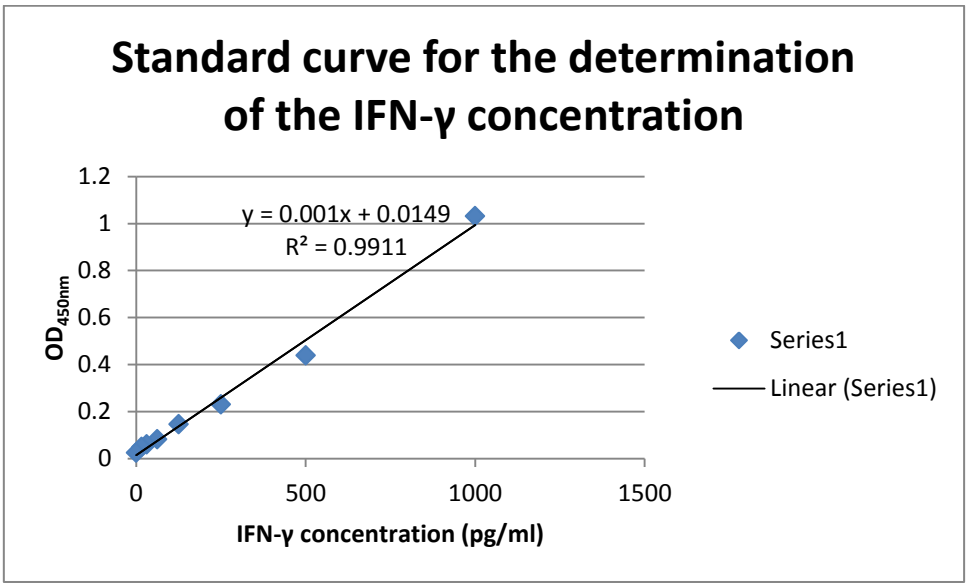

Plate 2:

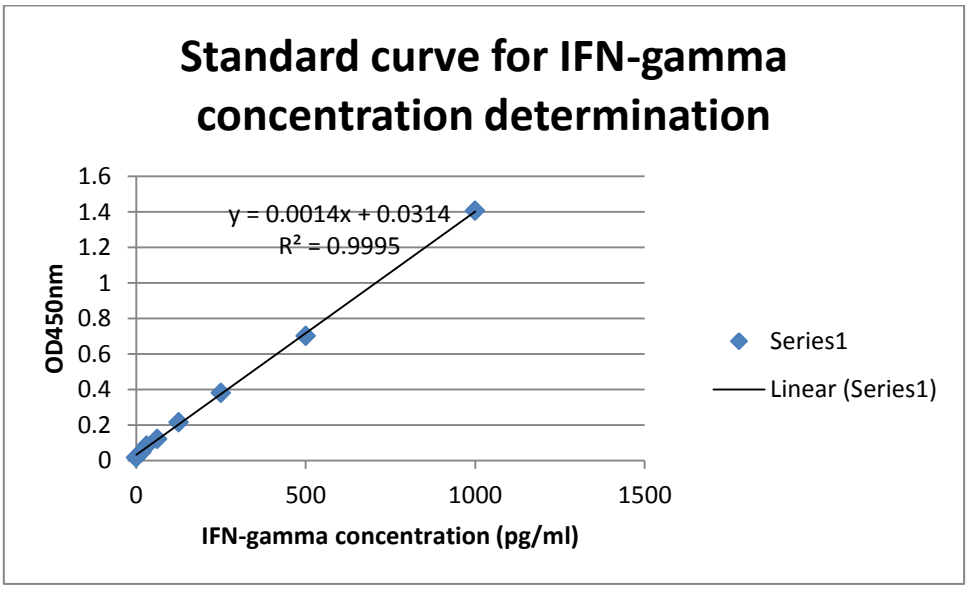

Plate 3:

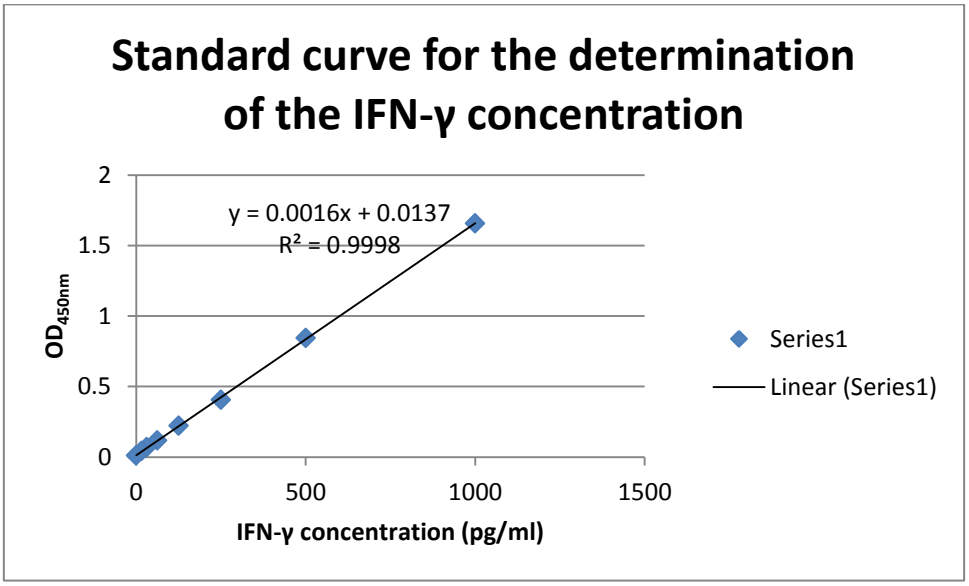

Plate 4:

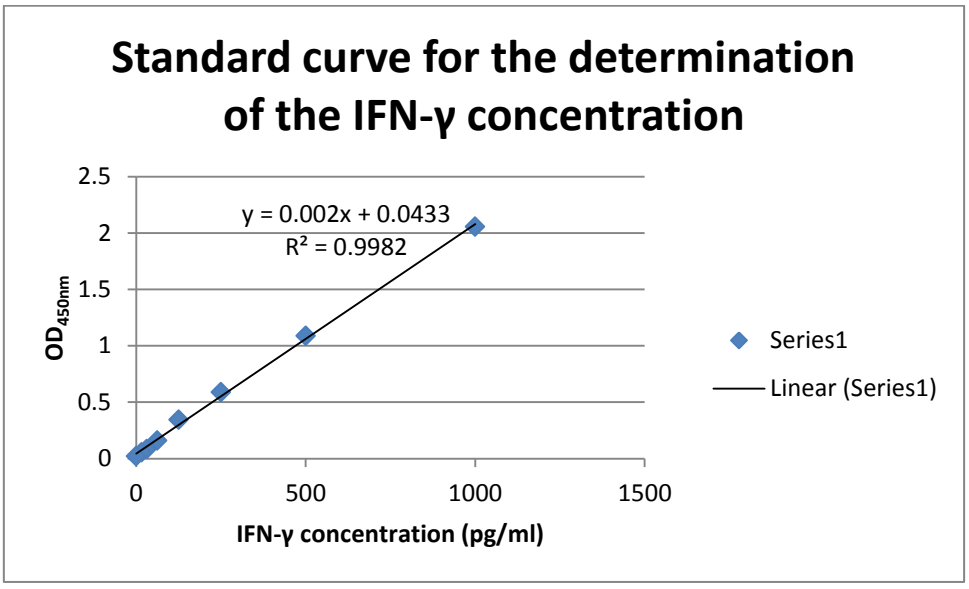

Standard curves for the determination of the IL-2 concentration

Plate 1:

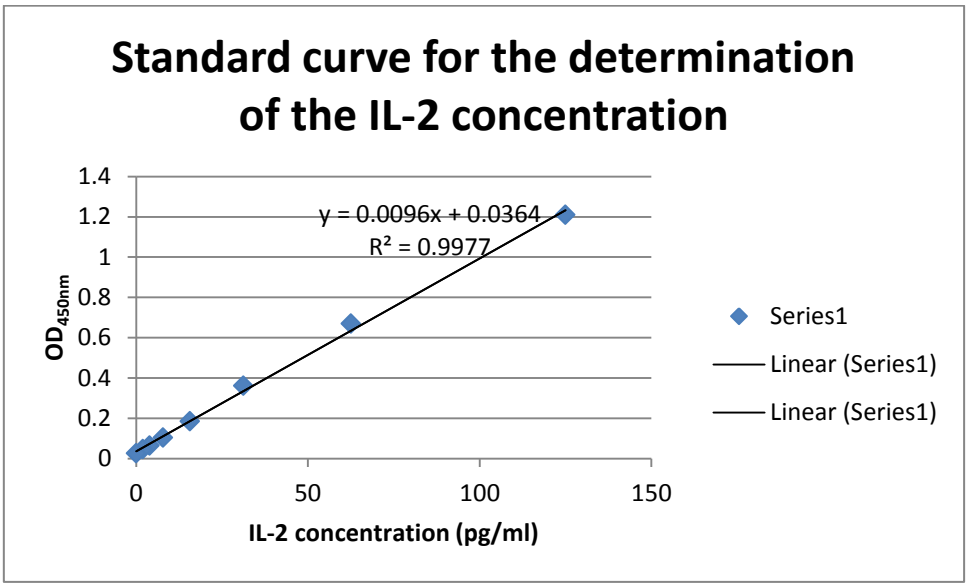

Plate 2:

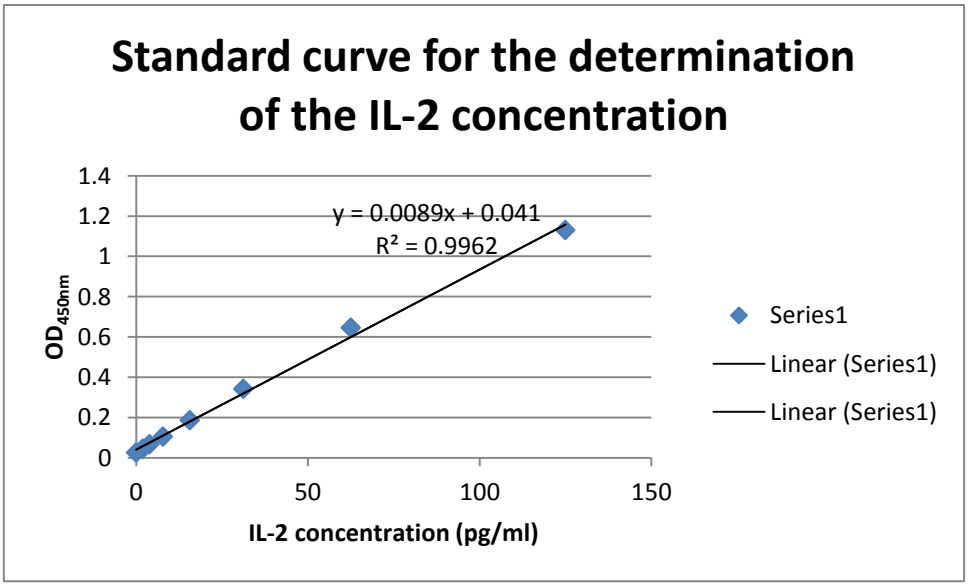

Plate 3:

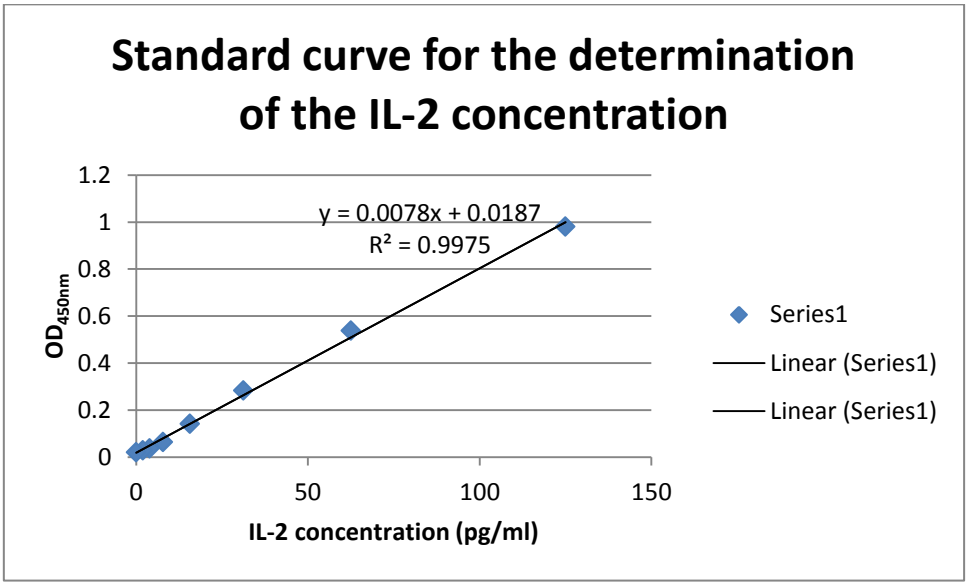

Plate 4:

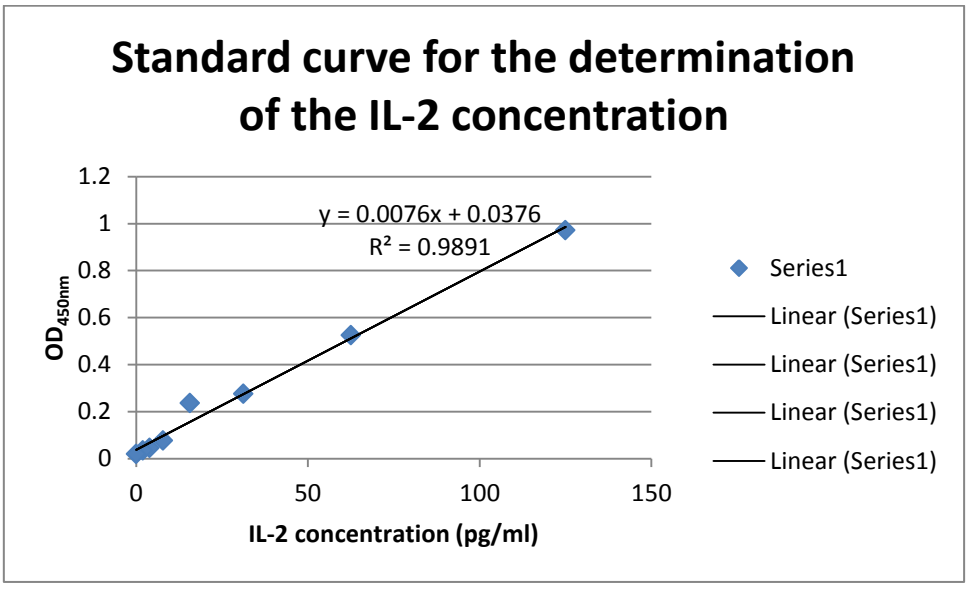

Standard curves for the determination of the IL-4 concentration

Plate 1:

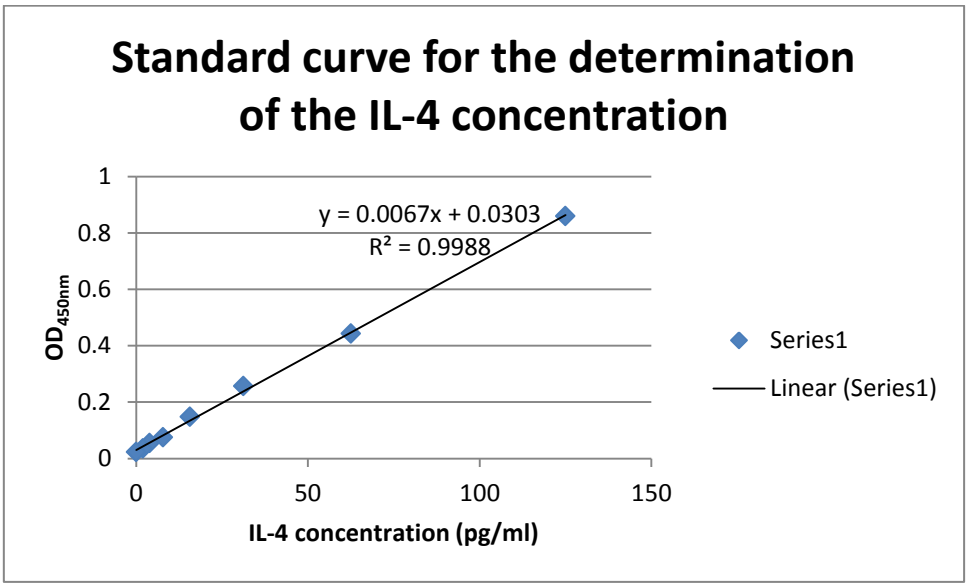

Plate 2:

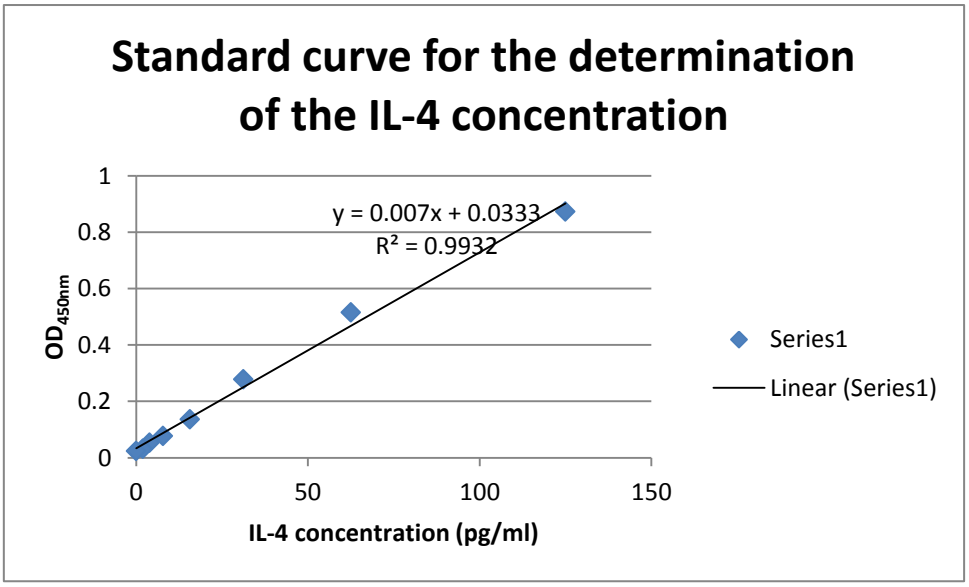

Plate 3:

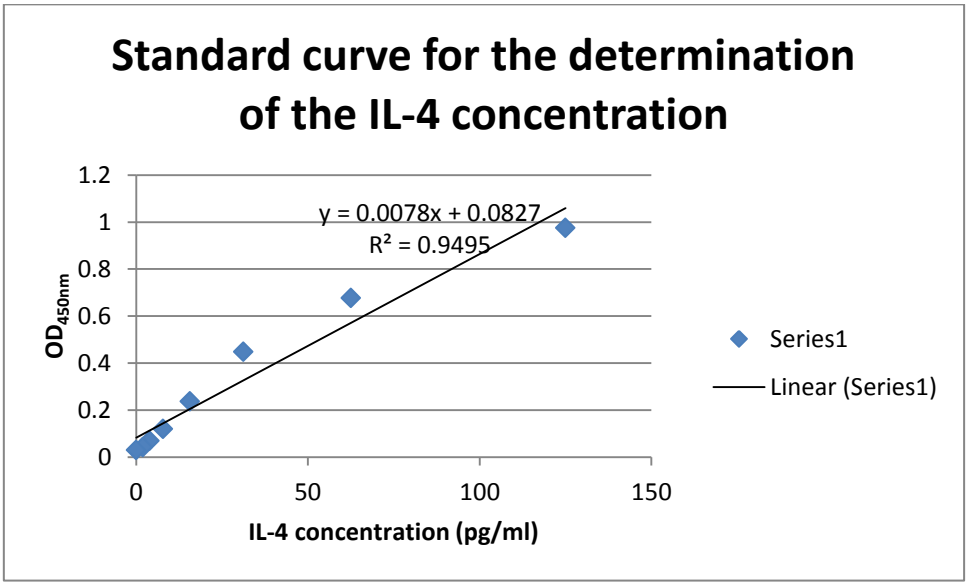

Plate 4:

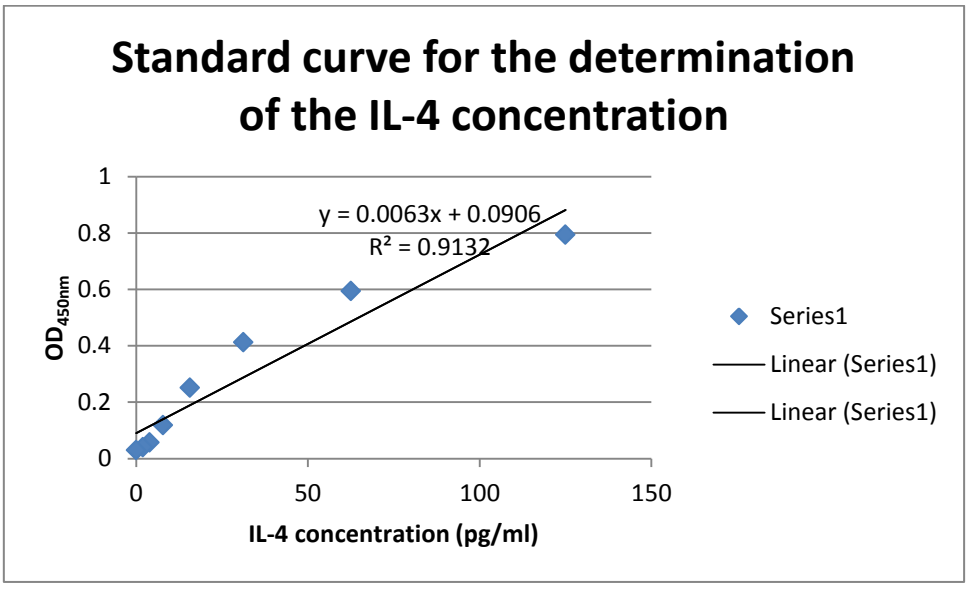

Standard curves for the determination of the IL-10 concentration

Plate 1:

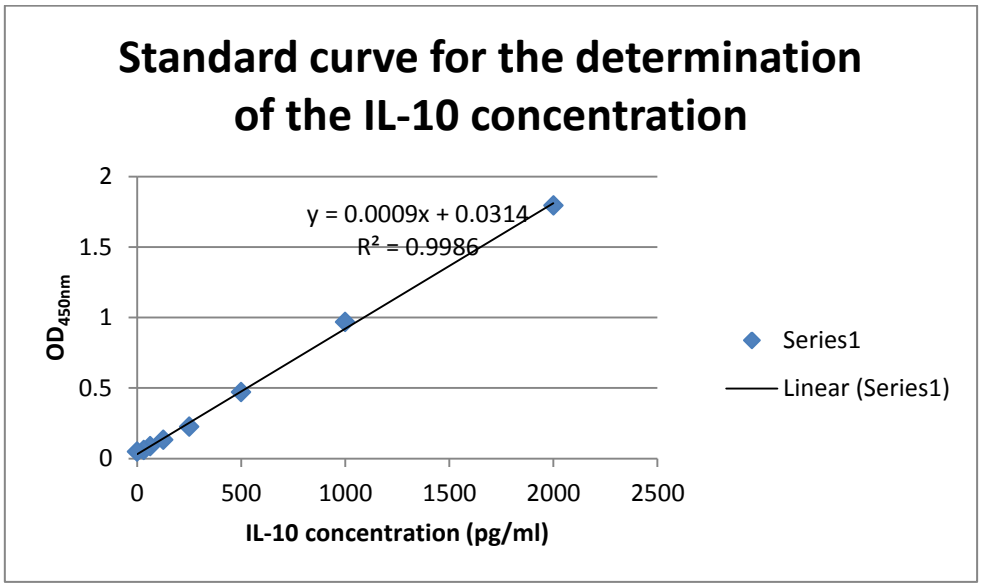

Plate 2:

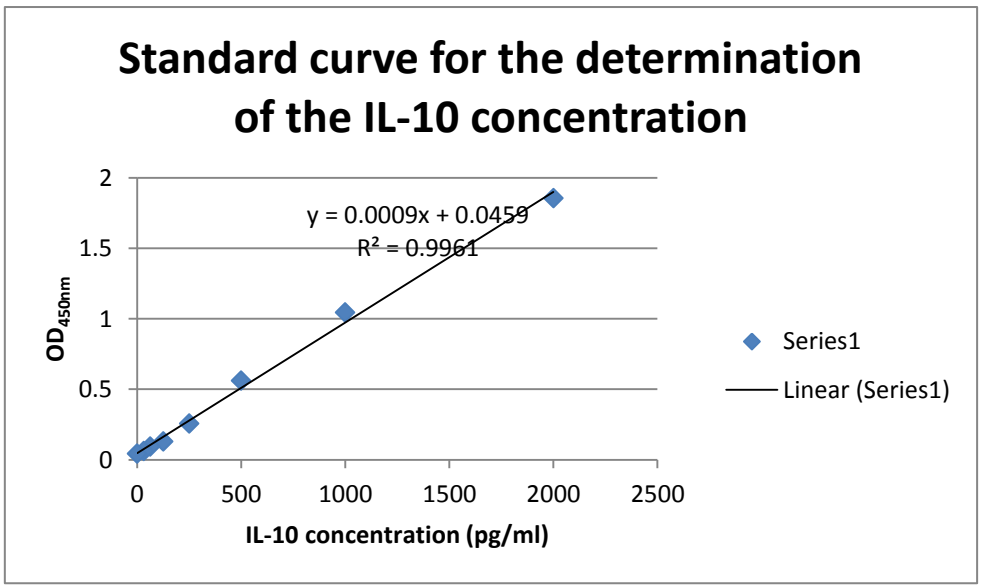

Plate 3:

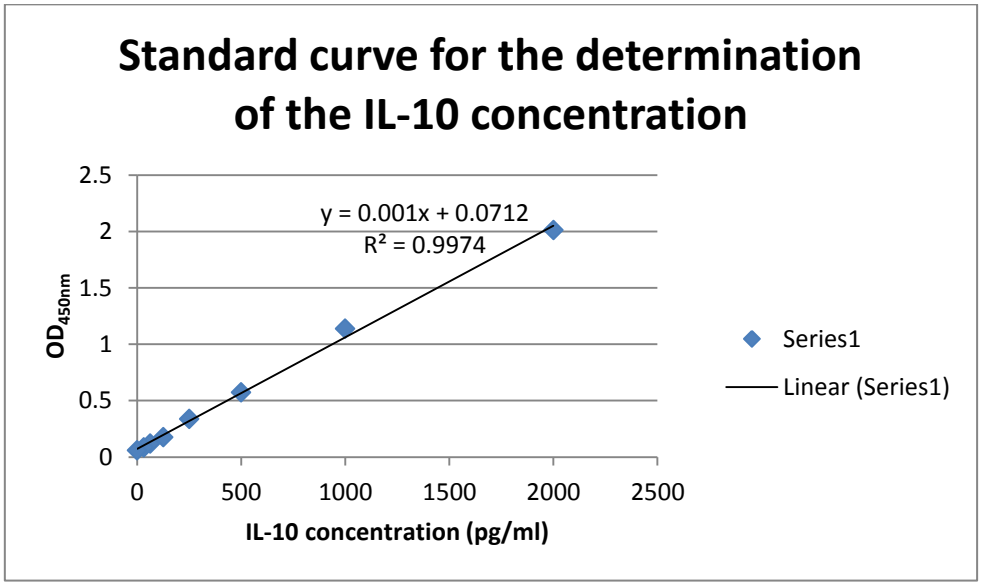

Plate 4:

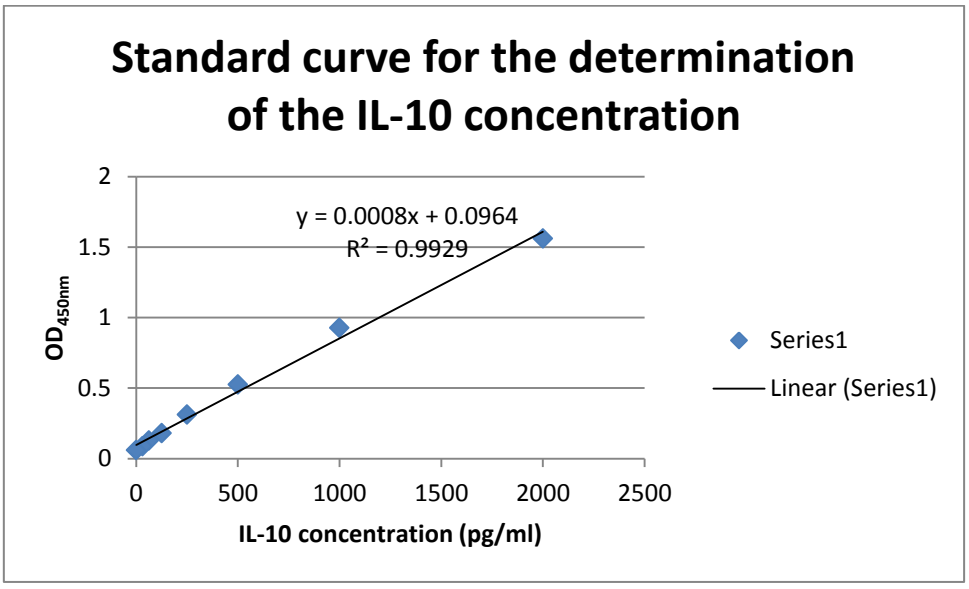

Appendix F: Composition of buffers, media and solutions

Composition of buffers

1. 50X TAE (1 L)

Dissolve 242 g Tris in 500 ml deionised water, add 100 ml 0,5 M EDTA at a pH of 8,0 and 57,1 ml glacial acetic acid. Adjust volume to 1 L using deionised water and store at room temperature. Dilute to 1X working concentration by the addition of 40 ml 50X TAE in a final volume of 2 L deionised water.

2. 10X PBS (1 L)

Dissolve 80 g of NaCl, 2 g of KCl, 17,8 g of $Na_2HPO_4 \cdot 2H_2O$ and 2,4 g of KH_2PO_4 in 800 ml. Adjust pH to 7,4 using HCl and adjust volume to 1 L using deionised water. Autoclave and store at room temperature. Dilute to 1X working concentration by the addition of 200 ml 10X PBS in a final volume of 2 L deionised water.

3. Transfer buffer (1 L)

Dissolve 2,9 g glycine, 5,8 g Tris and 0,37 g SDS in 200 ml methanol. Adjust volume to 1 L using deionised water and store at 4°C.

4. 1X TBS (1 L)

Dissolve 6,05 g Tris and 8,76 g NaCl in 800 ml deionised water. Adjust pH to 7,5 using 1 M HCl, adjust volume to 1 L using deionised water and store at 4°C.

5. BBS (1 L)

Prepare 1,5 M NaCl by dissolving 87,7 g NaCl in 1 L deionised water, 0,5 M boric acid by dissolving 30,9 g H_3PO_3 in 1 L deionised water and 1 N NaOH by dissolving 40 g NaOH in 1 L deionised water. Prepare a working solution using 8 ml 1,5 M NaCl, 10 ml 0,5 M H_3PO_3 and 2,4 ml 1 N NaOH solution. Adjust the volume to 1 L using deionised water, confirm a pH of 9,0, autoclave and store at room temperature.

Composition of media

1. **SOC media (1 L)**

Dissolve 20 g of Bacto-Tryptone, 5 g of Bacto-Yeast Extract, 0,5 g NaCl and 2,5 ml of 1 M KCl in 900 ml deionised water. Adjust the pH to 7,0 using 10 M NaOH and adjust volume to 970 ml. Add 10 ml 1 M $MgCl_2$ and 20 ml 1 M glucose before use and store at 4°C.

2. **LB media (1 L)**

Dissolve 10 g Bacto-tryptone, 5 g Bacto-yeast extract and 10 g NaCl in 800 ml deionised water. Adjust the pH to 7,5 using 1 M NaOH and adjust volume to 1 L using deionised water. Autoclave, allow to cool and store at 4°C.

3. **2X TY media (1 L)**

Dissolve 16 g Bacto-tryptone, 10 g Bacto-yeast extract and 5 g NaCl in 800 ml deionised water. Adjust the volume to 1 L using deionised water. Autoclave, allow to cool and store at 4°C.

Agar plates were prepared by the addition of 15 g Bacto-agar per 1 L of liquid media. After sterilisation by autoclaving, media was allowed to cool, was poured in sterile plates and stored in an inverted position at 4°C after solidification.

Composition of solutions

1. **0,1 M IPTG (50 ml)**

Dissolve 1,19 g IPTG in 40 ml deionised water, adjust the volume to 50 ml using deionised water and filter-sterilise using a 0,22 µm syringe filter. Store at -20°C.

2. **20 mg/ml X-gal (20 ml)**

Dissolve 0,4 g X-gal in 20 ml N,N'-dimethyl formamide and store at -20°C.

3. 125 mM EDTA

Prepare 0,5 M EDTA by dissolving 186,12 g $Na_2EDTA \cdot 2H_2O$ in 800 ml deionised water, adjust the pH to 8,0 using NaOH pellets and adjust the volume to 1 L using deionised water. Sterilise by autoclaving and store at room temperature. Dilute to a final concentration of 125 mM in the desired volume using nuclease-free water.

4. 0,9% sterile saline solution (10 ml)

Dissolve 90 mg NaCl in 10 ml DNase/RNase free water and filter-sterilise using a 0,22 µm syringe filter.

5. 0,2% Coomassie Brilliant Blue stain (1 L)

Dissolve 1 g Coomassie Brilliant Blue in 450 ml methanol and 100 ml glacial acetic acid. Adjust volume to 1 L using deionised water and store at room temperature.

6. Destaining solution (2 L)

Mix 600 ml methanol, 200 ml glacial acetic acid and 1,2 L deionised water and store at room temperature.

Appendix G: Letters of ethics approval

Letter of approval for animal ethics

UNIVERSITY OF THE FREE STATE
UNIVERSITEIT VAN DIE VRYSTAAT
YUNIVESITHI YA FREISTATA
UFS UV

[redacted]

Internal Post Box / Interne Posbus G40
Faks / Fax (051) 4444359

E-mail address: StraussHS@ufs.ac.za

Me / Ms H Strauss

2014-03-20

PROF F BURT
DEPT OF MICOBIOLOGY AND VIROLOGY
FACULTY OF HEALTH SCIENCES
UNIVERSITY OF THE FREE STATE

Dear Prof Burt

ANIMAL EXPERIMENT NR 24/2011
RESEARCHER: PROF F BURT, DEPT OF MEDICAL MICROBIOLOGY AND VIROLOGY
PROJECT TITLE: CHARACTERIZATION OF IMMUNE RESPONSES TO FLAVIVIRUS PROTEINS FOR VACCINE DEVELOPMENT.

You are hereby kindly informed that at the meeting held on 27 February 2014 the Interfaculty Animal Ethics Committee condoned the approval of the following with regard to the above study:

a) **Modifications to the protocol**
b) **Renewal to Dec 2014**

Remarks by die Committee members:
As this route may be more painful, please increase the monitoring intervals of the animals to three times daily, for the first 2 days after inoculation. Monitor for signs of activity, lameness and localised pain and swelling for the first batch of inoculations. If no adverse side-effects are observed, the monitoring frequency may be reduced thereafter.

Kindly take note of the following:

1. ***Fully completed and signed applications have to be submitted electronically to StraussHS@ufs.ac.za and a hard copy has to be submitted too.***
2. ***A signed progress report with regard to the above study has to be submitted electronically to StraussHS@ufs.ac.za while a hard copy has to be submitted to Ms H Strauss, Room D115, Francois Retief building, Faculty of Health Sciences. A report has to be submitted when animals are physically involved and after completion of the study. Guidelines with regard to progress reports are available from the secretary and on the Faculty Intranet.***
3. ***Researchers that plan to make use of the Animal Experimentation Unit must ensure to request and receive a quotation from the Head, Mr Seb Lamprecht***
4. ***Fifty (50%) of the quoted amount is payable when you receive the letter of approval.***

Regards

.....
CHAIR:
INTERFACULTY ANIMAL ETHICS COMMITTEE

Letter of ethics approval for project

UNIVERSITY OF THE FREE STATE
UNIVERSITEIT VAN DIE VRYSTAAT
YUNIVESITHI YA FREISTATA
UFS UV

Internal Post Box G40
☎(051) 4052812
Fax (051) 4444359

[redacted]
E-mail address: StraussHS@ufs.ac.za

Ms H Strauss/hv

2014-04-14

REC Reference nr 230408-011
IRB nr 00006240

PROF FJ BURT
DEPARTMENT OF MEDICAL MICROBIOLOGY AND VIROLOGY
FACULTY OF HEALTH SCIENCES
UFS

Dear Prof Burt

ECUFS NR 34/2013A
PROF FJ BURT DEPARTMENT OF MEDICAL MICROBIOLOGY AND VIROLOGY
PROJECT TITLE: DEVELOPMENT AND EVALUATION OF NOVEL VACCINES FOR MEDICALLY SIGNIFICANT ARBOVIRAL DISEASES.

1. You are hereby kindly informed that the Ethics Committee approved the following at the meeting on 8 April 2014:

   - *Permission is requested to extend the current protocol to include investigating mechanisms for enhancing immunogenicity of vaccines for two medically significant arboviruses, CCHFV and YFV*
   - *CV of Research Assistant, Ms N Bafazini*
   - *Extension Study*:
     - *Ecufs nr 34/2013B*
       Researcher: Student Miss N Viljoen (M.Med.Sc.)
       Project title: Preparation and immunogenicity of a candidate replicon based yellow fever vaccine.

2. Committee guidance documents: Declaration of Helsinki, ICH, GCP and MRC Guidelines on Bio Medical Research. Clinical Trial Guidelines 2000 Department of Health RSA; Ethics in Health Research: Principles Structure and Processes Department of Health RSA 2004; Guidelines for Good Practice in the Conduct of Clinical Trials with Human Participants in South Africa, Second Edition (2006); the Constitution of the Ethics Committee of the Faculty of Health Sciences and the Guidelines of the SA Medicines Control Council as well as Laws and Regulations with regard to the Control of Medicines.

3. Any amendment, extension or other modifications to the protocol must be submitted to the Ethics Committee for approval.

4. The Committee must be informed of any serious adverse event and/or termination of the study.

5. All relevant documents e.g. signed permission letters from the authorities, institutions, changes to the protocol, questionnaires etc. have to be submitted to the Ethics Committee before the study may be conducted (if applicable).

6. A progress report should be submitted within one year of approval of long term studies and a final report at completion of both short term and long term studies.

Abstract

Yellow fever virus (YFV), a mosquito-borne virus that belongs to the family *Flaviviridae* and genus *Flavivirus*, is a significant cause of morbidity and mortality in yellow fever endemic areas, especially in West Africa. In humans, YFV causes yellow fever, a disease characterised by renal failure, jaundice, and/or haemorrhage. The burden of disease is highest in Africa constituting approximately 90% of reported cases worldwide. Despite the availability of highly efficacious live attenuated vaccines against YFV, the estimated prevalence for yellow fever in Africa was 130 000 severe cases and 78 000 deaths for 2013. The available live attenuated vaccines have been contraindicated for use in immunocompromised patients and individuals with hypersensitivity to eggs and/or chicken. Vaccine-associated neurotropic adverse events that result in the development of meningoencephalitis in infants and vaccine-associated viscerotropic adverse events that result in disease resembling wild-type yellow fever have been reported. Vaccine-associated viscerotropic adverse events are associated with fatality rates exceeding 40%. Therefore, there is a need for a safer alternative to complement the use of the available live attenuated vaccines. The aim of this study was to construct a DNA-launched candidate vaccine against YFV and to determine the immunogenicity of the DNA-launched pSinED-lll replicon, which would provide information regarding the applicability of DNA-launched replicons as an approach to vaccine development.

The pSinGFP replicon encoding the green fluorescent protein (GFP) was kindly provided by Prof. Mark Heise. Expression of the GFP was confirmed in mammalian cell culture post-transfection with the pSinGFP replicon, thus confirming the functioning of the replicon elements and subsequent expression of the encoded protein. The gene encoding the GFP was excised and replaced with a synthesised codon-optimised gene encoding the YFV ED-lll protein using directional cloning. The nucleotide sequence was confirmed by bidirectional sequencing at the site of insertion and subsequently protein expression was confirmed in selected mammalian cell lines. Protein expression was confirmed by detection of the C-terminal histidine tag by immunofluorescence using anti-His_6 mouse monoclonal antibody. Thereafter, the expressed protein was characterised by immunofluorescence using mouse immune sera previously shown to contain anti-YFV ED-lll antibody. Reactivity of the expressed protein with anti-YFV ED-lll antibody substantiated the use of the pSinED-lll replicon in a mouse immunisation study.

Mice were immunised intramuscularly according to pre-approved immunisation regimes consisting of DNA only, as well as mixed modal immunisation regimes. Serum samples were collected and spleens were harvested two weeks after the administration of the final

immunisations. Serum samples were screened for anti-YFV antibodies by an enzyme-linked immunosorbent assay (ELISA) and immunofluorescence to determine the induction of a humoral immune response. Five of the twenty mice in groups immunised with the DNA-launched pSinED-lll replicon developed low level antibody responses illustrating the potential of the pSinED-lll replicon to induce a humoral immune response. Splenocytes were stimulated in cell culture with concanavalin A, YFV ED-lll protein, or no stimulant to facilitate the detection of cytokine release using ELISA's. A predominantly T-helper 1 cell-mediated immune response characterised by high level release of interferon-γ post-stimulation with the YFV ED-lll protein *in vitro* was elicited. The release of interleukin-10 post-stimulation may be associated with the prevention of immunologically mediated damage to the host by preventing an overzealous inflammatory immune response. Antibody-mediated anti-vector immunity should not negatively impact the immunogenicity of the DNA-launched pSinED-lll replicon as antibody directed against the encoded Sindbis virus non-structural proteins was not detected in mouse sera.

In conclusion, the pSinED-lll replicon was shown to have the potential to induce both a cell-mediated and a humoral immune response post-immunisation. However, optimisation of the humoral immune response will be required.

Keywords: yellow fever virus; envelope domain lll protein; DNA-launched vaccine; replicon-based; cell-mediated; humoral; immune response

Opsomming

Geelkoorsvirus (GKV), ‘n muskiet-oordraagbare virus wat behoort tot die familie *Flaviviridae* en genus *Flavivirus*, is ‘n belangrike oorsaak van morbiditeit en mortaliteit in geelkoors endemiese gebiede, veral in Wes-Afrika. In die mens veroorsaak GKV, geelkoors, ‘n siekte wat gekenmerk word deur nierversaking, geelsug en/of bloeding. Die las van die siekte is die hoogste in Afrika waar ongeveerd 90% van aangemeldte gevalle wêreldwyd voorkom. Ten spyte van die beskikbaarheid van hoogs effektiewe lewend verswakte entstowwe teen GKV is die beraamde voorkoms van geelkoors in Afrika vir 2013 steeds 130 000 ernstige gevalle en 78 000 sterftes. Die beskikbare lewend verswakte entstowwe is teenaangedui vir gebruik in immuunonderdrukte pasiënte en individue met eier en/of hoenderallergieë. Entstof-verwante neurotropiese newe-effekte wat lei tot die ontwikkeling van meningoenkefalitis/breinvliesontsteking in babas en entstof-verwante viserotropiese newe-effekte wat lei tot siekte wat natuurlike infeksie met GKV naboots is aangemeld. Entstof-verwante viserotropiese newe-effekte word geassosieer met ‘n sterftekoers wat 40% oorskry. Daar is dus ‘n behoefte vir ‘n veiliger alternatief wat die gebruik van die beskikbare lewend verswakte entstowwe kan aanvul. Die doel van hierdie studie was die voorbereiding van ‘n DNS-geloodsde replikon teen GKV en om die immunogenisiteit van die DNS-geloodsde pSinED-lll replikon te bepaal wat insae sal verskaf tot die toepaslikheid van DNS-geloodsde replikons vir entstof ontwikkeling.

Die pSinGFP replikon enkodeer die groen fluoresserende proteïen (GFP) en is goedkunstiglik deur Prof. Mark Heise verskaf. Die uitdrukking van die GFP is bevestig in geselekteerde soogdierselle na transfeksie met die pSinGFP replikon en gevolglik was die werking van die replikon elemente en die uitdrukking van die kodeerde proteïen bevestig. Die geen wat die GFP kodeer was verwyder uit die pSinGFP replikon en vervang met ‘n vervaardigde kodon-geoptimiseerde geen wat die GKV omhulsel domain lll (OD-lll) proteïen kodeer met behulp van gerigte klonering. Die nukleotiedvolgorde was bevestig deur tweerigting volgordebepaling in die gebied wat die ingevoegde geen bevat. Daarna was die uitdrukking van die kodeerde proteïen bevestig in geselekteerde soogdierselle. Proteïen uitdrukking was bevestig deur die opsporing van die C-terminale histidien merker met behulp van teen-His_6 muis monoklonale teenliggame. Die uitgedrukte proteïen is daarna gekarateriseer deur immunofluoressensie met muis immuunserum wat voorheen bepaal is om teen-GKV OD-lll teenliggame te bevat. Reaktiwiteit van die uitgedrukte proteïen met teen-GKV OD-lll teenliggame het die gebruik van die DNS-geloodsde pSinOD-lll replikon vir ‘n muis immunisering studie bekragtig.

Muise was binnespiers ingeënt volgens ‘n vooraf goedgekeurde immuniseringskema wat bestaan het uit slegs DNS, sowel as gemengde modale immuniseringskemas. Serum monsters was ingesamel en die milt was asepties verwyder twee weke na die toediening van die finale inentings. Teenliggame teen GKV was opgespoor in serum monsters met behulp van ‘n ensiem-gekoppelde immunosorbent toets (ELISA) en immunofluoressensie om te bepaal of ‘n humorale immuunrespons ontlok was. In 5/20 muise in groepe ingeënt met pSinOD-lll replikon DNS was ‘n lae vlak teenliggaam respons opgespoor wat die potensiaal van die pSinOD-lll replikon om ‘n humorale immuunrespons te ontlok illustreer. Om die opsporing van sitokiene met behulp van ‘n ELISA te fasiliteer was miltselle met konkanavalien A, GKV OD-lll proteïen of met geen stimulant gestimuleer in selkultuur. ‘n Oorwegend T-helper 1 sel-bemiddelde immuunrespons gekenmerk deur ‘n hoë vlak van interferon-γ vrystelling was bepaal na stimulasie met die GKV OD-lll proteïen *in vitro*. Die vrystelling van interleukin-10 na stimulasie kan moontlik geassosieer word met die voorkoming van immunologies bemiddelde skade aan die gasheer deur die voorkoming van ‘n opruiende inflammatoriese immuunrespons. Teenliggaam-bemiddelde teen-vektor immuniteit behoort nie die immunogenisiteit van die DNS-geloodsde pSinOD-lll replikon te affekteer nie, aangesien geen teenliggame teen die kodeerde Sindbis virus nie-strukturele proteïene opgespoor was in die serum van die muise nie.

Ten slotte was die potensiaal van die DNS-geloodsde pSinOD-lll replikon om ‘n sel-bemiddelde en ‘n humorale immuunrespons na inenting te ontlok gedemonstreer. Die humorale immuunrespons wat ontlok was sal egter versterk moet word.